ROYAUME DU MAROC
Université Mohammed V - RABAT -
جامعة محمد الخامس – الرباط –
Faculté des sciences
كلية العلوم
CENTRE D'ÉTUDES DOCTORALES - SCIENCES ET TECHNOLOGIES

N° d'ordre : 3835

THÈSE

en vue de l'obtention du : **DOCTORAT**

Structure de Recherche : Laboratoire de Physique des Hautes Energies, Modélisation et Simulation
Discipline : Physique
Spécialité : Physique Mathématique

Présentée et Soutenue le : *21/09/2023*

par :

Youssra BOUJAKHROUT

Integrable Spin Chains in 4D Chern-Simons Gauge Theory

Devant le JURY :

Lalla Btissam DRISSI	PES	Faculté des Sciences, Université Mohammed V, Rabat	Président
Allal GHANMI	PES	Faculté des Sciences, Université Mohammed V, Rabat	Examinateur/Rapporteur
Abdeljalil RACHADI	PH	Faculté des Sciences, Université Mohammed V, Rabat	Examinateur/Rapporteur
Mohamed GOUIGHRI	PH	Faculté des Sciences, Université Ibn Tofail, Kénitra	Examinateur/Rapporteur
Mohcine DRISSI EL BOUZAIDI	PA	École Nationale d'Architecture, Tétouan	Invité
Rachid AHL LAAMARA	PES	Faculté des Sciences, Université Mohammed V, Rabat	Co-Directeur de thèse
El Hassan SAIDI	PES	Faculté des Sciences, Université Mohammed V, Rabat	Directeur de thèse

Année Universitaire : 2023 – 24

Remerciements

La présente thèse est le fruit d'une collaboration de quatre ans au sein du Laboratoire des Hautes Energies, Modélisation et Simulation, du département de physique de la Faculté des Sciences, de l'Université Mohammed V de Rabat. Sa réalisation n'aurait pas été faisable sans l'aide indispensable des membres de cette structure de recherche accueillante, pour lesquels je suis reconnaissante.

En particulier, je tiens à remercier chaleureusement Mr. **Rachid AHL LAAMARA**, Professeur de l'enseignement supérieur à la Faculté des Sciences de Rabat, et le directeur de cette thèse, pour ses conseils avisés, son soutien inconditionnel à chaque occasion au cours des six dernières années, ainsi que pour ses efforts considérables déployés pour nous fournir les conditions de travail les plus favorables possibles au sein du laboratoire.

Un énorme merci va également à Mr. **El Hassan SAIDI**, Professeur de l'enseignement supérieur à la Faculté des Sciences de Rabat et co-directeur de cette thèse. Je serais toujours reconnaissante pour son temps précieux, son suivi et dédication continus pour mon projet de recherche, ainsi que pour les connaissances énormes qu'il m'a généreusement partagées. Mais surtout, pour son encouragement sincère et sa méthodologie de travail et de réflexion inspirantes qui m'ont poussé à découvrir et employer mes compétences de recherche scientifique.

J'adresse de sincères remerciements à Mme **Lalla Btissam DRISSI**, Professeur de l'enseignement supérieur à la Faculté des Sciences de Rabat, de l'honneur qu'elle m'a fait en acceptant de présider mon jury de thèse.

De même pour les rapporteurs et examinateurs de ma thèse, Mr. **Allal GHANMI**, professeur de l'enseignement supérieur à la Faculté des Sciences de Rabat, Mr. **Abdeljalil RACHADI**, professeur habilité au sein du même établissement, ainsi que Mr. **Mohamed GOUIGHRI**, professeur habilité de la faculté des Sciences, de l'université Ibn Tofail de Kénitra, je suis redevable.

J'associe à ces remerciements, Mr. **Mohcine DRISSI EL BOUZAIDI**, professeur associé de l'Ecole Nationale d'Architecture de Tetouan, qui a bien voulu assister à la soutenance de cette thèse, et participer au jugement de sa qualité.

En fin, je voudrais profiter de cette occasion pour remercier tous les membres de ma famille
et mon entourage qui ont aidé à la réalisation de ce projet de près ou de loin, en particulier mes parents qui m'ont soutenu et cru en moi tout au long de mon cursus d'études, et ma grand-mère pour ses prières sincères.

Résumé

Cette thèse est basée sur la correspondance reliant les modèles intégrables en deux dimensions à la théorie de jauge de Chern-Simons à quatre dimensions. En se concentrant sur les systèmes de chaînes de spin, on montre que leurs solutions caractéristiques peuvent être réalisées dans le cadre de la théorie de jauge duale en termes de croisement de défauts linéaires en 4D. En particulier, les opérateurs de Lax sont calculés à partir du comportement des faisceaux de champs de Jauge, et comparés aux résultats connus des chaînes de spin de types A_n, B_n, C_n et D_n.

En profitant de la puissance de cette correspondance, on génère aussi des solutions concernant les chaînes de spin ayant des symétries de Lie exceptionnelles e_6 et e_7. Pour l'ensemble de ces opérateurs de Lax oscillatoires de la liste ABCDE, on associe des diagrammes de Quiver topologiques permettant d'interpréter le comportement intrinsèque des états quantiques.

Ensuite, on étend la correspondance pour les super-symétries de Jauge, et on élabore une formule de super opérateurs de Lax, qui nous permet de dériver des nouvelles solutions pour les chaînes de superspin ayant les symétries internes A(m|n), B(m|n), C(n) et D(m|n).

On finit par réaliser la chaîne de superspin en termes de branes dans les cordes de type IIA et la théorie-M en se concentrant sur la symétrie sl(m|n). Ceci motive un super analogue de la correspondance Algèbre/ Homologie où on étend les géométries Du val pour la super singularité.

Mots-clefs : Chaines de spin, Opérateur de Lax, Théorie de Chern-Simons, Défauts topologiques linéaires, Théorie des cordes.

Abstract

This thesis is based on the correspondence linking two-dimensional integrable models to four-dimensional Chern Simons gauge theory. By focusing on the spin chain, we show that their characterizing solutions can be realized in the framework of a dual gauge theory in terms of line defects crossing in 4D. In particular, Lax operators are calculated from the behavior of gauge field bundles, and compared with known results for spin chains of types A_n, B_n, C_n and D_n.

By taking advantage of the power of this correspondence, we also generate solutions for spin chains with exceptional Lie symmetries e_6 and e_7. For this set of oscillator Lax operators in the ABCDE list, we associate topological Quiver diagrams allowing to interpret the intrinsic behavior of quantum states.

After that, we extend the correspondence for Gauge super symmetries, and work out a formula of super Lax operators, that allow us to derive new solutions for superspin chains with internal symmetries described by A(m|n), B(m|n), C(n) and D(m|n).

We end up by realizing the superspin chain in terms of branes in Type IIA strings and M-theory by focusing on the sl(m|n) symmetry. This motivates a super analog of the Algebra/ Homology correspondence where we extend Du val geometries to super singularity.

Key Words : Spin chains, Lax operator, Chern-Simons theory, Topological line defects, String theory.

LIST OF FIGURES

CONTENTS

CHAPTER 1

INTRODUCTION

Integrability and gauge theories represent two distinct areas of modern physics, with major success in both experiment and theory. The ability to bridge their mathematical formulations represents a meaningful and exciting step towards the unification of the different, yet equivalent descriptions of the physical reality. The fascinating discovery of the appearance of two-dimensional integrable lattice models in the framework of four-dimensional Chern-Simons gauge theory [1]- [3], which can be termed as the Integrability/ 4D CS Correspondence, lead to promising findings and a better understanding of both sides of the correspondence [4]- [10], and opened the door for a larger network of dualities with connections to other theories living on different dimensions, especially supersymmetric quiver gauge and string theories [11]- [27].

On one side, a quantum gauge field theory consists of gauge connections and vector bundles constrained by the non-redundancy (or locality) in space-time, which results in a symmetry-rich configuration allowing to model elementary particles as well as their interactions in terms of fields equations. The gauge theory we are interested in here is given by a four-dimensional Chern Simons originally formulated by Costello as a deformation of the well-known three-dimensional Chern-Simons theory [28],[29]. This special four-dimensional formulation is characterized by a mixed topological-holomorphic nature; it is defined on the product of a two dimensional real manifold interpreted as space-time, and a one-dimensional complex manifold representing the spectral parameter.

On the other side, an integrable model is a system of particles or atoms, that is exactly solvable on a non-perturbative level thanks to an infinite number of non trivial conserved quantities. A simple way to put it is that an integrable model is a "nice" or "ordered" system in space-time that enjoys rich symmetries and offers enough information allowing to comprehend its evolution throughout time, and generate explicit solutions describing its dynamics [30]-[40]. Examples of integrable systems include the famous Heisenberg spin chain, the eight-vertex model and multi-dimensional harmonic oscillators. The interesting broad of the experimental manifestations of these systems comprehends many problems of condensed matter physics such as ice, ferromagnetic solids... etc [41]. An important fraction of these models are theoretically represented by two-dimensional lattices in space-time, with lines standing for particles' worldlines [42]-[47]. In this picture, the crossing of two lines describes the scattering of the two particles, yielding the R-matrix. This quantity plays the role of the main macroscopic observable appearing in the Yang Baxter equation of integrability; it characterizes these integrable models and classifies them into sub-families corresponding to rational, elliptic and trigonometric types of solutions.

For integrable spin chain systems, consisting of nodes (particles) aligned following one direction and carrying spin states, the analog of the R-matrix is given by the Lax operator, the main ingredient of the present study. This quantity can be defined at each node of the chain

as a solution to the RLL equation equivalent to the Yang Baxter. In practice, it is used as a building block for the construction of the transfer matrix and therefore the family of commuting operators that allow to diagonalize the Hamiltonian and solve the system on quantum level [48]- [84]. The mathematical hunt for these solutions has entailed tremendous efforts since the 60s for the various sppin chain systems with various internal symmetries. Even lattice models that aren't yet experimentally realizable, such as superspin chains with $\mathbb{Z}_2$ graded spin values, are extensively studied in theoretical high energy physics [85],[86]. The first reason for this interest is their surprising appearance in the framework of other field theories such as the weekly coupled N=4 Yang-Mills where they can be used to provide scattering amplitudes [87]-[98]; or the AdS/CFT in string theory where essential non-perturbative calculations allow to verify the duality on first order [99], as well as other applications [100]-[113]. The second reason is simply why not? Since they provide a rich and elegant mathematical underlying structure that can be used as an elementary pilar for the understanding of more complicated (non integrable) physical problems, they represent a promising research direction and continue on yielding connections with other study areas.

In the integrability literature, these solvable systems are approached by means of algebraic techniques like the Bethe ansatz and the Quantum Inverse Scattering Method where solutions such as the R-matrix or the Lax operator are realized as representations of Yangian algebras. These large extended symmetries are given by deformations of Lie algebras where the role of the deformation parameter is played by the spectral parameter z. However, these "traditional" techniques can be cumbersome and limited for some symmetries due to the complexity of their algebraic structures and the non existence of a Yangian uplifting for some representations of Lie algebras. This becomes even more intricate for Lie superalgebras where calculations of explicit solutions were only possible for linear superspin chains. To overcome this shortage and classify more exactly solvable models, research is directed towards new mathematical techniques and even new rationales.

In the present study, we take advantage of a recently discovered correspondence unveiling that integrable two-dimensional lattice systems are linked to, or come from, a higher-dimensional Chern-Simons gauge theory in 4D. The latter (4D CS theory) is defined on the product of a real plane Σ and a holomorphic curve C, by the field action [1]

$$S_{4DCS} = \int_{\Sigma\times C} dz \wedge tr(\mathcal{A}\wedge d\mathcal{A} + \frac{2}{3}\mathcal{A}\wedge\mathcal{A}\wedge\mathcal{A}) \tag{1.1}$$

and carries a complexified gauge symmetry G. This special topological-holomorphic theory provides a shortcut towards the investigation of lowed- dimensional integrable systems. By endowing it with crossing line defects that appear as curves in Σ, and points in C, one can build the two-dimensional lattice model in Σ, and compute integrability solutions and important quantities of without recourse to the conventional integrability literature methods [114]-[121].

The leading successful prove to this duality was the recovery of the scattering R-matrix by Feynmann diagrams calculations of the crossing of two Wilson lines in the 4D CS. These line defects are characterized by electrical charges given by highest weights of G, such that their associated curves in Σ carry internal quantum states valued in a representation of g (the Lie algebra of G), and therefore are assimilated to worldlines of electrically charged particles. More astonishingly, the additional complex dimension C plays a crucial role in this interpretation. The positions of line defects in the complex C correspond to the spectral parameters z_i appearing in the of Yangian representations realizations of the Yang Baxter equation, and the latter is directly verified by the line defects construction thanks to the diffeomorphism invariance in the four-dimensional space.

In the same spirit, the integrable XXX spin chain which we are interested in here, can be realized in the dual 4D CS with symmetry G, by a set of parallel Wilson lines placed at the chain

sites and carrying degrees of freedom of identical particles with spins in a representation of g. The magnetic interaction between these spins is modelled by a 't Hooft line defect characterized by a magnetic charge equivalent to a coweight μ of G, and perpendicularly crossing the Wilson lines [123],[124]. This image yields a Lax operator solving the RLL equation at each node of the chain as the crossing of a Wilson line with the 't Hooft line. Using this gauge fields construction, the oscillator realization of the Lax operator can be obtained by simply identifying the dispersion of gauge field bundles due to the presence of the singular magnetic 't Hooft line, to the decomposition of elements of the Lie algebra g due to the action of the magnetic coweight μ. This idea was behind the factorized Lax operator formula $\mathcal{L}^{\mu}(z) = e^{X} z^{\mu} e^{Y}$ given in [123] for any gauge group G. The μ represents the adjoint action of a minuscule coweight, and X and Y are determined from the Levi decomposition of g with respect to μ. This general expression was proven by building explicit oscillator realizations of RLL solutions for sl_N and so_{2N} -type spin chains, in agreement with literature results.

In this thesis work, we study integrable XXX spin chain systems characterized by RLL equations, and realized by means of line defects in dual 4D Chern-Simons gauge theories in order to:

• Recover the list of oscillator Lax operators for spin chains with A_n, B_n, C_n and D_n bosonic symmetries and compare them to results of the spin chain literature to further reinforce the correspondence.

• Construct novel solutions concerning spin chains with exceptional e_6 and e_7 symmetries to enrich the spin chain literature by using the correspondence.

• Give an interpretation of the internal transport of quantum data of the Lax operators calculated in 4D CS in terms of gauge quiver diagrams and topological matter.

• Extend the correspondence in order to realize superspin chains in dual 4D CS theories with super gauge symmetries.

• Build explicit super Lax operators as solutions for superspin chains with linear as well as ortho-symplectic internal symmetries.

These results are presented in the present thesis after the first introduction chapter, and the second literature review chapter introducing spin chains as integrable lattice systems, the 4D Chern-Simons gauge theory and its line defects, as well as the correspondence linking these two theories. The third chapter is then dedicated to the investigation of bosonic spin chains with symmetries A_n, B_n, C_n, D_n, E_6 and E_7 respectively. For each of these integrable systems, we yield the oscillator realizations of Lax operators associated to minuscule coweights, and then the associated Quiver diagrams. In the fourth chapter we treat superspin chains in dual 4D CS theories; we explicitly compute super Lax matrices corresponding to the basic Lie superalgebras $A(m|n)$, $B(m|n)$, $C(n)$ and $D(m|n)$. The fifth chapter takes a slightly different direction from the others, its main objective is focused on:

• Embedding superspin chains in superstring theory as a first step towards the realization and verification of the correspondence in a higher dimensional unifying viewpoint.

In that chapter, we closely analyse the degrees of freedom and symmetries of the $sl(m|n)$ superspin chain to motivate its realization in terms of branes in Type IIA Strings and M-theory. We also motivate a super analog of complex manifolds with ADE singularities to justify brane compactifications. We end by a conclusion chapter where we recall main results, give others, and discuss possible extensions of this work.

Finally, notice that the present thesis is based on the following papers list:

- Y. Boujakhrout, E.H Saidi, R. Ahl Laamara, L.B Drissi, 't Hooft lines of ADE-type and Topological Quivers, DOI : 10.21468/SciPostPhys.15.3.078, arXiv:2303.13879 [hep-th].

- Y. Boujakhrout, E.H Saidi, R. Ahl Laamara, L.B Drissi, Embedding Integrable Superspin

Chain in String Theory, DOI: 10.1016/j.nuclphysb.2023.116156, arXiv:2304.03152v1 [hep-th].

- Y. Boujakhrout, E.H Saidi, R. Ahl Laamara, L.B Drissi, Lax Operator and superspin chains from 4D CS gauge theory, J.Phys.A 55 (2022) 41, 415402, DOI: 10.1088/1751-8121/ac9355, arXiv:2209.07117 [hep-th].
- Y. Boujakhrout, E.H Saidi, Minuscule ABCDE Lax Operators from 4D Chern-Simons Theory, Nucl.Phys.B 981 (2022) 115859, DOI: 10.1016/j.nuclphysb.2022.115859, arXiv:2207.14777 [hep-th].
- Y. Boujakhrout, E.H Saidi, On Exceptional 't Hooft Lines in 4D-Chern-Simons Theory, Nucl.Phys.B 980 (2022) 115795, DOI: 10.1016/j.nuclphysb.2022.115795, arXiv:2204.12424 [hep-th].
- Y. Boujakhrout, E.H Saidi, R. Ahl Laamara, L.B Drissi, Superspin Chains Solutions from 4D Chern Simons Theory, arXiv:2209.07117 [hep-th].

CHAPTER 2

INTEGRABILITY IN 4D CHERN-SIMONS THEORY

This chapter is dedicated to a background review where we give a very brief introduction to the basic notions of this study, in particular the Integrability/ 4D CS correspondence and its results which we'll build on in the next chapters. We begin by defining ingredients of the two-dimensional integrable lattice systems, by focusing on spin chains and the Lax operator. Then, we recall the mathematical formulation of the four-dimensional Chern-Simons gauge theory, and the interpretation of its main line defects and their crossings, in order to set the connection between the two sides of the correspondence.

2.1 Introduction to Integrability

Classically, a system is said to be integrable if it possesses a number of conserved quantities (motion integrables) at least equal to the number of its degrees of freedom; thus allowing for its complete solvability [125]-[129]. Quantum mechanically, the integrability of a physical system is translated by the ability to explicitly determine the hamiltonian eigenvalues [130]-[135]. This can be achieved by means of different mathematical approaches such as the Algebraic Bethe Ansatz (ABA) [136]-[144], or the Quantum Inverse Scattering Method (QISM) [145]-[159]. The latter represents the main method used for the study of lattice models that we will focus on here. We will begin here by briefly recalling the rationale behind the Quantum Inverse Scattering Method. Then, we focus our attention on integrable spin chains as one-dimensional lattice models, where we represent their basic solving steps that will be relevant for the dual gauge theory construction.

2.1.1 Quantum Inverse Scattering Method

As the name indicates, the Quantum Inverse Scattering Method investigates the solvability of a system based on the dynamics of the system particles' scattering. The main observable for this approach is the R-matrix which describes the scattering of two particles P_1 and P_2 modeled as one-dimensional quantum systems [160],[161]. This matrix acts on the tensor product of the two vector spaces V_1, V_2 carrying the quantum states of the incoming particles, and maps it onto itself

$$R_{12}(z_1 - z_2) : V_1 \otimes V_2 \to V_1 \otimes V_2 \tag{2.1}$$

This is a function of the difference $z_1 - z_2$ of the complex spectral parameters interpreted in terms of rapidities of the particles. It is graphically sketched as a vertex of two intersecting straight lines representing two worldlines of P_1 and P_2 in space-time (Figure 2.1).

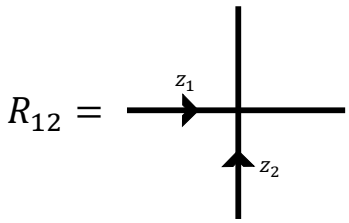

Figure 2.1: Graphical representation of the scattering R-matrix as a two-lines vertex.

The idea behind the QISM is that for an integrable quantum system, every multi-particles scattering process can be factorized into "two to two" scatterings such that their ordering doesn't matter. In general, this can be reproduced from the following three particles crossing image, where the particles P_1 and P_2 can intersect with each other before or after intersecting with the third P_3, See Figure 2.2.

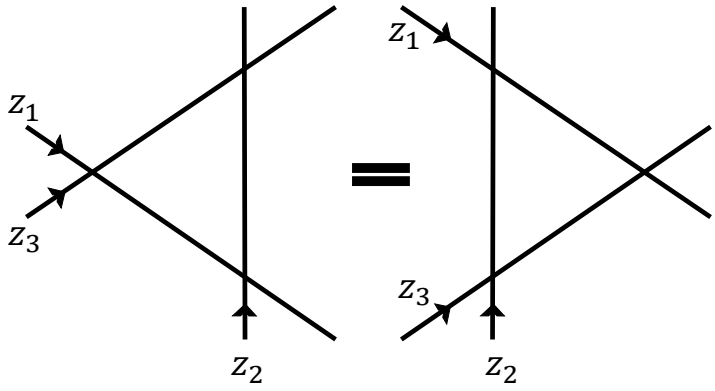

Figure 2.2: Graphical representation of the Yang Baxter equation in 2D space-time. Time is given by the vertical direction.

Mathematically, this is translated by the famous Yang Baxter Equation including three R-matrices

$$R_{12}(z_1 - z_2)R_{13}(z_1 - z_3)R_{23}(z_2 - z_3) = R_{23}(z_2 - z_3)R_{13}(z_1 - z_3)R_{12}(z_1 - z_2) \tag{2.2}$$

where the matrix R_{ij} with $i, j = 1, 2, 3$ acts on the spaces tensor $V_i \otimes V_j \otimes V_k$ with trivial action on V_k like

$$R_{ij}(z_i - z_j) = R_{ij} \otimes I \tag{2.3}$$

The Yang Baxter equation (2.2) represents a powerful sufficient integrability condition costraining two-dimensional quantum field theories [162],[163]. It was proven to admit three types of solutions, refered to as the rational, elliptic and trigonometric R-matrices [164]-[171]. In general, solutions to the Yang Baxter are determined up to an overall factor of z, which is fixed by means of the unitarity condition

$$R_{12}(z_1 - z_2)R_{13}(z_1 - z_3) = I \tag{2.4}$$

The simplest solution is written for two particles with identical internal vector spaces of dimension n

$$V_i = V_j = \mathbb{C}^n \tag{2.5}$$

in terms of their spectral parameters difference $z = z_i - z_j$ as

$$R(z) = z + P \tag{2.6}$$

The permutation tensor P is given by an $n^2 \times n^2$ matrix acting on the product of vectors $v_i \otimes v_j \in \mathbb{C}^n \otimes \mathbb{C}^n$ like

$$P(v_i \otimes v_j) = v_j \otimes v_i \tag{2.7}$$

2.1.2 Spin Chains and the Lax operator

In the present study, we are mainly interested in integrable rational XXX spin chain systems. These can be thought of as a simple one-dimensional lattice since they are formed by a set of identical particles aligned following one direction [172]-[186]. These particles sit on equally distanced nodes of the chain and carry spins valued in a representation $\mathbf{R}$ of a lie algebra g which defines the internal symmetry of the spin chain; we say that the spin chain is of type g. Superspin chains that will be treated later on, are constructed in the same way, such that their internal symmetries are given by Lie superalgebras. The simplest and most studied model corresponds to the Heisenberg chain with magnetic spins $\frac{1}{2}$ (sl_2 internal symmetry). It is defined by the nearest neighbor interactions Hamiltonian [187]

$$H_{Heisenberg} = J \sum_{i=1}^{L} \left(\vec{S}_i \vec{S}_{i+1} \right) \tag{2.8}$$

where $\vec{S}_i = \frac{1}{2}\vec{\sigma}_i$ and $\vec{\sigma}_i$ being the Pauli matrix at node i of the chain. Such spin chain with L nodes is said to be of length L; it can be either open, or closed with boundary condition reading as

$$\vec{S}_{L+1} = \vec{S}_1 \tag{2.9}$$

Since each of the L particles has an internal vector space V_i equal for the case of internal symmetry sl_2 to $\mathbb{C}^2$, the total Hilbert space of the system on which the Hamiltonian acts is given by the tensor product

$$(\mathbb{C}^2)^{\otimes L} \tag{2.10}$$

Unlike other lattice models , particles of a spin chain system do not scatter since they are placed on chain nodes. However, the nearest spins interactions create a magnetic field along all the chain. This is theoretically modeled as a fictional magnetically charged particle, which carries an unconstrained auxiliary space $\mathcal{A}$, in contrast to vector spaces carried by the spins. The analog of the scattering R-matrix in this model is given by the Lax operator which appears at each node and acts on the vector space of that node

$$L_i : V_i \to V_i \tag{2.11}$$

with operational entries acting on $\mathcal{A}$. This special R-matrix can be interpreted as describing the coupling of an electrically charged particle with the total magnetic field. By taking one of the three spaces in 2.2 as arbitrary, say V_3, the Yang Baxter equation turns into the RLL equation, which defines the integrability of a spin chain system

$$R_{12}(z_1 - z_2) L_{13}(z_1) L_{23}(z_2) = L_{23}(z_2) L_{13}(z_1) R_{12}(z_1 - z_2) \tag{2.12}$$

This relation is defined on $V_1 \otimes V_2 \otimes \mathcal{A}$ and uniquely defines the Lax matrix as a characterizing solution of the integrable spin chain. This operator serves as a building block of the monodromy matrix transporting information (the auxiliary magnetic space) along all the chain [188]. We write

$$M(z) = L_1(z - z_1) L_2(z - z_2) ... L_L(z - z_L) \tag{2.13}$$

where the product is ordered following the L nodes of the chain. For a closed spin chain with boundary conditions, we obtain the transfer matrix by tracing out the auxiliary space $aux = \mathcal{A}$ [189]-[192]

$$T(z) = tr_{aux} M(z) \tag{2.14}$$

Following from the RLL relations satisfied by the Lax operators, the transfer (or equivalently the monodromy) matrix obeys the RTT equation

$$R_{12}(z_1 - z_2) T_{13}(z_1) T_{23}(z_2) = T_{23}(z_2) T_{13}(z_1) R_{12}(z_1 - z_2) \tag{2.15}$$

meaning that for different spectral parameters z_1 and z_2, one has a family of commuting operators

$$[T(z_1), T(z_2)] = 0 \tag{2.16}$$

These commuting operators provide the key for the system solving; they are used to simultaneously diagonalize the Hamiltonian matrix using Bethe ansatz methods and generate its eigenvalues [193]-[196].

2.2 Four dimensional Chern-Simons and line defects

In the gauge side of the Integrability/ Gauge correspondence we are employing here, we have a particular four-dimensional Chern-Simons gauge field theory. It was first introduced by Costello in [28], and further elaborated by establishing its line and surface defects in [1]-[3] and [123]. We briefly present in this section the main elements and observables of motion of this gauge theory that allow for the realization of degrees of freedom of lower-dimensional integrable models. We focus on the construction of the Wilson line and the 't Hooft line defects since they will play a major role in calculating the R-matrix and Lax operator.

To begin, the 4D Chern-Simons theory lives on the four-dimensional manifold $\boldsymbol{M}_4$ which is given by the product of a topological real plane Σ and a holomorphic curve C

$$\boldsymbol{M}_4 = \Sigma \times C \tag{2.17}$$

In general, we can consider $\Sigma = \mathbb{R}^2$ parameterised by the real (x, y), and the complex C, that we will mainly take as $\mathbb{C}$, parameterized by a complex parameter z. The 4D CS (four-dimensional Chern-Simons) is defined on $\boldsymbol{M}_4$ by the field action

$$S_{4DCS} = \int_{\boldsymbol{M}_4} dz \wedge \mathcal{A} \wedge d\mathcal{A} + \frac{2}{3} \mathcal{A} \wedge \mathcal{A} \wedge \mathcal{A} \tag{2.18}$$

where the 1-form gauge potential $\mathcal{A}$ is invariant by the gauge symmetry G that should be complex; it expands in terms of generators t_a of the complex Lie algebra g of G as

$$\mathcal{A} = t_a \mathcal{A}^a \tag{2.19}$$

with the gauge connection $\mathcal{A}^a$ expanding in the four-dimensional space as

$$\mathcal{A}^a = dx \mathcal{A}^a_x + dy \mathcal{A}^a_y + d\bar{z} \mathcal{A}^a_{\bar{z}} \tag{2.20}$$

This is a partial one-form connection because its lacks the contribution of the component $dz\mathcal{A}^a_z$ as justified in [1]. The dynamics of this theory are described by the equation of motion such that the gauge curvature vanishes in absence of external sources

$$\mathcal{F}_2 = d\mathcal{A} + \mathcal{A} \wedge \mathcal{A} = 0 \tag{2.21}$$

This ground state is deformed by implementing the line or surface defects, which are the only observables that can be defined on this topological- holomorphic theory. We will introduce here below two types of line defects that allow to define electric and magnetic charges in the 4D CS.

2.2.1 Wilson line and the R-matrix

The Wilson line defect is an electrically charged line operator on which travel gauge field vectors $\mathcal{A}$ in a representation $\boldsymbol{R}$ of g. It is sketched in four dimensions as a curve ξ_z expanding in the topological plan $\mathbb{R}^2$ and sitting in a position z of the complex C. Its associated observable is denoted as $W^{\mathbf{R}}_{\xi_z}$, and is given by the trace over a representation $\mathbf{R}$ of g of the exponential of the gauge transport along ξ_z

$$W^{\mathbf{R}}_{\xi_z} = Tr_{\mathbf{R}}\left[\mathrm{P}\exp\left(\int_{\xi_z}\mathcal{A}\right)\right] \tag{2.22}$$

with P expressing the ordering operator. Notice that each Wilson line is labeled by a representation $\mathbf{R}$, or equivalently its highest weight state $\lambda_{\mathbf{R}}$ which describes the vector electrical charge. This allows to interpret the $W^{\boldsymbol{R}}_{\xi_z}$ as an electrically charges particle such that :
• The curve ξ_z represents the worldline of the particle in space-time.
• The internal quantum states of the particle are valued in the representation $\mathbf{R}$ acting as a vector space V.
• The position in C describes the spectral parameter z, interpreted in terms of the rapidity of the particle.

As a result of this interpretation, the R-matrix measuring the amplitude of the scattering of two particles with vector spaces $V = \mathbf{R}$ and $V' = \mathbf{R}'$ and spectral parameters z and z' is realized in the dual 4D Chern-Simons gauge theory as the crossing of two Wilson lines $W^{\boldsymbol{R}}_{\xi_z}$ and $W^{\boldsymbol{R}'}_{\xi'_{z'}}$. This crossing is depicted in the two-dimensional $\mathbb{R}^2$ in Figure 2.3.

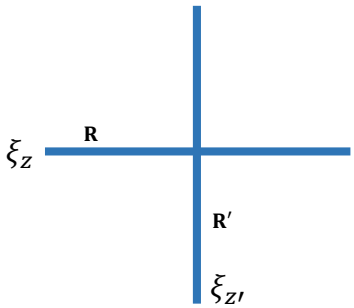

Figure 2.3: Graphical representation of the R-matrix in terms of Wilson lines crossing in the four-dimensional Chern-Simons.

Notice however that these lines do not actually intersect in four dimensions, since they sit in different positions z and z' in the complex dimension, which provides the theory with a diffeomorphism invariance. In fact, having a set of line defects with distinct spectral parameters, one can freely move one line past other lines or their crossing without discontinuity. This property leads to the verification of the Yang Baxter equation 2.2 of integrability on the graphic level, which is given by the Wilson lines image in **Figure** 2.4.

Hence, integrable 2D quantum lattice models can be realized in terms of crossing line defects in the four-dimensional Chern-Simons theory. In this context, the Yang Baxter solutions can be easily generated by Feynman diagrams calculations of the vertices amplitudes. This was demonstrated in [1, 2] by recovering the first order expansions of the three known solutions of the Yang Baxter equation: the rational, elliptic and trigonometric R-matrices which correspond to the three possible choices of the complex space C. Here, we consider the case $C = \mathbb{C}$ which yields integrable systems of rational type.

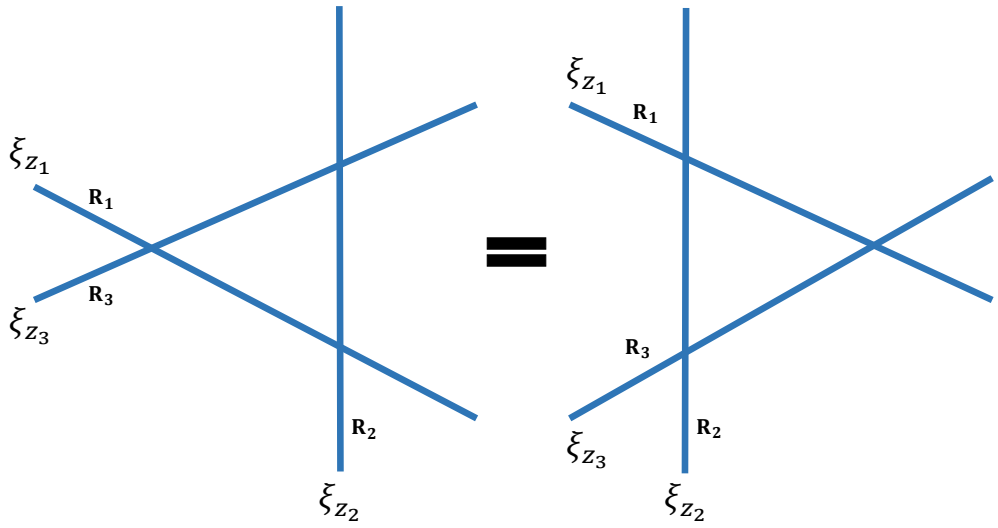

Figure 2.4: Graphical representation of the Yang Baxter equation verified by means of Wilson lines in the 4D CS.

2.2.2 't Hooft line and the Lax operator

The analog of a magnetically charged hypothetic particle, or a Dirac monopole, is given in the framework of the four-dimensional Chern Simons by the 't Hooft line operator. Similarly to a Wilson line, this line defect $\mathrm{tH}^{\tilde{\lambda}}_{\gamma_z}$ is also implemented as a curve $\gamma_z \in \mathbb{R}^2$ and a point $z \in C$. However, it is particular in the sense that it's a disorder operator. It carries a magnetic charge which is given by a coweight $\tilde{\lambda}$ of he gauge group G; and when implemented into the theory, it creates a Dirac-like singularity in the neighbouring gauge field configuration. Thus 't Hooft lines do not carry gauge fields travelling along them, they are mathematically defined by the measure of the parallel transport of gauge bundles past them, i.e. perpendicularly to γ_z) :

$$L^{[\tilde{\lambda}]}(z) = \mathrm{P}\exp\left(\int_{\perp\gamma_z} \mathcal{A}^{[\tilde{\lambda}]}\right) \tag{2.23}$$

In order to exploit this expression, we consider in what follows the particular 't Hooft line $\mathrm{tH}^{\tilde{\lambda}=\mu}_{\gamma_0}$. This line it is placed on the curve $\gamma_0 = \{y = 0, z = 0\}$ dividing the real plane into two patches

$$\mathbb{R}^2 = \mathbb{R}^2_{y\leq 0} \cup \mathbb{R}^2_{y\geq 0} \qquad , \qquad \gamma_0 = \mathbb{R}^2_{y\leq 0} \cap \mathbb{R}^2_{y\geq 0} \tag{2.24}$$

Therefore, the transport (2.23) is measured perpendicularly to γ_0 from $\mathbb{R}^2_{y\leq 0}$ to $\mathbb{R}^2_{y\geq 0}$

$$L^{[\tilde{\lambda}]}(z) = \mathrm{P}\exp\left(\int_{\mathrm{y}} dy \mathcal{A}^{[\tilde{\lambda}]}_y\right) \tag{2.25}$$

Moreover, the magnetic charge of $\mathrm{tH}^{\tilde{\lambda}=\mu}_{\gamma_0}$ is given by a minuscule coweight μ of G. Such coweight acts on elements of the Lie algebra g by only three eigenvalues $0, \pm 1$ [197], and therefore divides g into three subspaces. This is referred to as the Levi decomposition of g with respect to μ which reads as

$$g = n_- \oplus l_\mu \oplus n_+ \tag{2.26}$$

The l_μ is called the Levi subalegbra of g and contains elements with vanishing charge with respect to μ, and $n_\pm$ are nilpotent subspaces carrying charges ± 1 of μ. This algebra splitting plays a very important role in the evaluation of the L-operator (2.23) valuation. In [123], the

gauge field bundles dispersed into regions $\mathbb{R}^2_{y\leq 0}$ and $\mathbb{R}^2_{y\geq 0}$ due to the 't Hooft singularity were identified with the nilpotent subspaces n_- and n_+ of (2.26); while the local Dirac singularity (at the 't hooft line) acting as an isomorphism between the two bundles was associated to l_μ. For visualization, the gauge configuration $A^{[\mu]}$ can be written as

$$\mathcal{A}^{[\mu]} \sim \mathcal{A}_{\mathbf{n}_-} + \mathcal{A}_{\boldsymbol{l}_\mu} + \mathcal{A}_{\mathbf{n}_+} \tag{2.27}$$

and the L-operator takes the factorized form

$$L^{[\mu]}(z) = g_1 z^\mu g_2 \tag{2.28}$$

The $g_1(z)$ and $g_2(z)$ are gauge transformations with values in e^{n_+} and e^{n_-}, and the $z^\mu \in e^{l_\mu}$ is given by the operator $exp(log(z)\mu)$ where μ is the adjoint action of the minuscule coweight. We will see in what follows, that in practice, the L-operator is explicitly calculated by placing a Wilson line perpendicularly to the 't Hooft line such that the operators in (4.164) act on the representation carried by the Wilson.

2.3 Spin chains and the Lax operator in 4D CS

In the framework of a 4D Chern-Simons gauge theory with complex gauge symmetry G living in $\mathbb{R}^2 \times C$, a rational integrable XXX spin chain of length L and internal symmetry described by g, the Lie algebra of G, is realized by means of:

• L Wilson lines $W^{\boldsymbol{R}}_{\xi^i_z}$ placed in parallel in positions x_i in the topological plane $\mathbb{R}^2$, and the same position z in C, such that each Wilson line represents a node of the spin chain with spin given by the representation $\boldsymbol{R}$.

• A 't Hooft line $\mathrm{tH}^\mu_{\gamma_0}$ sitting at a distinct $z = 0$, and extanding along the x-axis of the plane $\mathbb{R}^2$, perpendicularly crossing all the Wilson lines. This line plays the role of the monodromy matrix of the chain.

This construction is represented in Figure 2.5 where the Wilson lines are drawn vertically in blue, and the 't Hooft horizontally in red.

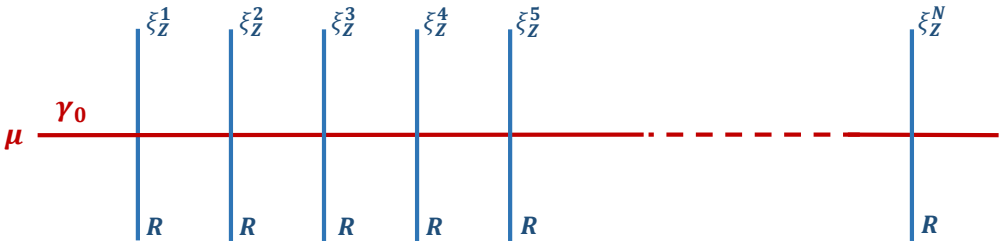

Figure 2.5: The spin chain realization in the Chern-Simons theory: L Wilson lines represented by the blue vertical lines crossed by a $\mathrm{'tH}^\mu_\gamma$ represented by the red horizontal line.

To each node of this spin chain, we associate a Lax operator equal to the crossing of a Wilson line $W^{\mathbf{R}}_{\xi_z}$ characterised by $(\xi_z; \boldsymbol{R})$ with the 't Hooft $\mathrm{tH}^\mu_{\gamma_0}$ characterized by $(\gamma_0; \mu)$. This lines' crossing operator is defined by the coupling of this data (Figure 2.6). We say that this Lax operator (or L-operator) acts on the representation $\mathbf{R}$ of g, and corresponds to the coweight μ, or equivalently a node of the Dynkin diagram of G.

$$\mathcal{L}^\mu_{\mathbf{R}}(\gamma_0, \xi_z) = \left\langle tH^\mu_{\gamma_0}, W^{\mathbf{R}}_{\xi_z} \right\rangle \tag{2.29}$$

For a minuscule magnetic charge μ, we can take advantage of (2.28) to write the Lax operator

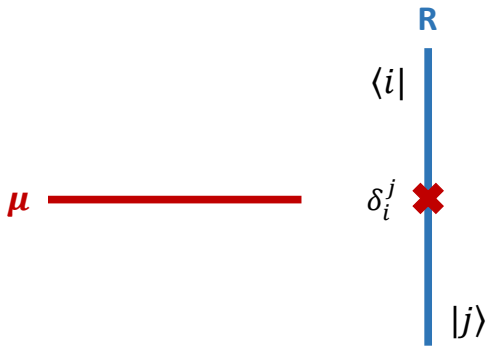

Figure 2.6: Line defects in the real plane $\mathbb{R}^2$. On the left, a horizontal 't Hooft line with magnetic charge μ expanding along the x-axis ($y = 0$) at $z = 0$. On the right, a vertical Wilson line expanding along the y-axis ($x = 0$) at $z \neq 0$ with electric charge in some representation $\boldsymbol{R}$. Notice that the 't Hooft line is in fact paired to a similar one located at $z = \infty$ with magnetic charge $-\mu$, see [123, 124].

as the factorization [123]

$$\mathcal{L}^{\mu}_{\boldsymbol{R}}(z) = e^{X_{\boldsymbol{R}}} z^{\mu_R} e^{Y_{\boldsymbol{R}}} \tag{2.30}$$

with $X_{\boldsymbol{R}}$ and $Y_{\boldsymbol{R}}$ being nilpotent matrices contained in n_+ and n_- respectively, and acting on state vectors in the representation $\boldsymbol{R}$. The μ_R is the adjoint action of the coweight μ on states of the representation $\boldsymbol{R}$. These operators verify the following commutation relations indicating their charges emerging from the Levi decomposition

$$[z^{\mu_R}, X_{\boldsymbol{R}}] = +X_{\boldsymbol{R}} \qquad , \qquad [z^{\mu_R}, Y_{\boldsymbol{R}}] = -Y_{\boldsymbol{R}} \tag{2.31}$$

As shown in Figure 2.6, the Wilson line carries quantum states $|i\rangle$ belonging to the $\mathbf{R}$ and propagating along it and. The incoming particle states vector is denoted by the bra $\langle i|$ and the outgoing states vector by the ket $|j\rangle$ with

$$\langle i|j\rangle = \delta^j_i \tag{2.32}$$

The L-operator (Figure 2.7 -a) acts as the typical matrix operator

$$\left\langle i|\mathcal{L}^{(\mu)}_{\boldsymbol{R}}(z)|j\right\rangle = L^j_i(z) \tag{2.33}$$

with representative matrix L^j_i valued in the algebra $\mathfrak{A}$ of functions on the phase space of $\mathrm{tH}^{\mu}_{\gamma_z}$. We write

$$\mathcal{L}^{\mu}_{\boldsymbol{R}} \in \mathfrak{A} \otimes End(\mathbf{R}) \tag{2.34}$$

This operator verifies the RLL equation encoding the commutation relations between two L-operators at z and z'

$$L^r_j(z)\, R^{ik}_{rs}(z - z')\, L^s_l(z') = L^i_r(z)\, R^{rs}_{jl}(z - z')\, L^k_s(z') \tag{2.35}$$

This equivalence is interpreted in terms of line defects as in Figure 2.7 -b, where the red 't Hooft line crosses two Wilson lines in different orders with equivalent configurations thanks to the diffeomorphism invariance of the 4D Chern-Simons.

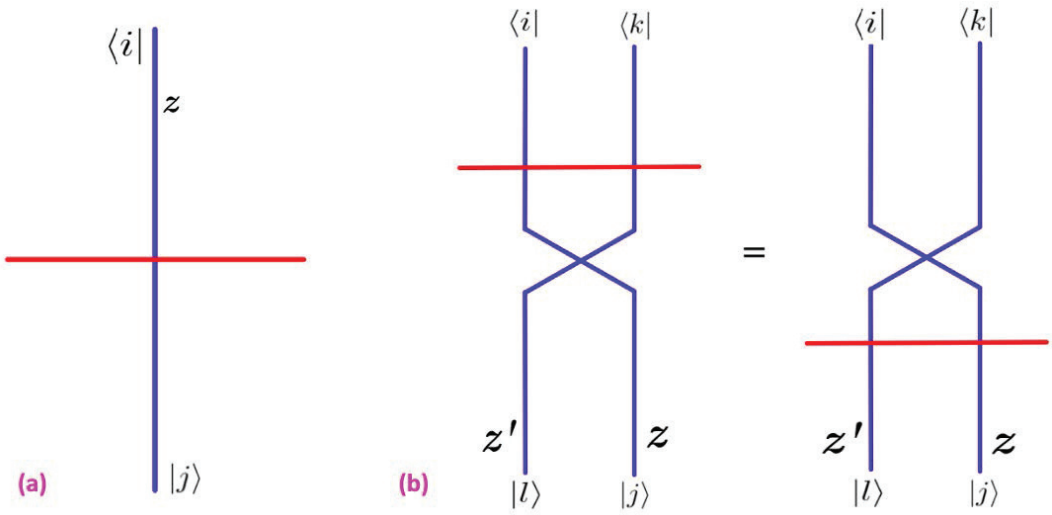

Figure 2.7: (**a**) The operator $\mathcal{L}(z)$ encoding the coupling between a 't Hooft line at z=0 (in red) and a Wilson line at z (in blue) with incoming $\langle i|$ and out going $|j\rangle$ states. (**b**) RLL relations encoding the commutation relations between two L-operators at z and z'.

2.3.1 Oscillator Realization from a Dynkin diagram

Thanks to the power of the Integrability/ 4D CS correspondence, the Lax operator characterizing the integrability of an XXX spin chain system with internal symmetry g, can be explicitly computed in the framework of the dual 4D CS theory by using the Levi decomposition of g with respect to a minuscule coweight of G. In fact, the Levi decomposition has a simple interpretation in terms of nodes' cutting in the Dynkin diagram description of the symmetry algebra. We will take advantage of this property to present here a direct method allowing to explicitly realize minuscule L-operators of oscillator type, from Dynkin diagrams with minuscule nodes.

The diagrammatic description of a Lie algebra g of rank N is given by a Dynkin diagram containing N nodes representing the N simple roots of g such that each simple root α is dual to a fundamental coweight $\tilde{\lambda}$. If the node α is associated to a minuscule representation of g [197], or equivalently to a minuscule coweight μ, than the cutting of that node from the Dynkin diagram yields two or three Dynkin sub-diagrams depending on wether the node is extremal or non-extremal. These sub-diagrams correspond to sub-algebras of g including the $sl_2 \simeq so_2$ of the isolated cut node. The sum of these sub-algebras form the Levi-subalgebra l_μ of g with respect to the considered minuscule coweight. We can write

$$g = n_- \oplus l_\mu \oplus n_+ \tag{2.36}$$

The $n_\pm$ appear in this decomposition as subspaces with equal dimensions, and can be identified as irreducible bi-representations of the l_μ, acting as links between its sub-algebras. Following from this decomposition (2.36), the minuscule Lax operator associated to the minuscule coweight μ is given by the general formula

$$\mathcal{L}^{\mu}_{\mathbf{R}_G} = e^X z^\mu e^Y \tag{2.37}$$

where X and $Y \in n_+$ and n_-. However, in order to explicitly realize this Lax matrix, one needs to determine the representation $\boldsymbol{R}$ of g on which $\mathcal{L}^{\mu}_{\mathbf{R}_G}$ acts. In this regard, notice that as the minuscule μ induces a Levi-decomposition of g, it also splits a representation $\boldsymbol{R}_g$ into a sum of irreducible representations $\mathbf{R}_a^{\boldsymbol{l}_\mu}$ of the sub-algebras of l_μ. We write

$$\mathbf{R}_g = \oplus_a \mathbf{R}_a^{\boldsymbol{l}_\mu} \tag{2.38}$$

This is referred to in literature as the branching rules [198]-[202] where each subspace $\mathbf{R}_a$ carries a fractional Levi charge $m_{\mathbf{R}_a}$. The action of the charge operator μ is given by the sum of actions on these representations. It explicitly reads in terms of projectors $\varrho_{\mathbf{R}_a}$ on these subspaces as follows

$$\mu = \sum_{\mathbf{R}_a} m_{\mathbf{R}_a} \varrho_{\mathbf{R}_a} \tag{2.39}$$

where

$$\sum_{\mathbf{R}_a} \varrho_{\mathbf{R}_a} = \mathbf{1}_{\boldsymbol{R}} \qquad , \qquad \varrho_{\mathbf{R}_a} \varrho_{\mathbf{R}_b} = \delta_{ab} \varrho_{\mathbf{R}_a} \tag{2.40}$$

Since $\mu \in l_\mu$, the trace of its action on the representation $\boldsymbol{R}$ is equal to zero

$$Tr_{\boldsymbol{R}}(\mu) = \sum m_i Tr(\varrho_i) = 0 \tag{2.41}$$

yielding the following constraint relation on Levi-charges

$$\sum_{\mathbf{R}_a} m_{\mathbf{R}_a} = 0 \tag{2.42}$$

which can be used to determine the charges $\mathbf{R}_a^{\boldsymbol{l}_\mu}$.
Regarding the operators X and Y, they expand in the generators basis X_i of n_+ and Y^i of n_-, in terms of parameters b^i, c_i with $i = 1, \ldots, \dim n_+ = \dim n_-$ as follows

$$X = b^i X_i \qquad ; \qquad Y = c_i Y^i \tag{2.43}$$

The action of the basis matrices on the representation $\boldsymbol{R}$, can be realized by identifying the root subsystem corresponding to the nilpotents. In fact, the $n_\pm$ contain roots of g that depend on the minuscule cut root, say β. We write

$$\Phi_{\mathbf{N}_\pm} = \left\{ \pm\alpha \in \Phi_{\mathbf{g}}, \quad \frac{\partial \alpha}{\partial \beta} \neq 0 \right\} \tag{2.44}$$

$$\Phi_{\boldsymbol{l}_\mu} = \left\{ \pm\alpha \in \Phi_{\mathbf{g}}, \quad \frac{\partial \alpha}{\partial \beta} = 0 \right\} \tag{2.45}$$

The distinction between the roots and therefore generators of n_+ and n_- is done by solving the Levi-conditions

$$\begin{array}{rcl} [\mu, X_i] & = & +X_i \\ [\mu, Y^i] & = & -Y^i \end{array} \tag{2.46}$$

such that X_i should carry a positive unit charge $+1$ and Y^i carries a negative unit charge -1. Moreover, we have

$$\left[X_i, Y^j\right] = \delta_i^j \mu \tag{2.47}$$

and

$$\left[b^i, c_j\right] = \delta_j^i \tag{2.48}$$

thus the parameters of the L-operator act as Weyl oscillators of the auxiliary phase space of the 't Hooft line. We say that the constructed spin chain solutions are of oscillator nature.

2.3.2 Topological quivers

As we will see in the next chapter, the Lax operator construction elaborated above yields several solutions for spin chains with different internal symmetries having minuscule coweights. These Lax matrices constructed from the algebraic analysis of Levi decompositions have a similar

general structure that can be unified and encoded into descriptive diagrams. We introduce here what we refer to as "toplogical quiver diagrams" that we associate to each minuscule oscillator Lax operator calculated in the 4D CS theory. These are named quiver diagrams due to their formal similarity with the well known diagrams of supersymmetric quiver gauge theories [203]-[211]. This similarity will allow us to interpret the internal data and gauge fields behavior carried by the L-operators in terms of adjoint and bi-fundamental matter of the gauge symmetry of the 4D CS theory.
To begin, recall that for a supersymmetric quiver gauge theory having a unitary gauge symmetry G factorised as

$$G = \prod_{i=1}^{n_0} U\left(M_i\right) \tag{2.49}$$

and Lie algebra as,

$$\boldsymbol{g} = \oplus_{i=1}^{n_0} u\left(M_i\right) \tag{2.50}$$

one can draw a gauge quiver denoted like $\mathrm{Q}_{gauge}^{susy}$ illustrating the matter content of the gauge theory. This diagram is constructed of :

• A number n_0 of nodes $\mathcal{N}_1, ..., \mathcal{N}_{n_0}$ in one to one with the gauge group factors $G_1, ..., G_{n_0}$ that describe "adjoint matter" transforming in the adjoint representations of the symmetry

$$adjU\left(M_i\right) = \boldsymbol{M}_i \times \bar{\boldsymbol{M}}_i \tag{2.51}$$

• A number n_{link} of links L_{ij} connecting the nodes $(\mathcal{N}_i, \mathcal{N}_j)$ and describing bi-fundamental matter of the gauge symmetry transforming in representations of the form

$$\boldsymbol{M}_i \times \bar{\boldsymbol{M}}_j \in U\left(M_i\right) \times U\left(M_j\right) \tag{2.52}$$

In our case, we will use this dictionary to give interpretations to the content of the Lax operators constructed in 4D CS. This interpretation will turn out to be useful especially for examples constructed in the next chapter. For now, we consider in the general case a Lax operator characterized by $(G; \boldsymbol{R}; \mu)$ where μ is a minuscule coweight decomposing the Lie algebra g of the gauge symmetry G as in (2.36), and where the representation $\boldsymbol{R}$ splits into p irreducible representations R_{m_i} like,

$$\boldsymbol{R} = \sum_{i=1}^{p} \boldsymbol{R}_{m_i} = \sum_{i=1}^{p} \boldsymbol{R}_i$$

These p irreps correspond to sub-algebras of l_μ, i.e. of the Lie algebra g in analogy to (2.50). Moreover, these different subspaces carry different charges m_i with respect to the adjoint action of the $so(2)$ of μ

$$\mu = \sum_{i=1}^{p} m_i \varrho_i, \qquad \sum_{i=1}^{p} \varrho_i = \mathbf{1}_{\boldsymbol{R}}$$

The gauge symmetry configuration resulting from this particular decomposition can be associated to a quiver diagram $\mathrm{Q}_{\boldsymbol{R}}^{\mu}$ formed by p nodes $\mathcal{N}_i$, such that each node is labeled by the data $\boldsymbol{R}_{m_i} \equiv (\boldsymbol{R}_i, m_i)$ where the charge is denoted as a subscript of the irrep, and $2(p-1)$ oriented links $L_{i \to j}$ and $L_{j \to i}$ connecting $\mathcal{N}_i$ and $\mathcal{N}_j$. In order to circulate the Levi-charges in the quiver, the links carry charges that agree with the difference between the nodes charges

$$m_i - m_{i+1} = \pm 1, \qquad m_i - m_j = \pm k$$

Here $k = 1, ..., p-1$ is an integer, and thus we can predict that the quantities carried by these links should be polynomials of the Weyl oscillators $\mathbf{b} = (b^\alpha)$ and $\mathbf{c} = (c_\alpha)$, since these carry

unit charges ∓ 1 with respect to μ. This can be seen from the neutral global charge of the exponentials below with the nilpotents $n_\pm$ carrying charges ± 1.

$$e^X = e^{b^\alpha_{(-1)} X_{\alpha(+1)}}, \qquad e^Y = e^{c_{\alpha(+1)} Y^\alpha_{(-1)}}$$

Hence, given two nodes $\mathcal{N}_i$ and $\mathcal{N}_j$ with Levi-charges verifying $m_j - m_i = k$, the link $L_{i\to j}$, carrying the charge $+k$, is generated by polynomials of the form $\mathbf{c}^{k+l}\mathbf{b}^l$ with leading element given by $\mathbf{c}^k$. Similarly, the link $L_{j\to i}$, carrying a Levi charge $-k$ should be generated by $\mathbf{b}^{k+l}\mathbf{c}^l$ with leading monomial $\mathbf{b}^k$. The arrows should be added to distinguish these links according to the proper circulation of the Levi charge.
In the associated Lax matrix $\mathcal{L}$, the explicit contributions of these nodes and links can be determined by using the resolution of the identity operator ($\sum \Pi_i = \mathbf{1}_{\boldsymbol{R}}$). We write

$$\begin{aligned} \mathcal{L} &= \mathbf{1}_{\boldsymbol{R}} \mathcal{L} \mathbf{1}_{\boldsymbol{R}} \\ &= \sum_i \varrho_i \mathcal{L} \varrho_i + \sum_{i>j} \varrho_i \mathcal{L} \varrho_j + \sum_{i<j} \varrho_i \mathcal{L} \varrho_j \end{aligned}$$

where we can deduce that the nodes $\mathcal{N}_i$ are associated to the diagonal sub-blocks $\varrho_i \mathcal{L} \varrho_i$ acting on adjoint representations $\boldsymbol{R}_i \times \boldsymbol{R}_i$, while the links correspond to the off-diagonal blocks $L_{ij} = \varrho_i \mathcal{L} \varrho_j$ acting on bi-representations $\boldsymbol{R}_i \times \boldsymbol{R}_j$. We will see in explicit examples that this interpretation agrees with the sub-blocks of the minuscule Lax operators built in the next chapter.
Finally, concerning the topological naming of these quivers, it is due to the topological nature of the basic parameters of the Lax operators, i.e. the phase space coordinates b^a and c_a of the topological 't Hooft line defects of 4D CS. Using the killing form of the Lie algebra to write $b^a = tr\,(XY^a)$ and substitute by $X = \log\left(\mathcal{L}^{\mu_k} e^{-Y} z^{-\mu_k}\right)$, we can directly express the b^a and c_a in terms of the topological line defect

$$b^a = tr\left(\log\left(\mathcal{L}^{\mu_k} e^{-Y} z^{-\mu_k}\right) Y^a\right) \quad , \quad c_a = tr\left(\log\left(z^{-\mu_k} e^{-X} \mathcal{L}^{\mu_k}\right) X_a\right) \tag{2.53}$$

CHAPTER 3

MINUSCULE LAX OPERATORS FOR ABCDE SPIN CHAINS AND TOPOLOGICAL QUIVERS

In this chapter, we study integrable spin chain systems with bosonic ABCDE internal symmetries in the framework of their dual 4D Chern-Simons gauge theories. By exploiting the Lax operator formula elaborated before (2.37), we yield explicit oscillator realizations of minuscule Lax matrices as solutions to RLL equations, based only on Levi decompositions of the Lie algebras. Notice that for the infinite A_n, B_n, C_n and D_n symmetries, the minuscule oscillator L-matrices were already computed in the integrability side by using Yangian representations -based methods. These results will be compared here with our solutions calculated in the dual gauge theory side for reference. Concerning exceptional symmetries E_6 and E_7, they are still lacking in the spin chain literature, thus this deficiency will be covered thanks to the correspondence. We we will also associate to each minuscule Lax matrix calculated in this chapter, a gauge quiver diagram illustrating its internal data, in order to understand the unified behaviour of these observables, and predict the form of other L-matrices without explicit computations.

3.1 A-type spin chain

The firs spin chain system we will treat is of of A-type, meaning that its spins take values in a representation of the linear sl_N Lie symmetry. This integrable system can be realized in the framework of a four dimensional Chern-Simons theory with $SL(N)$ gauge symmetry by considering Wilson lines in a representation $\mathbf{R}$ of sl_N, and a 't Hooft line with magnetic charge given by a coweight of $SL(N)$. We will focus here on the fundamental $\mathbf{R} = \mathbf{N}$ for simplicity, and we will take the magnetic charge as a minuscule coweight μ in order to calculate minuscule L-operators $\mathcal{L}^{\mu}_{\mathbf{N}}$ using (2.37). However, for this A-type symmetry, all fundamental coweights are of minuscule type. As depicted in **Figure 3.1**, the Dynkin diagram of the sl_N Lie algebra has $N-1$ simple roots reading in terms of space vectors as

$$\alpha_i = \epsilon_i - \epsilon_{i+1}; \qquad 1 \leq i \leq N-1 \tag{3.1}$$

These are dual to $N-1$ minuscule fundamental coweights μ_i such that

$$\alpha_i \mu_j = \delta_{ij}; \qquad 1 \leq i, j \leq N-1 \tag{3.2}$$

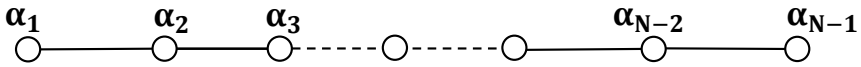

Figure 3.1: The Dynkin diagram for the sl_N family, it has $N-1$ simple roots, all corresponding to minuscule coweights

This means that we can define in the $SL(N)$ Chern-Simons gauge theory $N-1$ minuscule 't Hooft lines with distinct magnetic charges. Their different couplings with the Wilson $W_{\xi_z}^{\boldsymbol{R}=\mathbf{N}}$ leads to $N-1$ families of minuscule Lax operators labeled by the coweights μ_i. These L-operators will be casted here into two sets. The first one concerns the extremal nodes μ_1 and μ_{N-1} of the Dynkin diagram that can be treated on the same footing, while non-extremal nodes are classified by the integer $2 \leq k \leq N-2$ and are associated to a generic coweight μ_k. This discrimination is due to the fact that for a fixed representation $\boldsymbol{R}$, the form of the L-operator is based on the Levi decomposition emerging from the action of the minuscule coweight. As we will see for the A-type Dynkin diagram, this action depends on wether the associated node is extremal or not.
We begin here below by studying the Levi decomposition in the first case and constructing the associated solutions $\mathcal{L}_{\mathbf{N}}^{\mu_1}$ and $\mathcal{L}_{\mathbf{N}}^{\mu_{N-1}}$; then, we turn to the family $\mathcal{L}_{\mathbf{N}}^{\mu_k}$ in the second subsection.

3.1.1 L-operator for extremal nodes of sl_N

We consider the Dynkin diagram **Figure 3.1** of sl_N, and cut an extremal node corresponding to the simple root α_1 or α_{N-1}. As depicted in **Figures 3.2** and **3.3**, we obtain in the two cases an isolated extremal node representing the A_1 algebra, and a Dynkin sub-diagram of type A_{N-2}. This graphical splitting is written as

$$DD_{A_{N-1}} \to DD_{A_1} + DD_{A_{N-2}} \tag{3.3}$$

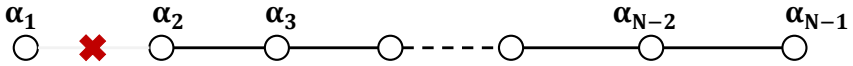

Figure 3.2: If we cut the first node from the Dynkin diagram for the sl_N family, we obtain the two sub-Dynkin diagrams corresponding to sl_1 and sl_{N-1}.

On the level of the Lie algebra, this node cutting operation leads to a Levi decomposition of sl_N which reads for the two cases as

$$sl(N) \to n_- \oplus sl(1) \oplus sl(N-1) \oplus n_+ \tag{3.4}$$

where the Levi subalgebra is

$$l_{\mu_1} = l_{\mu_{N-1}} = sl(1) \oplus sl(N-1) \tag{3.5}$$

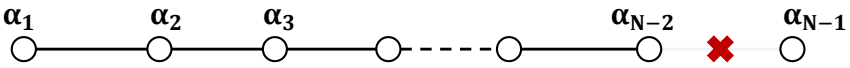

Figure 3.3: If we cut the last node from the Dynkin diagram for the sl_N family, we obtain the two sub-Dynkin diagrams corresponding to sl_{N-1} and sl_1.

and the nilpotents are given by representations of the $sl(N-1)$ such that

$$\dim n_+ = \dim n_- = N-1 \tag{3.6}$$

One can deduce from this similarity that the corresponding minuscule L-operators are equivalent up to a basis change.

$$\mathcal{L}^{\mu_1}_{\boldsymbol{R=N}}(z) \sim \mathcal{L}^{\mu_{N-1}}_{\boldsymbol{R=N}}(z) \tag{3.7}$$

We can choose to focus here on the coupling of the Wilson line $W^{\boldsymbol{R=N}}_{\xi_z}$ with the 't Hooft line $tH^{\mu_1}_{\gamma_0}$ in order to detail the construction of $\mathcal{L}^{\mu_1}_{\boldsymbol{N}}(z)$. In this case, the branching rule of the fundamental representation N following from the decomposition (3.4) reads as [198]

$$\mathbf{N} \to \mathbf{1}_{\frac{N-1}{N}} \oplus (\mathbf{N-1})_{-\frac{1}{N}} \tag{3.8}$$

This is visualized in Figure 3.4 as the splitting of gauge fields carried by the line defects in the 4D CS theory. Notice that the charges in (3.8) verify the vanishing trace condition

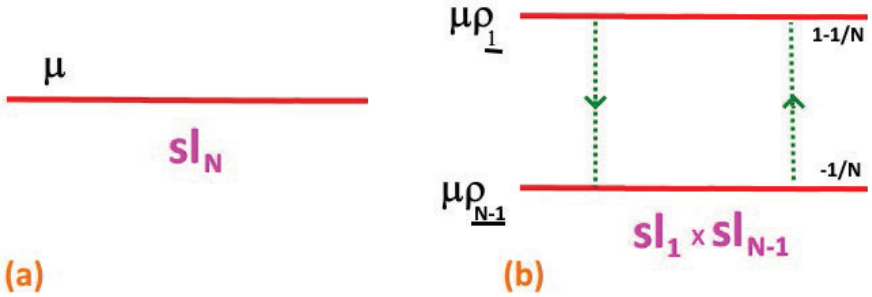

Figure 3.4: (**a**) Magnetic 't Hooft with charge μ_1 from the point of view of global sl_N symmetry. (**b**) The same line from the point of view of internal $sl_1 \oplus sl_{N-1}$. Here, the line μ splits into two sub-lines $\mu\varrho_1$ and $\mu\varrho_{N-1}$ as described in eq.(3.8).

$$\frac{N-1}{N} + N - 1 \times -\frac{1}{N} = 0 \tag{3.9}$$

which leads to the following basis choice for the space $\mathbf{N}$

$$\{|1\rangle, |a\rangle \qquad ; 2 \leq a \leq N\} \tag{3.10}$$

The adjoint action of the minuscule coweight μ_1 is written in this basis as

$$\mu_1 = \frac{N-1}{N}|1\rangle\langle 1| - \frac{1}{N}\sum_{a=2}^{N}|a\rangle\langle a| \tag{3.11}$$

and the operator

$$z^{\mu_1} = z^{\frac{N-1}{N}} \varrho_1 + z^{-\frac{1}{N}} \varrho_{\bar{1}} \tag{3.12}$$

where we have set

$$\varrho_1 = |1\rangle\langle 1| \qquad ; \qquad \varrho_{\bar{1}} = \sum_{a=2}^{N} |a\rangle\langle a| \tag{3.13}$$

as the projectors on $\mathbf{1}$ and $\mathbf{N-1}$ respectively with $\varrho_1 + \varrho_{\bar{1}} = I_{\mathbf{N}}$.

Now concerning the other operators $X \in n_+$ and $Y \in n_-$ appearing in the Lax operator formula, they can be realized by specifying the associated roots action. We make use of the following table giving the explicit splitting of the root system of the sl_N algebra resulting from the Levi decomposition (3.4)

	sl_N	$sl(1)$	$sl(N-1)$	$n_+ \oplus n_-$
Rank	$N-1$	1	$N-2$	$-$
Roots	$\pm\alpha_{ij}; 1 \leq i \neq j \leq N$	$-$	$\pm\alpha_{ij}; 2 \leq i \neq j \leq n$	$\pm\alpha_{1i}; 2 \leq i \leq N$
Number of roots	$N(N-1)$	$-$	$(N-1)(N-2)$	$N-1$
Generators	$h_i; E_{\pm\alpha_{ij}}; 1 \leq i \neq j \leq N$	h_1	$h_i; E_{\pm\alpha_{ij}}; 2 \leq i \neq j \leq N$	$E_{\pm\alpha_{1i}}; 2 \leq i \leq N$
Dimension	N^2-1	1	$(N-1)^2-1$	$2(N-1)$

(3.14)

In this table, the roots read as $\alpha_{ij} = \varepsilon_i - \varepsilon_j$, while the h_i are Cartan generators and $E_{\pm\alpha_{ij}}$ are root generators corresponding to the $\pm\alpha_{ij}$ such that $E_{+\alpha_{ij}} = \overline{E_{-\alpha_{ij}}}$. Notice that the nilpotents $n_\pm$ are formed by positive (negative) roots of $sl(n)$ that depend on α_1. Their distinction is insured by the Levi conditions

$$[\mu_1, n_\pm] = \pm n_\pm \tag{3.15}$$

This allows to realize the operators X_a and Y^a of $n_\pm$ as known root generators. In the basis (3.10), these are given by the $N \times N$ triangular matrices

$$\begin{array}{rcl} X_a & = & |1\rangle\langle a| \\ Y^a & = & |a\rangle\langle 1| \end{array} \tag{3.16}$$

Eventually, we can write the elements of $n_\pm$ as the combinations

$$X = \sum_{a=1}^{N-1} b^a |1\rangle\langle a| \qquad , \qquad Y = \sum_{a=1}^{N-1} c_a |a\rangle\langle 1| \tag{3.17}$$

where the parameters b^a and c_a play the role of oscillators of the phase space of the 't Hooft line with the poisson bracket

$$\{b^a, c_b\}_{PB} = \delta^a_b \tag{3.18}$$

The matrices (3.17) verify the nilpotency property because $X^2 = Y^2 = 0$; their exponentials simply expand as

$$e^X = I + X \qquad ; \qquad e^Y = I + Y \tag{3.19}$$

We finally replace into the L-operator formula

$$\mathcal{L}^{\mu_1}_{\mathbf{N}}(z) = (I+X)\, z^{\mu_1}\, (I+Y) \tag{3.20}$$

which is simplified by using special properties of the realization (3.17); mainly

$$\begin{array}{rcl@{\qquad,\qquad}rcl} X_a\varrho_1 = & = & 0 & \varrho_1 Y^a & = & 0 \\ X_a\varrho_{\bar{1}} & = & X_a & \varrho_{\bar{1}} Y^a & = & Y^a \end{array} \tag{3.21}$$

We write in terms of the projectors (4.67)

$$\mathcal{L}_{\mathbf{N}}^{\mu_1} = z^{\frac{N-1}{N}} \varrho_1 + z^{-\frac{1}{N}} \varrho_{\bar{1}} + z^{-\frac{1}{N}} \varrho_1 X \varrho_{\bar{1}} + z^{-\frac{1}{N}} \varrho_{\bar{1}} Y \varrho_1 + z^{-\frac{1}{N}} \varrho_1 XY \varrho_1 \tag{3.22}$$

which allows to represent the L-operator in the basis (3.10) as a four sub-blocks matrix

$$\mathcal{L}_{\mathbf{N}}^{\mu_1} = \begin{pmatrix} \varrho_1 \mathcal{L}_{\mathbf{N}}^{\mu_1} \varrho_1 & \varrho_1 \mathcal{L}_{\mathbf{N}}^{\mu_1} \varrho_{\bar{1}} \\ \varrho_{\bar{1}} \mathcal{L}_{\mathbf{N}}^{\mu_1} \varrho_1 & \bar{\varrho}_1 \mathcal{L}_{\mathbf{N}}^{\mu_1} \varrho_{\bar{1}} \end{pmatrix} \tag{3.23}$$

which is equal to

$$\mathcal{L}_{\mathbf{N}}^{\mu_1} = \begin{pmatrix} z^{\frac{N-1}{N}} + XY & z^{-\frac{1}{N}} X \\ z^{-\frac{1}{N}} Y & z^{-\frac{1}{N}} I_{N-1} \end{pmatrix} \tag{3.24}$$

In terms of the oscillators of the auxiliary phase space, we have

$$\mathcal{L}_{\mathbf{N}}^{\mu_1} = \begin{pmatrix} z^{\frac{N-1}{N}} + z^{-\frac{1}{N}} b^a c_a & z^{-\frac{1}{N}} b^a \\ z^{-\frac{1}{N}} c_a & z^{-\frac{1}{N}} I_{N-1} \end{pmatrix} \tag{3.25}$$

Here, the b^a and c_a are respectively row and column vectors of $N-1$ dimensions, and the quantity $b^a c_a$ is scalar. Concerning the Lax operator $\mathcal{L}_{\mathbf{N}}^{\mu_{N-1}}(z)$ associated to the last extremal node of the Dynkin diagram, it is simply recovered from the matrix (3.25) by a basis change, where the states of the fundamental representation would be ordered as $\{|a\rangle, |N\rangle; 1 \leq a \leq N-1\}$.

3.1.2 L-operator for non-extremal nodes of sl_N

The second family of the minuscule L-operators that we can construct from the Chern Simons theory concerns the non-extremal nodes of the Dynkin diagram, i.e. 't Hooft lines with magnetic charge given by minuscule coweights μ_k with $2 \leq k \leq N-2$. Following the same steps as before, we begin by studying the Levi decompositions of the sl_N algebra generated by the cutting of non-extremal nodes of the Dynkin diagram of sl_N. In fact, for a generic node labeled by k with $2 \leq k \leq N-2$, the cutting operation (Figure 3.5) leaves us with three sub-Dynkin diagrams of A-type

$$DD_{A_{N-1}} \to DD_{A_{k-1}} + DD_{A_1} + DD_{A_{N-k-1}} \tag{3.26}$$

The $sl(N)$ Lie algebra decomposes in this case as

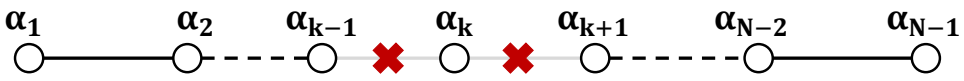

Figure 3.5: If we cut a non extremal node from the Dynkin diagram for the sl_N family, we obtain two sub-Dynkin diagrams of A-type in addition to the cut node.

$$\begin{aligned} sl(N) &\to n_-^k l_{\mu_k} \oplus n_+^k && (3.27) \\ l_{\mu_k} &= sl(k) \oplus sl(1) \oplus sl(N-k) && (3.28) \\ n_\pm^k &= \mathbf{k}\,(\mathbf{N}-\mathbf{k})_\pm && (3.29) \end{aligned}$$

This Levi decomposition is behind the construction of the Lax operator $\mathcal{L}_{\mathbf{N}}^{\mu_k}(z)$ describing the coupling of a 't Hooft line $\mathrm{tH}_{\gamma_0}^{\mu_k}$ with a Wilson line $W_{\xi_z}^{\mathbf{N}}$ in the fundamental representation.

Notice that the Levi decomposition (3.4) cannot be recovered from (4.169) by taking $k = 1$, hence why we study them separately here.
Following the action of a μ_k (4.169), the fundamental representation also splits into irreducible representations of the l_{μ_k} like

$$\mathbf{N} \to \mathbf{k}_{\frac{N-k}{N}} \oplus (\mathbf{N}-\mathbf{k})_{-\frac{k}{N}} \tag{3.30}$$

This splitting gives us a prediction of the behaviour of the gauge states at the line defects' coupling as depicted in Figure 3.6. The vector states of $\mathbf{N}$ are therefore represented in the basis

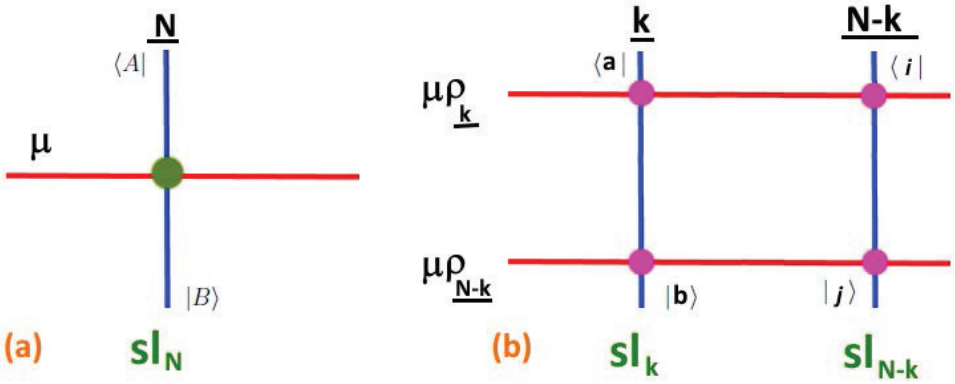

Figure 3.6: (a) A horizontal minuscule 't Hooft line with magnetic charge μ_k crossing a vertical Wilson line with electric charge $\boldsymbol{R} = \mathbf{N}$. The green dot describes the coupling given by the Lax operator $\langle A|L^{\mu_k}_{\boldsymbol{R}}|B\rangle$. (b) Intrinsic structure of the Lax operator taking into account the Levi decomposition of sl_N with respect to μ_k.

as

$$\{|i\rangle, |a\rangle; 1 \leq i \leq k; k+1 \leq a \leq N\} \tag{3.31}$$

We can define the projectors on these subspaces as

$$\Pi_k = |i\rangle\langle i|, \qquad \Pi_{\bar{k}} = |a\rangle\langle a|, \qquad \Pi_k + \Pi_{\bar{k}} = I_{\mathbf{N}} \tag{3.32}$$

The μ_k acts on the states of $\mathbf{N}$ with the sl_1 charges like

$$\mu_k = \frac{N-k}{N}\Pi_k - \frac{k}{N}\Pi_{\bar{k}} \tag{3.33}$$

The X and Y are realized in terms of the $k(N-k)$ couples of oscillators $(b^{i\alpha}, c_{i\alpha})$

$$\begin{array}{rcll} X & = & b^{i\alpha}|i\rangle\langle k+\alpha| & , \quad 1 \leq i \leq k \\ Y & = & c_{i\alpha}|k+\alpha\rangle\langle i| & , \quad 1 \leq \alpha \leq N-k \end{array} \tag{3.34}$$

These verify the Levi constraints as well as the nilpotency features

$$\begin{array}{l} [\mu_k, X] = \left(\frac{N-l}{N} + \frac{l}{N}\right) X = X \quad , \quad XX = 0 \\ [\mu_k, Y] = \left(-\frac{l}{N} - \frac{N-l}{N}\right) Y = -Y \quad , \quad YY = 0 \end{array} \tag{3.35}$$

in addition to other properties like

$$\begin{array}{l} X\Pi_k = 0 \quad , \quad \Pi_k Y = 0 \\ X\Pi_{\bar{k}} = X \quad , \quad \Pi_{\bar{k}} Y = Y \end{array} \tag{3.36}$$

The L-operator for a generic node k, in the fundamental representation expands as

$$\begin{array}{rcl} \mathcal{L}^{\mu_k}_{\mathbf{N}} & = & (I+X)\, z^{\mu_k}\, (I+Y) \\ & = & z^{\mu_k} I + X z^{\mu_k} + z^{\mu_k} Y + X z^{\mu_k} Y \end{array} \tag{3.37}$$

with

$$z^{\mu_k} = z^{\frac{N-k}{N}}\Pi_k + z^{-\frac{k}{N}}\Pi_{\bar{k}} \tag{3.38}$$

and X and Y as in (3.34). The matrix form in the basis (4.155) reads as

$$\mathcal{L}^{\mu_k}_{\mathbf{N}} = \begin{pmatrix} \left(z^{\frac{N-k}{N}} + z^{-\frac{k}{N}} b^{i\alpha} c_{i\alpha}\right) I_k & z^{-\frac{k}{N}} b^{i\alpha} \\ z^{-\frac{k}{N}} c_{i\alpha} & z^{-\frac{k}{N}} I_{N-k} \end{pmatrix} \tag{3.39}$$

One can observe that the $\mathcal{L}^{\mu_1}_{\mathbf{N}}$ of (3.25) can be obtained from (3.39) by taking $k = 1$, and similarly the $\mathcal{L}^{\mu_{N-1}}_{\mathbf{N}}$ is obtained with $k = N-1$. Hence, this matrix (3.39) represents the general expression of the L-matrix for any node k of sl_N with $1 \leq k \leq N-1$. Notice that this result was already obtained using the 4D CS theory in [123]. It also agrees perfectly with the L-operators calculated in the spin chain literature in [55].

3.1.3 topological quiver of A-type

In this subsection, we give the first examples of topological quiver diagrams corresponding to L-operators of the sl_N spin chain. As mentioned above, the general Lax operator for an arbitrary node $k; 1 \leq k \leq N-1$ is given by the matrix $\mathcal{L}^{\mu_k}_{\mathbf{N}}$. This matrix represents the internal splitting of the quantum states of the fundamental representation of the Wilson line when coupling to a 't Hooft line with a magnetic charge μ_k. This general behaviour can be actually directly deduced from the decomposition as explained in Figure 3.6.

$$\mathbf{N} \to \mathbf{k}_{\frac{N-k}{N}} \oplus (\mathbf{N}-\mathbf{k})_{-\frac{k}{N}} \tag{3.40}$$

Interestingly, it can be moreover interpreted into adjoint and bi-fundamental matter like those of a quiver gauge diagram. The expression of the matrix (3.39) in the projectors basis describes this explicit action of μ_k on the subspaces $\mathbf{k}$ of sl_k and $\mathbf{N}-\mathbf{k}$ of sl_{N-k}. The four sub-blocks of are translated into two nodes $\mathcal{N}_k, \mathcal{N}_{\bar{k}}$ and two links $L_{k\bar{k}}, L_{\bar{k}k}$ of the topological gauge quiver $\mathrm{Q}^{\mu_k}_{\mathbf{N}}$. The nodes correspond to diagonal blocks on the representations $\mathbf{k}$ and $\mathbf{N}-\mathbf{k}$

$$\mathcal{N}_{\mathbf{k}} \simeq \Pi_{\bar{k}} \mathcal{L}^{\mu_k}_{\mathbf{N}} \Pi_k \qquad , \qquad \mathcal{N}_{(\mathbf{N}-\mathbf{k})} \simeq \Pi_{\bar{k}} \mathcal{L}^{\mu_k}_{\mathbf{N}} \Pi_{\bar{k}} \tag{3.41}$$

which are interpreted as topological self-dual matter of the gauge groups SL_k and SL_{N-k}. The off-diagonal blocks describe bi-fundamental matter of $SL_k \times SL_{N-k}$ linking between the two nodes

$$L_{k\bar{k}} = L_{\mathbf{k}\to(\mathbf{N}-\mathbf{k})} \simeq \Pi_k \mathcal{L}^{\mu_k}_{\mathbf{N}} \Pi_{\bar{k}} \qquad , \qquad L_{\bar{k}k} = L_{(\mathbf{N}-\mathbf{k})\to\mathbf{k}} \simeq \Pi_{\bar{k}} \mathcal{L}^{\mu_k}_{\mathbf{N}} \Pi_k \tag{3.42}$$

This interpretation is illustrated in Figure **3.7** where the charges under μ_k are depicted.

Notice that indeed, the total charges of the quantities carried by the nodes and the links are in agreement with the conservation of the exchange in the quiver. Moreover, by using the Killing form, the b^α and c_α can be related to the links $L_{k\bar{k}}$ and $L_{\bar{k}k}$ as

$$b^{ia} = z^{\frac{k}{N}} Tr\left(L_{k\bar{k}} Y^{ia}\right) \qquad , \qquad c_{ia} = z^{\frac{k}{N}} Tr\left(L_{\bar{k}k} X_{ia}\right) \tag{3.43}$$

We can take advantage of this quiver diagram interpretation of the minuscule Lax matrix in the framework of the four-dimensional gauge theory in order to predict the structure of other solutions of the model, without going through explicit calculations. For instance, Lax matrices corresponding to higher dimensional representations of the A-type symmetry are cumbersome to calculate, and still missing in the literature. By application of the quiver diagram's construction steps provided in the previous chapter, we give here quiver graphs describing the inner structure

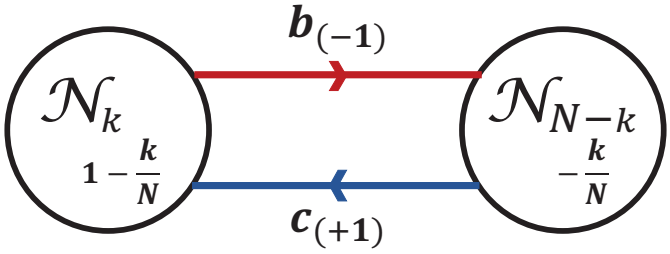

Figure 3.7: The topological quiver representing $\mathcal{L}^{\mu_k}_{\boldsymbol{N}}$ of sl_N. It has 2 nodes and 2 links. The nodes describe self-dual topological matter and the links describe bi-matter.

of such solutions. We start by listing the branching rules of different representations of sl_N with respect to μ_1 [198]. Notice that these splittings all follow from the Levi decomposition (3.4).

sl_N	$sl_1 \oplus sl_{N-1}$
$\boldsymbol{N}^{\wedge k}$	$\left(\boldsymbol{F}^{\wedge(k-1)}\right)_{1-\frac{k}{N}} \oplus \left(\boldsymbol{F}^{\wedge k}\right)_{-\frac{k}{N}}$
$\boldsymbol{N} \vee \boldsymbol{N}$	$\mathbf{1}_{2-\frac{2}{N}} \oplus \boldsymbol{F}_{1-\frac{2}{N}} \oplus (\boldsymbol{F} \vee \boldsymbol{F})_{-\frac{2}{N}}$
$\boldsymbol{N} \times \bar{\boldsymbol{N}}$	$\mathbf{1}_{1-\frac{1}{N}} \otimes \mathbf{1}_{\frac{1}{N}-1} + \mathbf{1}_{1-\frac{1}{N}} \otimes \boldsymbol{F}_{\frac{1}{N}} + \boldsymbol{F}_{-\frac{1}{N}} \otimes \mathbf{1}_{\frac{1}{N}-1} + \boldsymbol{F}_{-\frac{1}{N}} \otimes \boldsymbol{F}_{\frac{1}{N}}$
$\boldsymbol{adj}\,(sl_N)$	$\boldsymbol{F}_{-1} \oplus [\mathbf{1}_0 \oplus \boldsymbol{adj}\,(sl_{N-1})_0] \oplus \boldsymbol{F}_{+1}$

(3.44)

Here, the representation $\boldsymbol{F} = \boldsymbol{N} - \mathbf{1}$ refers to the fundamental of sl_{N-1}. The gauge quivers resulting from these decompositions are drawn in Figures 3.8, 3.9, 3.10 and 3.11.

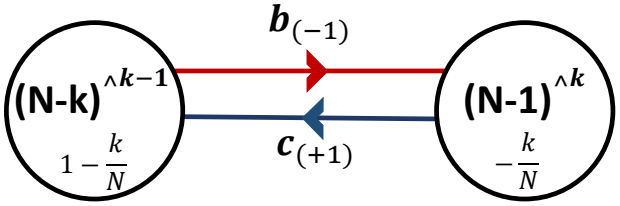

Figure 3.8: The topological quiver $\mathrm{Q}^{\mu_1}_{\boldsymbol{R}}$ for the representation $\boldsymbol{R} = \boldsymbol{N}^{\wedge \boldsymbol{k}}$.

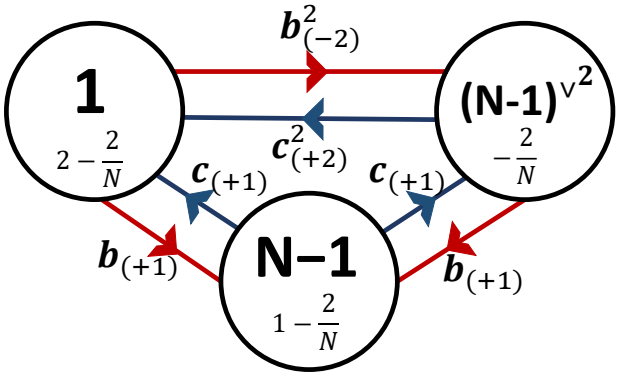

Figure 3.9: The topological quiver $\mathrm{Q}^{\mu_1}_{\boldsymbol{R}}$ for the representation $\boldsymbol{R} = \boldsymbol{N}^{\vee \mathbf{2}}$.

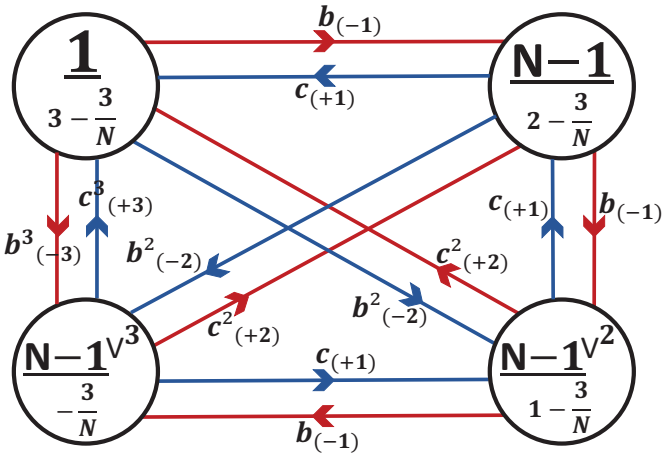

Figure 3.10: The topological quiver $\mathrm{Q}^{\mu_1}_{\boldsymbol{R}}$ for the representation $\boldsymbol{R} = \boldsymbol{N} \vee \boldsymbol{N} \vee \boldsymbol{N}$. This quiver has four nodes and 12 links.

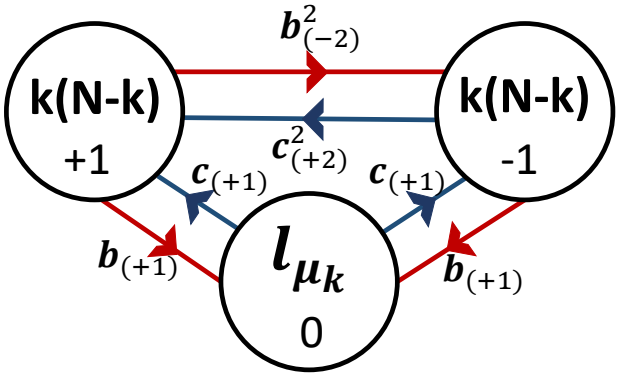

Figure 3.11: The topological quiver $\mathrm{Q}^{\mu_k}_{\boldsymbol{adj}(sl_N)}$ for the adjoint representation of sl_N. It has three nodes in one to one with the Levi subalgebra $\mathcal{N}_0 = \boldsymbol{l}_{\mu_k}$ and the nilpotent subspaces $\boldsymbol{n}_\pm = \boldsymbol{k}\,(\boldsymbol{N}-\boldsymbol{k})_\pm$.

3.2 B type spin chains

In the present section, we study the class of spin chains with B-type internal symmetry. In a similar fashion to the precedent section, we realize this integrable system using Wilson and 't Hooft line defects habiting a 4D Chern-Simons theory endowed with the orthogonal $SO(2N+1)$ gauge symmetry. By analyzing the algebraic properties of the so_{2N+1} symmetry, we recover the minuscule Lax operators $\mathcal{L}^{\mu_{SO(2N+1)}}_{\mathbf{R}}$ as the coupling of a Wilson line in the fundamental representation with a 't Hooft line having a minuscule magnetic charge. We show that this L-operator agrees with matrices obtained from anti-shifted Yangians.

3.2.1 Minuscule L-operator of B-type

Unlike the A-type symmetry, the so_{2N+1} Lie algebra actually has only one minuscule coweight and therefore one possible Levi decomposition for which we will calculate the associated Lax operator. For that purpose, recall that the B_N Lie algebra is of rank N and dimension $N(2N+1)$. Its Dynkin diagram is given in Figure 3.12 with N simple roots reading as

$$\alpha_i = e_i - e_{i+1}; 1 \leq i \leq N-1 \qquad , \qquad \alpha_N = e_{N-1} + e_N \tag{3.45}$$

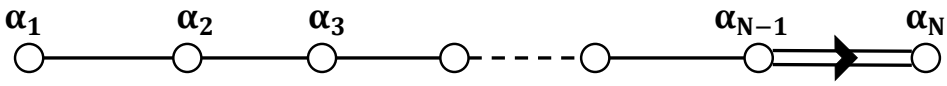

Figure 3.12: The Dynkin diagram associated to the B_N Lie algebra, it has N nodes.

The minuscule coweight $\mu_1 = e_1$ corresponds to the first node of the Dynkin diagram and is dual to the root $\alpha_1 = e_1 - e_2$, i.e. it verifies $\mu_1.\alpha_i = \delta_{1i}$. If we cutt this node from the Dynkin diagram as visualized in Figure 3.13, we can read the splitting

$$DD_{B_N} \to DD_{A_1} + DD_{B_{N-1}} \tag{3.46}$$

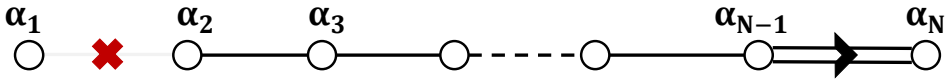

Figure 3.13: If we cut the minuscule node from the Dynkin diagram for the B_N Lie algebra, we obtain two sub-Dynkin diagrams corresponding to A_1 and B_{N-1}.

On the Lie algebra level, this corresponds to

$$\begin{aligned} so_{2N+1} &\to so_2 \oplus so_{2N-1} \oplus n_{\pm} && (3.47)\\ l_{\mu_1} &= so_2 \oplus so_{2N-1} && (3.48)\\ n_{\pm} &= (\mathbf{2N-1})_{\pm 1} && (3.49) \end{aligned}$$

which can be verified by the dimensions splitting

$$\dim \quad : \quad N(2N+1) \quad = \quad 1 + (2N-1)(N-1) + 2(2N-1) \tag{3.50}$$

The branching rules describe the decomposition on the level of the fundamental representation $\mathbf{2N+1}$ which yields a direct sum of representations of $l_{\mu_1} = so_2 \oplus so_{2N-1}$

$$\mathbf{2N+1} = \mathbf{2_0} \oplus (\mathbf{2N-1})_{\mathbf{0}} \tag{3.51}$$

where the zero label refers to the charge under the group $SO(2)$. By using the isomorphism $SO(2) \sim U(1)$, we can moreover substitute with $\mathbf{2_0} = \mathbf{1}_{+1} \oplus \mathbf{1}_{-1}$ to obtain the decomposition

$$\mathbf{2N+1} = \mathbf{1}_{+1} \oplus (\mathbf{2N-1})_0 \oplus \mathbf{1}_{-1} \tag{3.52a}$$

This indicates, we can conveniently represent the operator $\mathcal{L}^{\mu_1}_{\mathbf{2N+1}}$ using the basis kets

$$|\mathbf{2N+1}\rangle = \left\{ \begin{array}{c} |+\rangle \\ |i\rangle \\ |-\rangle \end{array} \right\} \tag{3.53}$$

where $i = 1, ..., 2N-1$ describes the states of the $\mathbf{2N-1}$, while $|\pm\rangle$ refer to the two complex singlets $\mathbf{1}_{\pm 1}$. This basis verifies the orthogonality relations $\langle +|-\rangle = \langle +|i\rangle = \langle i|-\rangle = 0$, as well $\langle +|+\rangle = \langle -|-\rangle = 1$ and $\langle i|j\rangle = \delta_{ij}$. The minuscule coweight acts in this basis as

$$\mu_1 = \varrho_+ + q\Pi - \varrho_- \tag{3.54}$$

with vanishing charge q, and projectors

$$\varrho_+ = |1_+\rangle\langle 1_+|\,, \qquad \Pi = \sum_i |i\rangle\langle i|\,, \qquad \varrho_- = |1_-\rangle\langle 1_-| \tag{3.55}$$

The $X = b^i X_i$ and $Y = c_i Y^i$ are realized by $(2N+1)\times(2N+1)$ matrices verifying the Levi conditions

$$[\mu, X] = +X \qquad , \qquad [\mu, Y] = -Y \tag{3.56}$$

These contain $2(2N-1)$ oscillators in one to one with generators

$$\begin{array}{rcl} X_i & = & |+\rangle\langle i| - |i\rangle\langle -| \\ Y^i & = & |i\rangle\langle +| - |-\rangle\langle i| \end{array} \tag{3.57}$$

The nilpotency of these generators is of order 3 because we have

$$\begin{array}{rcl} X_iX_j & = & -|+\rangle\,\delta_{ij}\,\langle -| \\ Y^iY^j & = & -|-\rangle\,\delta^{ij}\,\langle +| \end{array} \quad , \quad \begin{array}{rcl} X_iX_jX_k & = & 0 \\ Y^iY^jY^k & = & 0 \end{array} \tag{3.58}$$

We calculate the quantities

$$\begin{array}{lll} X^2 = -\mathbf{b}^2\,|+\rangle\langle -| & , & \mathbf{b}^2 = b^i\delta_{ij}b^j \\ Y^2 = -\mathbf{c}^2\,|-\rangle\langle +| & , & \mathbf{c}^2 = c_i\delta^{ij}c_j \end{array} \tag{3.59}$$

and

$$\begin{array}{l} e^X = 1 + X + X^2/2 \\ e^Y = 1 + Y + Y^2/2 \end{array} \tag{3.60}$$

as well as

$$z^\mu = z\varrho_+ + \Pi + z^{-1}\varrho_- \tag{3.61}$$

and then replace to the L-operator

$$\mathcal{L}^{\mu_1}_{\mathbf{2N+1}} = \left(1 + X + \frac{1}{2}X^2\right) z^{\mu_1} \left(1 + Y + \frac{1}{2}Y^2\right) \tag{3.62}$$

The expansion of this quantity can be simplified with help of the relations

$$\begin{array}{llll} X\varrho_+ & = 0 & , & \varrho_+ Y & = 0 \\ X^2\varrho_+ & = 0 & , & \varrho_+ Y^2 & = 0 \\ X^2\Pi & = 0 & , & \Pi Y^2 & = 0 \end{array} \tag{3.63}$$

which lead to

$$\begin{array}{rcl} \mathcal{L}^{\mu_1}_{\mathbf{2N+1}} & = & z\varrho_+ + \Pi + z^{-1}\varrho_- + X\left(\Pi + z^{-1}\varrho_-\right) + \left(\Pi + z^{-1}\varrho_-\right)Y \\ & & + X\left(\Pi + z^{-1}\varrho_-\right)Y + \frac{1}{2}z^{-1}X^2\varrho_- + \frac{1}{2}z^{-1}\varrho_-Y^2 \\ & & + \frac{1}{2}z^{-1}X^2\varrho_-Y + \frac{1}{2}z^{-1}X\varrho_-Y^2 + \frac{1}{4}z^{-1}X^2\varrho_-Y^2 \end{array} \tag{3.64}$$

After calculation, the minuscule L-matrix of the so_{2N} spin chain in the fundamental representation reads as

$$\mathcal{L}^{\mu_1}_{\mathbf{2N+1}} = \begin{pmatrix} z + \mathbf{bc} + \frac{1}{4}z^{-1}\mathbf{b}^2\mathbf{c}^2 & b^i + \frac{1}{2}z^{-1}b^i\mathbf{bc} & -\frac{1}{2}z^{-1}\mathbf{b}^2 \\ c_i + \frac{1}{2}z^{-1}c_i\mathbf{cb} & (1 + z^{-1}\mathbf{bc})\,I_{2N-1} & -z^{-1}b^i \\ -\frac{1}{2}z^{-1}\mathbf{c}^2 & -z^{-1}c_i & z^{-1} \end{pmatrix} \tag{3.65}$$

where $\mathbf{bc} = b^ic_i$ and $\mathbf{b}^2\mathbf{c}^2$ are scalars, and b^i and c_i are vectors. It agrees with the matrix calculated in the spin chain litterature using anti-dominant shifted Yangians based realisations [59].

3.2.2 Topological Quiver of B- type

Following the quiver diagrams construction introduced in the previous chapter, we translate the internal data carried by the L-operator (3.65) into the topological quiver $\mathrm{Q}^{\mu_1}_{\mathbf{2N+1}}$. This quiver describes the behaviour of internal states in the fundamental representation of so_{2N+1}, under the action of the minuscule vector coweight $\mu_1 = e_1$. The matrix (3.65) contains nine sub-blocks in result of the three subspaces of $\mathbf{2N+1}$. The three diagonal blocks are in one to one with three nodes of $\mathrm{Q}^{\mu_1}_{\mathbf{2N+1}}$, each one carrying the dimension and the charge of the corresponding irrepresentation

$$\mathcal{N}_{\mathbf{1}_+} \simeq \varrho_+ \mathcal{L}^{\mu_1}_{\mathbf{2N+1}} \varrho_+ \quad , \quad \mathcal{N}_{\mathbf{2N-1}_0} \simeq \Pi \mathcal{L}^{\mu_1}_{\mathbf{2N+1}} \Pi \quad , \quad \mathcal{N}_{\mathbf{1}_-} \simeq \varrho_- \mathcal{L}^{\mu_1}_{\mathbf{2N+1}} \varrho_- \tag{3.66}$$

These nodes are linked by six directed links that are given by the off-diagonal blocks, we have

$$\begin{array}{lll} L_{\mathbf{1}_+ \to \mathbf{2N-1}_0} \simeq \varrho_+ \mathcal{L}^{\mu_1}_{\mathbf{2N+1}} \Pi & , & L_{\mathbf{2N-1}_0 \to \mathbf{1}_+} \simeq \Pi \mathcal{L}^{\mu_1}_{\mathbf{2N+1}} \varrho_+ \\ L_{\mathbf{1}_+ \to \mathbf{1}_-} \simeq \varrho_+ \mathcal{L}^{\mu_1}_{\mathbf{2N+1}} \varrho_- & , & L_{\mathbf{1}_- \to \mathbf{1}_+} \simeq \varrho_- \mathcal{L}^{\mu_1}_{\mathbf{2N+1}} \varrho_+ \\ L_{\mathbf{1}_- \to \mathbf{2N-1}_0} \simeq \varrho_- \mathcal{L}^{\mu_1}_{\mathbf{2N+1}} \Pi & , & L_{\mathbf{2N-1}_0 \to \mathbf{1}_-} \simeq \Pi \mathcal{L}^{\mu_1}_{\mathbf{2N+1}} \varrho_- \end{array} \tag{3.67}$$

The resulting diagram is depicted below where we can see that the oscillators content of every link allows the circulation of $SO(2)$ chagres between the states spaces.

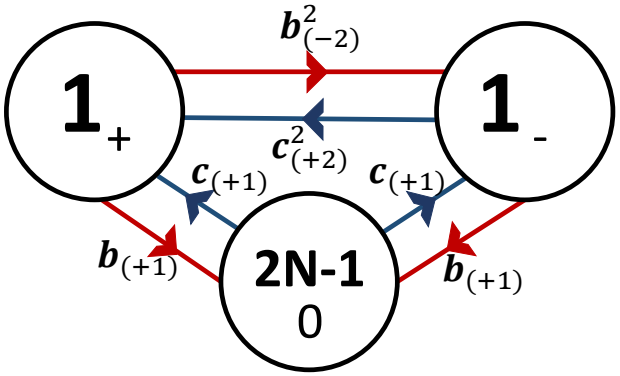

Figure 3.14: The topological quiver $\mathrm{Q}^{\mu_1}_{\mathbf{2N}}$ representing $\mathcal{L}^{\mu_1}_{\mathbf{2N}}$ of so_{2N}.

3.3 C type spin chains

This chapter aims to study the spin chains of C-type characterized by sp_{2N} internal symmetry, by employing the Integrability/ Gauge correspondence. We are interested here in the four-dimensional Chern-Simons theory with symplectic gauge symmetry, embedded with Wilson and 't Hooft lines. The crossing of these line defects serves as a bridge towards the oscillator realization of minuscule Lax operators solving the RLL relations of integrability. This quantity is to be compared with the L-matrix computed in the spin chain literature. We end by building the associated quiver diagram representation labeled as Q_{C_N}.

3.3.1 minuscule L-matrix of C-type

To begin, we recall the diagrammatic description of the C_N Lie algebra of $N(2N+1)$ dimensions. It is given in Figure 3.15, where we have N nodes in one to one with the N simple roots

$$\alpha_i = e_i - e_{i+1}; 1 \leq i \leq N-1 \quad , \quad \alpha_N = 2e_N \tag{3.68}$$

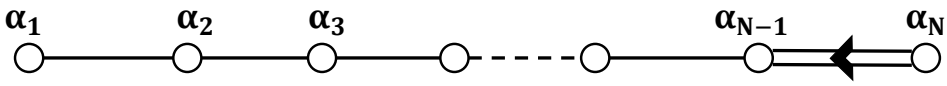

Figure 3.15: The Dynkin diagram associated to the C_N Lie algebra.

The last node associated to the simple root $\alpha_N = 2e_N$ is in fact associated to the only minuscule coweight of the symplectic $Sp(2N)$ group. This coweight correponds to the cospinor representation and is obtained using the condition $\mu_N.\alpha_i = \delta_{Ni}$ with simple roots α_i for $1 \leq i \leq N-1$. We write in terms of the vector space basis

$$\mu_N = \frac{1}{2}(e_1 + ... + e_N) \tag{3.69}$$

The cutting of this minuscule spinor-like node from the Dynkin diagram of Figure 3.15 is visualised in Figure 3.16.
It leads to a Levi ddecomposition of the form

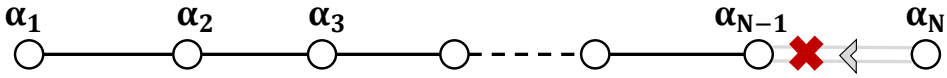

Figure 3.16: If we cut the minuscule (last) node from the Dynkin diagram for the C_N Lie algebra, we obtain the Dynkin diagram corresponding to sl_N in addition to the node A_1.

$$\begin{array}{rcc} sp_{2N} & = & so_2 \oplus sl_N \oplus n_+ \oplus n_- \\ l_\mu & = & so_2 \oplus sl_N \\ \dim n_\pm & = & \frac{N(N+1)}{2} \end{array} \tag{3.70}$$

where the Levi subalgebra contains the linear sl_N as can be noticed from the Dynkin diagram splitting, and verified by the dimensions sum

$$\begin{array}{rcccc} \dim & : & N(2N+1) & = & 1 + (N^2-1) + 2\left(\frac{N(N+1)}{2}\right) \\ rank & : & N & = & 1 + (N-1) \end{array} \tag{3.71}$$

Eventually, the fundamental vector representation of sp_{2N} also decomposes into irrepresentations of sl_N

$$\mathbf{2N} = \mathbf{N}_{+1/2} \oplus \mathbf{N}_{-1/2} \tag{3.72a}$$

In fact, $\mathbf{N}_{+1/2}$ and $\mathbf{N}_{-1/2}$ are the fundamental and anti-fundamental of sl_N carrying opposite charges $\pm 1/2$ with respect to the $SO(2)$ of the cutted minuscule node. This decomposition will lead to the calculation of the L-operator $\mathcal{L}^{\mu_N}_{\mathbf{2N}}$ associated to the last node of the Dynkin diagram, in the fundamental representation $\mathbf{2N}$. This matrix will be represented in a basis of the form

$$\left\{ |i\rangle, |\bar{i}\rangle ; i = 1, ..., N; \bar{i} = \bar{N}, ..., \bar{1} \right\} \tag{3.73}$$

with the property $\bar{\imath} = 2N + 1 - i$. This choice allows us to simply write the following quantities

$$\begin{array}{lll} \mu = \frac{1}{2}\Pi - \frac{1}{2}\bar{\Pi} & , & z^{\mu} = z^{\frac{1}{2}}\Pi + z^{-\frac{1}{2}}\bar{\Pi} \\ \Pi = \Pi_{\mathbf{N}_{+1/2}} = \sum_{i=1}^{N} |i\rangle \langle i| & , & \bar{\Pi} = \Pi_{\mathbf{N}_{-1/2}} = \sum_{\bar{\imath}=\bar{1}}^{\bar{N}} |\bar{\imath}\rangle \langle \bar{\imath}| \end{array} \tag{3.74}$$

Concerning the matrices X and Y, notice that each of the nilpotents $n_{\pm}$ of dimension $\frac{1}{2}N(N+1)$ which is nothing but the symmetric representation of sl_N. Its generators are realized by $N \times N$ matrices such that

$$\begin{array}{lll} X = b^{\{i\bar{j}\}} X_{\{i\bar{j}\}} & , & X_{\{i\bar{j}\}} = |i\rangle \langle \bar{j}| + |j\rangle \langle \bar{\imath}| \\ Y = c_{\{\bar{\imath}j\}} Y^{\{\bar{\imath}j\}} & , & Y^{\{\bar{\imath}j\}} = |\bar{\imath}\rangle \langle j| + |\bar{j}\rangle \langle i| \end{array} \tag{3.75}$$

The Levi constraints are verified appropriately such that the $N(N+1)$ oscillators verify

$$\left\{ b^{\{i\bar{j}\}}, c_{\{\bar{k}l\}} \right\}_{PB} = \delta^{i}_{\bar{k}} \delta^{\bar{j}}_{l} \tag{3.76}$$

We directly use the following relations

$$\begin{array}{lll} X\Pi = 0 & , & \Pi Y = 0 \\ X\bar{\Pi} = X & , & \bar{\Pi} Y = Y \\ X^2 = 0 & , & e^X = I_{2N} + X \\ Y^2 = 0 & , & e^Y = I_{2N} + Y \end{array} \tag{3.77}$$

to give the matrix form of the L-operator in question in the basis (3.73) as

$$\mathcal{L}^{\mu_N}_{\mathbf{2N}} = \begin{pmatrix} z^{\frac{1}{2}} I_N + z^{-\frac{1}{2}} XY & z^{-\frac{1}{2}} X \\ z^{-\frac{1}{2}} Y & z^{-\frac{1}{2}} I_N \end{pmatrix} \tag{3.78}$$

where the involved $N \times N$ matrices read explicitly like

$$X = \begin{pmatrix} b^{1\bar{1}} & \cdots & b^{1\bar{N}} \\ \vdots & \ddots & \vdots \\ b^{N\bar{1}} & \cdots & b^{N\bar{N}} \end{pmatrix}, \qquad Y = \begin{pmatrix} c_{\bar{1}1} & \cdots & c_{\bar{1}N} \\ \vdots & \ddots & \vdots \\ c_{\bar{N}1} & \cdots & c_{\bar{N}N} \end{pmatrix} \tag{3.79}$$

and

$$XY = \begin{pmatrix} b^{1\bar{\imath}} c_{\bar{\imath}1} & \cdots & b^{1\bar{\imath}} c_{\bar{\imath}N} \\ \vdots & \ddots & \vdots \\ b^{N\bar{\imath}} c_{\bar{\imath}1} & \cdots & b^{N\bar{\imath}} c_{\bar{\imath}N} \end{pmatrix} \tag{3.80}$$

with the symmetry property $b^{i\bar{j}} = b^{j\bar{\imath}}$, and similarly $c_{\bar{\imath}j} = c_{\bar{j}i}$. This solution is equivalent, up to multiplication by z, to the Lax-matrix of C-type obtained by using anti-dominant shifted Yangians in [59].

3.3.2 Topological Quiver of C-type

In a similar fashion to the exmples of topological gauge quivers build before to describe minuscule L-operators in the four-dimensional Chern-Simons gauge theory, we can now exploit the matrix (3.78) to build the $\mathrm{Q}^{\mu_N}_{\mathbf{2N}}$. Notice that this quiver concerns the states of the fundamental representation $2N$ of the symmetry C_N, and the minuscule coweight μ_N of spinor nature. This quiver will have two nodes

$$\mathcal{N}_{\mathbf{N}_{+1/2}} \simeq \Pi \mathcal{L}^{\mu_N}_{\mathbf{2N}} \Pi \qquad , \qquad \mathcal{N}_{\mathbf{N}_{-1/2}} \simeq \bar{\Pi} \mathcal{L}^{\mu_N}_{\mathbf{2N}} \bar{\Pi} \tag{3.81}$$

and two links relating them as

$$L_{\mathbf{N}_{+1/2}\to} \simeq \Pi \mathcal{L}^{\mu_N}_{\mathbf{2N}} \bar{\Pi} \qquad , \qquad L_{\mathbf{N}_{-1/2}\to} \simeq \bar{\Pi} \mathcal{L}^{\mu_N}_{\mathbf{2N}} \Pi \tag{3.82}$$

Its content is depicted in Figure 3.17 given here below.

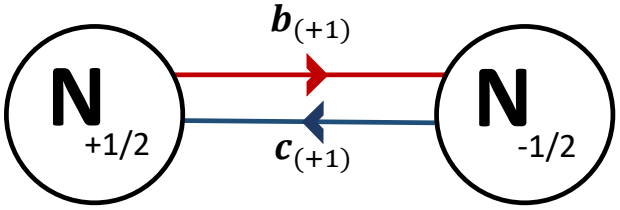

Figure 3.17: The topological quiver $\mathbb{Q}^{\mu_N}_{\mathbf{2N}}$ representing $\mathcal{L}^{\mu_N}_{\mathbf{2N}}$ of sp_{2N}.

3.4 D type spin chains

We turn our attention now to the orthogonal D-type spin chains family as the second most studied integrable spin chain in the literature along with the A-type, thanks to their simply laced symmetries. Oscillator L-operators for these orthogonal spin chains were constructed before for extremal nodes by generalizing the automorphism $A_3 \sim D_3$ to larger ranks. Following the work of [123], we will show how these results can be recovered more simply by taking advantage of the dual $SO(2N)$ 4D CS theory. We focus here on a Wilson line W in the fundamental **2N** representation, and evaluate its crossing with minuscule 't Hooft lines of the theory. Interestingly, the so_{2N} Lie algebra has three different minuscule coweights refered to as μ_1, μ_{N-1} and μ_N. These respectively correspond to the extremal nodes $1, N-1$ and N in the Dynkin diagram of Figure3.18. The set of simple roots for this symmetry is written as

$$\alpha_i = e_i - e_{i+1}; i \in [1, N-1] \qquad , \quad \alpha_N = e_{N-1} + e_N \tag{3.83}$$

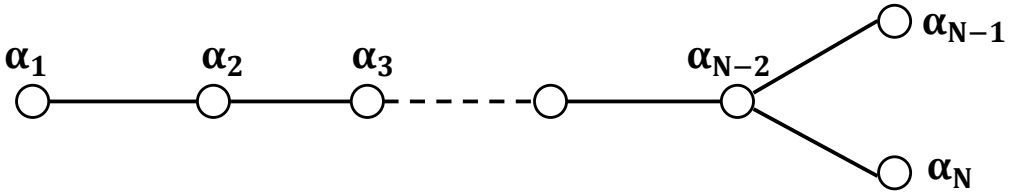

Figure 3.18: The Dynkin diagram associated to the D_N Lie algebras where the N simple roots α_i are exhibited.

We have three possible minuscule magnetic charges carried by three types of 't Hooft lines in the SO_{2N} 4D CS

$$\mathrm{tH}^{\mu_1}_{\gamma_0} \qquad , \qquad \mathrm{tH}^{\mu_{N-1}}_{\gamma_0} \qquad , \qquad \mathrm{tH}^{\mu_N}_{\gamma_0} \tag{3.84}$$

and hence, three families of minuscule Lax matrices that we will calculate here below using the general factorized formula of the L-operator.

$$\mathcal{L}^{\mu_1}_{\mathbf{2N}} \qquad , \qquad \mathcal{L}^{\mu_{N-1}}_{\mathbf{2N}} \qquad , \qquad \mathcal{L}^{\mu_N}_{\mathbf{2N}} \tag{3.85}$$

Notice that for the three cases we will be focusing on the fundamental representation $2N$ of the D_N symmetry.

3.4.1 L-operator for the vectorial node of so_{2N}

The first minuscule L-operator for the D_N spin chain will be referred to as the vectorial Lax operator. This is because it is associated to coweight μ_1, dual to the simple root α_1 which is related to the vectorial representation of the so_{2N} Lie algebra. We have

$$\mu_1 \alpha_i = \delta_{i1} \qquad \rightarrow \qquad \mu_1 = e_1 \tag{3.86}$$

We can deduce the action of this minuscule coweight on the elements of the so_{2N} Lie algebra directly from the Dynkin Diagram's node cutting depicted in Figure 3.19

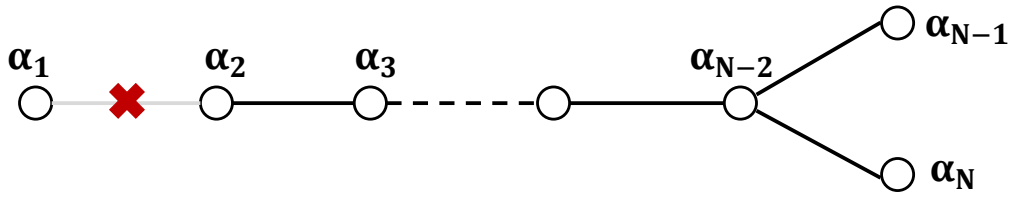

Figure 3.19: By cutting the vectorial like node α_1 from the Dynkin diagram associated of the D_N Lie algebra, we obtain two sub-Dynkin diagrams associated to D_{N-1} and A_1.

$$DD_{D_N} \to DD_{A_1} \oplus DD_{D_{N-1}} \tag{3.87}$$

with $A_1 \sim D_1$. On the Lie algebra level, this Levi decomposition reads us

$$so_{2N} \to so_2 \oplus so_{2N-2} \oplus n_+ \oplus n_- \tag{3.88}$$

where the Levi-subalgebra is $l_{\mu_1} = so_2 \oplus so_{2N-2}$ and the nilpotents are given by the fundamental and anti-fundamental representations of so_{2N-2}

$$n_\pm = (\mathbf{2N-2})_\pm \tag{3.89}$$

These resulting sub-algebras can be verified from the following explicit splitting of the root system of so_{2N} and its dimensions due to the Levi decomposition (3.88).

	so_{2N}	$so(2)$	so_{2N-2}	$n_+ \oplus n_-$
Rank	N	1	$N-2$	$-$
Roots	$\pm\alpha_{ij}; 1 \leq i \neq j \leq N$	$-$	$\pm\alpha_{ij}; 2 \leq i \neq j \leq n$	$\pm\alpha_{1i}; 2 \leq i \leq N$
Number of roots	$N(N-1)$	$-$	$(N-1)(N-2)$	$N-1$
Generators	$h_i; E_{\pm\alpha_{ij}}; 1 \leq i \neq j \leq N$	h_1	$h_i; E_{\pm\alpha_{ij}}; 2 \leq i \neq j \leq N$	$E_{\pm\alpha_{1i}}; 2 \leq i \leq N$
Dimension	N^2-1	1	$(N-1)^2-1$	$2(N-1)$

(3.90)

Recall that the Wilson line considered here in the orthogonal Chern-Simons theory carries states in the fundamental vectorial representation **2N** and the 't Hooft line is associated to the minuscule vectorial coweight. Hence, we need to determine the action of μ_1 on this representation.

$$\mathbf{2N} \to \mathbf{1}_+ \oplus (\mathbf{2N-2})_0 \oplus \mathbf{1}_- \tag{3.91}$$

This splitting is visualized in Figure 3.20. Hence, the crossing of these line defects in question

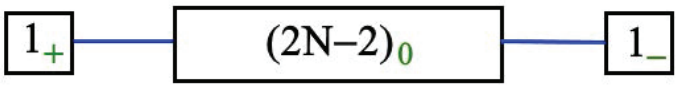

Figure 3.20: A graphic representation of the splitting of the vector 2N representation under the vectorial Levi decomposition. The projectors on these three blocks are $\varrho_+ = |+\rangle\langle+|$, $\sum \varrho_i = \sum |i\rangle\langle i|$ and $\varrho_- = |-\rangle\langle-|$.

can be understood as in Figure 3.21, where the internal behaviour of the gauge fields provides

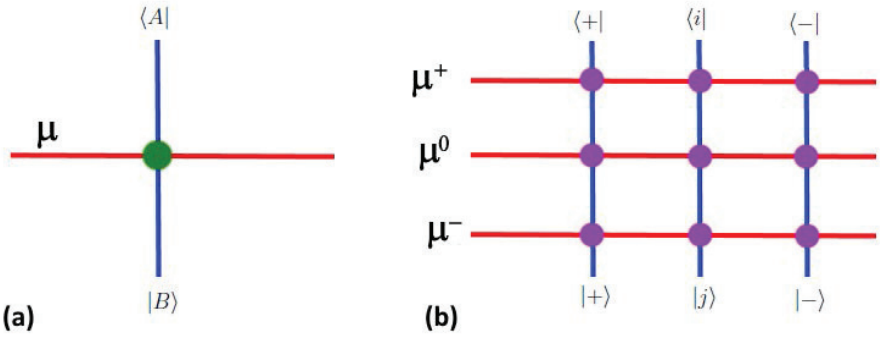

Figure 3.21: (**a**) A horizontal vector-like 't Hooft line with magnetic charge μ_1 crossing an electrically charged vertical Wilson line. The green dot refers to the coupling between the two lines; it is given by the Lax operator $\mathcal{L}^{\mu_1}_{\boldsymbol{R}}$. (**b**) Intrinsic structure of the Lax operator interpreted in terms of a topological gauge quiver with three nodes and 6 links.

a glimpse of the structure of the quiver diagram to be constructed later. . One can also notice at this point that this minuscule coweight acts in a very similar fashion to the minuscule coweight of the so_{2N+1} Lie algebra which is also of vector nature and also reads as $\mu_1 = e_1$. Their realizations are also analogous; in te present basis

$$|\mathbf{2N}\rangle = \left\{ \begin{array}{c} |+\rangle \\ |i\rangle_{1\leq i\leq 2N-2} \\ |-\rangle \end{array} \right\}, \tag{3.92}$$

with projectors

$$\varrho_+ = |+\rangle\langle+|\,, \qquad \Pi = \sum_i |i\rangle\langle i|\,, \qquad \varrho_- = |-\rangle\langle-|\,, \tag{3.93}$$

we write

$$\mu_1 = \varrho_+ + q\Pi - \varrho_- \tag{3.94}$$

Here, $q = 0$ is the charge of the states $|i\rangle_{1\leq i\leq 2N-2}$ with respect to the $SO\,(2)$ of the cutted node. The other operators appearing in the L-operator formula are conveniently realized as

$$z^{\mu_1} = z + \Pi_0 + z^{-1}\varrho_- \tag{3.95}$$

and

$$X = b^i X_i \in n_+ \quad , \quad Y = c_i Y^i \in n_- \tag{3.96}$$

with generators

$$X_i = |+\rangle\langle i| - |i\rangle\langle-| \quad , \quad Y^i = |i\rangle\langle+| - |-\rangle\langle i| \tag{3.97}$$

The exponential expansions are written as

$$e^X = e^X = I + X + \tfrac{1}{2}X^2 \quad , \quad e^Y = 1 + Y + \tfrac{1}{2}Y^2 \tag{3.98}$$

where

$$\begin{array}{lll} X^2 = -\mathbf{b}^2\,|+\rangle\langle-| & , & Y^2 = -\mathbf{c}^2\,|+\rangle\langle-| \\ \mathbf{b}^2 = b^i\delta_{ij}b^j & , & \mathbf{c}^2 = c_i\delta^{ij}c_j \end{array} \tag{3.99}$$

By substituting in (2.37), the resulting L-matrix $\mathcal{L}^{\mu_1}_{\mathbf{2N}}$ corresponding to the first node reads in terms of the $4N-4$ oscillators (b^i, c_i) of the phase space as

$$\mathcal{L}^{\mu_1}_{\mathbf{2N}} = z^{-1}\begin{pmatrix} z^2 + zb^ic_i + \frac{1}{4}\mathbf{b}^2\mathbf{c}^2 & zb^i + \frac{1}{2}\mathbf{b}^2c_i & -\frac{1}{2}\mathbf{b}^2 \\ zc_i + \frac{1}{2}b^i\mathbf{c}^2 & (z + b^ic_i)\,I_{2N-2} & -b^i \\ -\frac{1}{2}\mathbf{c}^2 & -c_i & 1 \end{pmatrix} \tag{3.100}$$

As expected, the structure of this matrix is to be compared with the minuscule L-operator of the type B_N spin chain; the only difference concerns the size of the middle block. This resemblance can be directly justified from the Dynkin diagrams features because the Dynkin Diagram of the B_N Lie algebra can actually be obtained from the Dynkin diagram of D_{N+1} by folding the two spinorial-like nodes. Notice that the vectorial minuscule coweight stays intact in this process and its action is similar on elements of the two Lie algebras.

3.4.2 L-operator for the spinorial nodes of so_{2N}

Besides the vector minuscule node μ_1, the spinor and co-spinor nodes of the Dynkin diagram 3.18 are also associated to minuscule coweights μ_N and μ_{N-1} respectively. They serve as magnetic charges for the minuscule 't Hooft lines $\mathrm{tH}_{\gamma_0}^{\mu_N}$ and $\mathrm{tH}_{\gamma_0}^{\mu_{N-1}}$. In this section, we will focus on these line defects and study their coupling to the Wilson $W_{\xi_z}^{\mathbf{2N}}$ in the $SO\,(2N)$ 4D CS (Figure 3.22) in order to calculate the minuscule L-operators $\mathcal{L}_{\mathbf{2N}}^{\mu_{N-1}}$ and $\mathcal{L}_{\mathbf{2N}}^{\mu_N}$. In these regards,

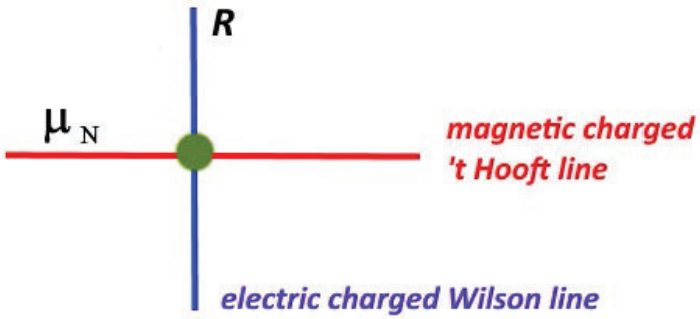

Figure 3.22: A horizontal 't Hooft line of D- type with spinor-like magnetic charge given by the minuscule coweight μ_N of SO_{2N} couples to a vertical Wilson line characterized by a representation $\boldsymbol{R}$ of so_{2N}.

remark that the Dynkin diagram 3.18 of the D_N Lie algebra has a Z_2 symmetry allowing to exchange the two spinorial like nodes α_{N-1} and α_N. The cutting any of these two nodes leads to the same Levi decomposition as depicted in Figure 3.23.

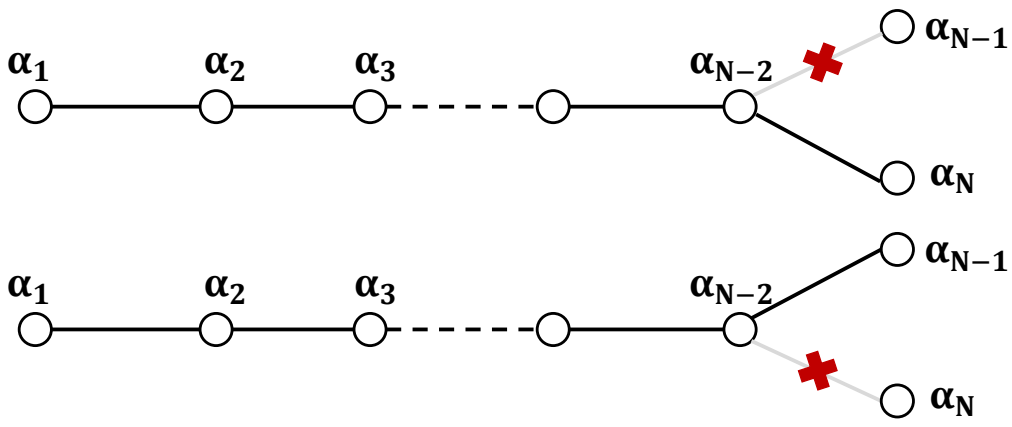

Figure 3.23: By cutting a spinorial like node α_{N-1} or α_N from the Dynkin diagram associated of the D_N Lie algebra, we obtain a Dynkin diagram associated to sl_N and the node A_1.

$$so_{2N} \to sl_1 \oplus sl_N \oplus n_{\pm} \tag{3.101}$$

The nilpotent subspaces are given by

$$n_{\pm} = \frac{N\left(N-1\right)}{2}_{\pm} \tag{3.102}$$

while the fundamental representation splits as

$$\boldsymbol{2N} \rightarrow \boldsymbol{N}_{+\frac{1}{2}} \oplus \boldsymbol{N}_{-\frac{1}{2}} \tag{3.103}$$

This indicates the equivalence of the two L-opertors

$$\mathcal{L}^{\mu_N}_{\mathbf{2N}} \qquad \simeq \qquad \mathcal{L}^{\mu_{N-1}}_{\mathbf{2N}} \tag{3.104}$$

In what follows, we will focus our attention on the computation of the spinor-like L-operator corresponding to the minuscule coweight μ_N. This coweight is dual to $\alpha_N = e_{N-1} + e_N$ and reads in terms of the weight vector basis e_i as

$$\mu_N = \frac{1}{2}\left(e_1 + ... + e_{N-1} + e_N\right) \tag{3.105}$$

Its action on the $2N$ representation is visualized in Figure 3.24.
For convenience, we work in the basis

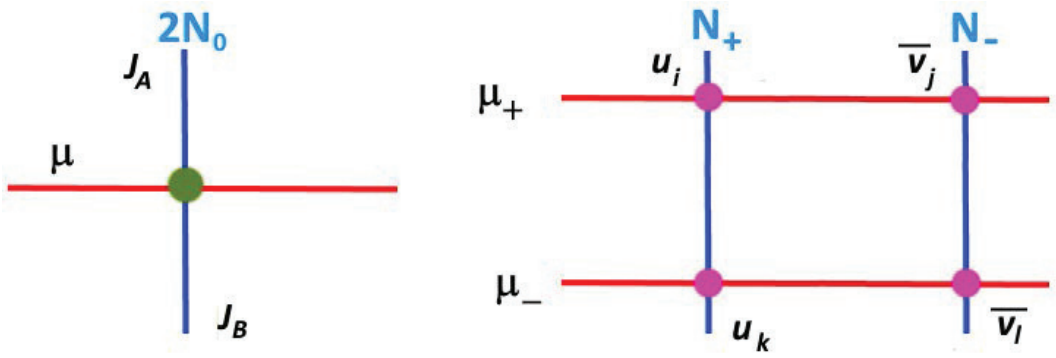

Figure 3.24: On the left, a horizontal spinorial like 't Hooft line crossing a vertical Wilson line carrying a current J_A the representation $2N$. On the right, The splitting of the current into two currents u_i and $\bar{v}^i$ traveling along the vertical lines.

$$\left\{\left|i\right\rangle, \left|\bar{\imath}\right\rangle \qquad ; \qquad 1 \leq i \leq N, \bar{\imath} = 2N+1-i\right\} \tag{3.106}$$

The adjoint action of the coweight (3.105) is written in terms of the projectors

$$\mu_N = \frac{1}{2}\sum_i \left|i\right\rangle\left\langle i\right| - \frac{1}{2}\sum_{\bar{\imath}} \left|\bar{\imath}\right\rangle\left\langle \bar{\imath}\right| \tag{3.107}$$

and the generators of the nilpotents $n_{\pm} = \boldsymbol{N}_{\pm\frac{1}{2}} \wedge \boldsymbol{N}_{\pm\frac{1}{2}}$ are given by the anti-symmetric $2N \times 2N$ matrices

$$\begin{array}{rcl} X_{i\bar{j}} & = & \left|i\right\rangle\left\langle \bar{j}\right| - \left|j\right\rangle\left\langle \bar{j}\right| \\ Y^{\bar{i}j} & = & \left|\bar{\imath}\right\rangle\left\langle j\right| - \left|\bar{j}\right\rangle\left\langle i\right| \end{array} \tag{3.108}$$

The Levi constraints are verified as follows

$$\left[\mu_N, X\right] = X \qquad , \qquad \left[\mu_N, Y\right] = -Y \tag{3.109}$$

where

$$X = b^{i\bar{j}} X_{i\bar{j}} \qquad Y = c_{i\bar{j}} Y^{\bar{i}j} \tag{3.110}$$

involving $N(N-1)$ oscillators of the phase space of the 't Hooft line, or equivalently the auxiliary space of the spin chain. The L-operator is directly calculated by substituting in (4.49). Notice that we have $X^2 = Y^2 = 0$ leading to

$$\mathcal{L}^{\mu_N}_{\mathbf{2N}} = \mathcal{L}^{\mu_{N-1}}_{\mathbf{2N}} = \begin{pmatrix} z^{\frac{1}{2}} + z^{-\frac{1}{2}} BC & z^{-\frac{1}{2}} B \\ z^{-\frac{1}{2}} C & z^{-\frac{1}{2}} \end{pmatrix} \tag{3.111}$$

The matrices B and C are anti-symmetric

$$X = \begin{pmatrix} b^{1\bar{1}} & \cdots & b^{1\bar{N}} \\ \vdots & \ddots & \vdots \\ b^{N\bar{1}} & \cdots & b^{N\bar{N}} \end{pmatrix}, \qquad Y = \begin{pmatrix} c_{\bar{1}1} & \cdots & c_{\bar{1}N} \\ \vdots & \ddots & \vdots \\ c_{\bar{N}1} & \cdots & c_{\bar{N}N} \end{pmatrix} \tag{3.112}$$

This matrix is similar to the minuscule spinorial like L-matrix (3.78) of the C-type spin chain, the latter also has four sub-blocks of dimension $N \times N$.

3.4.3 Topological gauge quivers of D-type

As expected from the resemblance of the structure of the vectorial Lax matrix of the D_N spin chain with the vectorial Lax matrix of B_N type, as well as between the spinorial Lax matrix of D_N type with the spinorial of the C_N spin chain, we will show that their associated quiver diagrams are also much alike and exhibit similar intrinsic behaviour. We begin by constructing the topological quiver $\mathrm{Q}^{\mu_1}_{\mathbf{2N}}$ associated to vector-like $\mathcal{L}^{\mu_1}_{\mathbf{2N}}$ (3.100) of the so_{2N} spin chain. This diagram illustrates the singular action of the magnetic charge μ_1 on quantum states in the representation **2N**, see (3.25).

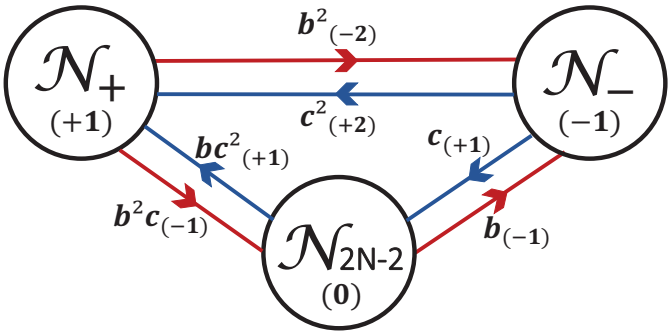

Figure 3.25: The topological quiver representing $\mathcal{L}^{vect}_{so_{2N}}$. It has three nodes and 6 links. The nodes describe self-dual topological matter and the links describe topological bi-matter.

It is formed by three nodes and six links in analogy to the quiver of B-type. The nodes are in one to one with irreducible presentations $\mathbf{1}_+$, $\mathbf{2N} - \mathbf{2}_0$ and $\mathbf{1}_-$.

$$\mathcal{N}_{\mathbf{1}_+} \simeq \varrho_+ \mathcal{L}^{\mu_1}_{\mathbf{2N+1}} \varrho_+ \qquad , \qquad \mathcal{N}_{\mathbf{2N-2}_0} \simeq \Pi \mathcal{L}^{\mu_1}_{\mathbf{2N+1}} \Pi \qquad , \qquad \mathcal{N}_{\mathbf{1}_-} \simeq \varrho_- \mathcal{L}^{\mu_1}_{\mathbf{2N+1}} \varrho_- \tag{3.113}$$

They are interpreted as adjoint matter, while bi-fundamental matter is given by the six links

$$\begin{array}{lcl} L_{\mathbf{1}_+ \to \mathbf{2N-2}_0} \simeq \varrho_+ \mathcal{L}^{\mu_1}_{\mathbf{2N}} \Pi & , & L_{\mathbf{2N-2}_0 \to \mathbf{1}_+} \simeq \Pi \mathcal{L}^{\mu_1}_{\mathbf{2N}} \varrho_+ \\ L_{\mathbf{1}_+ \to \mathbf{1}_-} \simeq \varrho_+ \mathcal{L}^{\mu_1}_{\mathbf{2N}} \varrho_- & , & L_{\mathbf{1}_- \to \mathbf{1}_+} \simeq \varrho_- \mathcal{L}^{\mu_1}_{\mathbf{2N}} \varrho_+ \\ L_{\mathbf{1}_- \to \mathbf{2N-2}_0} \simeq \varrho_- \mathcal{L}^{\mu_1}_{\mathbf{2N}} \Pi & , & L_{\mathbf{2N-2}_0 \to \mathbf{1}_-} \simeq \Pi \mathcal{L}^{\mu_1}_{\mathbf{2N}} \varrho_- \end{array} \tag{3.114}$$

We move now to the spinor minuscule Lax operator $\mathcal{L}^{\mu_N}_{\mathbf{2N}}$, that we translate into the topological gauge quiver $\mathrm{Q}^{\mu_N}_{\mathbf{2N}} =$ which is equivalent to $\mathrm{Q}^{\mu_N}_{\mathbf{2N}}$ because of (3.104). Following from the matrix (3.111), or equivalently from the Lie algebra decomposition 3.103, we obtain the diagrammatic representation of Figure 3.26 given here below. This quiver unveils the similarity with the

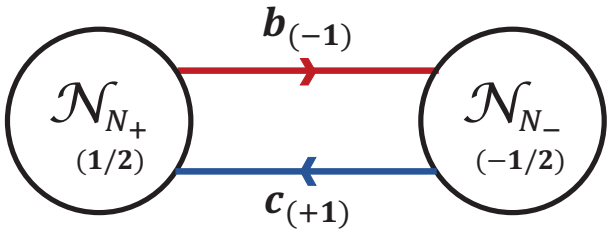

Figure 3.26: The topological quiver $\mathrm{Q}^{\mu_N}_{\boldsymbol{R}_v}$ representing the operator $\mathcal{L}^{\mu_N}_{\boldsymbol{R}_v}$. It has 2 nodes $\mathcal{N}_1$, $\mathcal{N}_2$; and 2 links L_{12}, L_{21}. The nodes describe self-dual topological matter and the links describe topological bi-matter.

diagram of Figure 3.17 regarding the C_N type spin chain. It also has two nodes with the same dimensions and charges

$$\mathcal{N}_{\mathbf{N}_{+1/2}} \simeq \Pi\mathcal{L}^{\mu_N}_{\mathbf{2N}}\Pi \quad , \quad \mathcal{N}_{\mathbf{N}_{-1/2}} \simeq \bar{\Pi}\mathcal{L}^{\mu_N}_{\mathbf{2N}}\bar{\Pi} \tag{3.115}$$

and therefore two links relating them as

$$L_{\mathbf{N}_{+1/2}\to} \simeq \Pi\mathcal{L}^{\mu_N}_{\mathbf{2N}}\bar{\Pi} \quad , \quad L_{\mathbf{N}_{-1/2}\to} \simeq \bar{\Pi}\mathcal{L}^{\mu_N}_{\mathbf{2N}}\Pi \tag{3.116}$$

3.5 E6 type

After the study of the spin chains systems with ABCD symmetries and the characterization of their RLL solutions, we move now to the investigation of the integrable spin chains with exceptional symmetries. These lattice systems are insufficiently studied in the spin chain literature due to the complexity of their algebraic structure. With the purpose of constructing explicit solutions for these systems, we rely on the power of the correspondence with the 4D Chern-Simons. In particular, we exploit gauge symmetries that admit minuscule coweights, i.e. the E_6 and E_7 families. The E_8 and G_2 symmetries don't have minuscule representations, and corresponding Lax matrices can't be generated in the present study using the formula (4.49). In this section, we put our attention on the e6 symmetry which is characterized by two minuscule coweights μ_1 and μ_5 that can be treated equivalently thanks to Z_2 symmetry. We will construct the corresponding Lax operators, as well as the topological gauge quiver.

3.5.1 Minuscule L-operators of E_6 type

The finite dimensional exceptional Lie algebra $\boldsymbol{e}_6$ is of rank 6 and 78 dimensions. Its Dynkin diagram is depicted in Figure 3.27
with simple roots reading as

$$\begin{array}{rcccl} \mathrm{E}_6 & : & \alpha_1 & = & \frac{1}{2}\left(\epsilon_1-\epsilon_2-\epsilon_3-\epsilon_4-\epsilon_5-\epsilon_6-\epsilon_7+\epsilon_8\right) \\ & & \alpha_i & = & \epsilon_i-\epsilon_{i-1} \quad , \quad i=1,2,3,4,5 \\ & & \alpha_6 & = & \epsilon_1+\epsilon_2 \end{array} \tag{3.117}$$

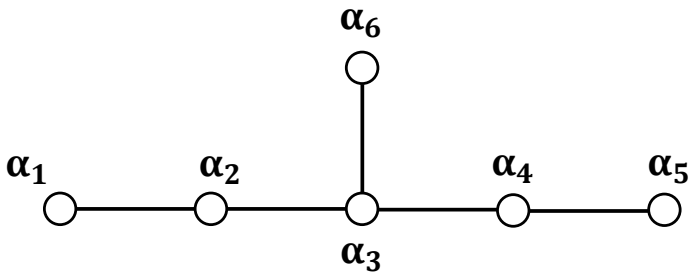

Figure 3.27: The Dynkin Diagram of e_6 Lie algebra having six nodes labeled by the simple roots α_i.

Their intersections are described by the Cartan matrix

$$K_{e_6} = \begin{pmatrix} 2 & -1 & 0 & 0 & 0 & 0 \\ -1 & 2 & -1 & 0 & 0 & 0 \\ 0 & -1 & 2 & -1 & 0 & -1 \\ 0 & 0 & -1 & 2 & -1 & 0 \\ 0 & 0 & 0 & -1 & 2 & 0 \\ 0 & 0 & -1 & 0 & 0 & 2 \end{pmatrix} \tag{3.118}$$

The other 72 roots of the root system Φ_{e_6} is divided to 36 positive root $\alpha \in \Phi^+_{e_6}$, and 36 negative $-\alpha \in \Phi^-_{e_6}$. They are all realized in the Euclidean $\mathbb{R}^8$ with basis generators $\{\epsilon_i\}_{1\leq i\leq 8}$. Explicitly, we have

root	realisation	labels	number
β^+_{ij}	$+\epsilon_i + \epsilon_j$	$1 \leq j < i \leq 5$	20
β^-_{ij}	$-\epsilon_i - \epsilon_j$	$2 \leq j < i \leq 5$	20
$\gamma^+_{q_i}$	$+\frac{1}{2}(q_i\epsilon_i - \epsilon_6 - \epsilon_7 + \epsilon_8)$	$\Pi^5_{i=1} q_i = 1$	16
$\gamma^-_{q_i}$	$-\frac{1}{2}(q_i\epsilon_i - \epsilon_6 - \epsilon_7 + \epsilon_8)$	$\Pi^5_{i=1} q_i = 1$	16

(3.119)

where $q_i \pm 1$ with the condition $\Pi q_i = 1$. The fundamental coweights dual to the six simple roots (3.117) read like

fund- ω_i	in terms of roots	height	Repres
ω_1	$\frac{4}{3}\alpha_1 + \frac{5}{3}\alpha_2 + 2\alpha_3 + \frac{4}{3}\alpha_4 + \frac{2}{3}\alpha_5 + \alpha_6$	8	27_+
ω_2	$\frac{5}{3}\alpha_1 + \frac{10}{3}\alpha_2 + 4\alpha_3 + \frac{8}{3}\alpha_4 + \frac{4}{3}\alpha_5 + 2\alpha_6$	15	351_+
ω_3	$2\alpha_1 + 4\alpha_2 + 6\alpha_3 + 4\alpha_4 + 2\alpha_5 + 3\alpha_6$	21	2925_0
ω_4	$\frac{4}{3}\alpha_1 + \frac{8}{3}\alpha_2 + 4\alpha_3 + \frac{10}{3}\alpha_4 + \frac{5}{3}\alpha_5 + 2\alpha_6$	15	351_-
ω_5	$\frac{2}{3}\alpha_1 + \frac{4}{3}\alpha_2 + 2\alpha_3 + \frac{5}{3}\alpha_4 + \frac{4}{3}\alpha_5 + \alpha_6$	8	27_-
ω_6	$\alpha_1 + 2\alpha_2 + 3\alpha_3 + 2\alpha_4 + \alpha_5 + 2\alpha_6$	11	78_0

(3.120)

In what concerns us here, the two minuscule coweights μ_1 and μ_5 allow us to define two families of minuscule 't Hooft lines in the framework of the 4D Chern-Simons theory with gauge symmetry given by the E_6 gauge group, they are labeled as

$$\mathrm{tH}^{\mu_1} \qquad , \qquad \mathrm{tH}^{\mu_5} \tag{3.121}$$

These minuscule nodes correspond to the fundamental **27** and anti-fundamental $\bar{\mathbf{27}}$ minuscule representations, and are exchangeable by the Z_2 $\mathbb{Z}_2^{aut}$ outer- automorphism symmetry acting like $\alpha_i \to \alpha_{6-i}$ with $i = 1, ..., 5$. In permutation symmetry language, the $\mathbb{Z}_2^{aut}$ is generated by the double transposition $(15)(24)$, i.e:

$$\mathbb{Z}_2^{aut} = \{I_{id}, (15)(24)\} \tag{3.122}$$

We will focus in what follows on the construction of the minuscule L-operator corresponding to μ_1, and show that the other minuscule L-operator can be easily deduced. In fact, the Levi decomposition of the e_6 Lie algebra with respect to these minuscule coweights is the same, as presented in Figure 3.28.

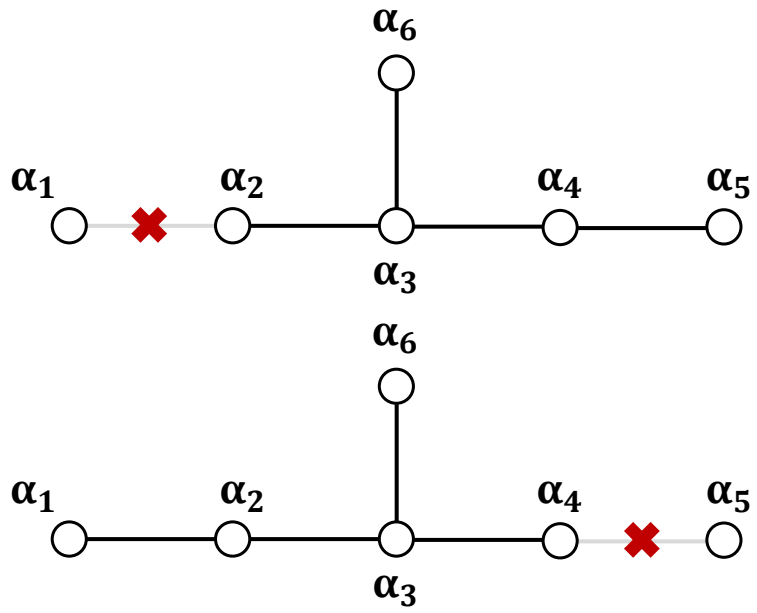

Figure 3.28: If we cut the node α_1 or α_5 from the Dynkin diagram of the e_6 Lie algebra, we obtain in both cases sub-Dynkin diagrams corresponding to the D_5 and A_1 algebras.

The cutting of the α_1 or α_5 node yields the splitting

$$DD_{E_6} \to DD_{D_1} \oplus DD_{D_5} \tag{3.123}$$

revealing the orthogonal so_{10} as a subalgebra of the exceptional e_6

$$\begin{array}{rcl} e_6 & \to & so_2 \oplus so_{10} \oplus n_{\pm} \\ l_{\mu_1} & = & so(2) \oplus so(10) \end{array} \tag{3.124}$$

with the nilpotents given by the spinor representations of so_{10}, i.e.

$$n_{\pm} = \mathbf{16}_{\pm} \tag{3.125}$$

We can justify this interesting decomposition by tracking each root in Φ_{e_6}. As remarked from (3.117), the simple root α_1 is the only one of exceptional nature, its cutting leaves us with the usual simple roots of a D-type Dynkin diagram. Regarding the rest of the root system, it is divided by the Levi decomposition into 40 roots that don't depend on α_1

$$\frac{\delta \beta_{so_{10}}}{\delta \alpha_1} = 0 \tag{3.126}$$

and correspond to the subalgebra so_{10}; and 32 one belonging to $n_{\pm}$ and verifying

$$\frac{\delta \beta_{so_{10}}}{\delta \alpha_1} \neq 0 \tag{3.127}$$

These are respectively given by

$$\begin{array}{lll} \pm\left(\epsilon_i \pm \epsilon_j\right) & 1 \leq j < i \leq 5 & 40 \\ \pm\frac{1}{2}\left(q_i\epsilon_i - \epsilon_6 - \epsilon_7 + \epsilon_8\right) & q_i = \pm 1; \Pi_{i=1}^{5} q_i = 1 & 32 \end{array} \tag{3.128}$$

Now regarding the fundamental representation **27** which is characterizes the Wilson line taken here, its branching yields three irrepresentations: the singlet of so_2, the vector **10** and the spinor **16** of so_{10} as illustrated in Figure 3.29.

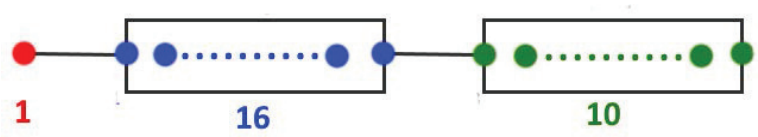

Figure 3.29: A graphical illustration of the Levi decomposition of the representation 27 of e_6 in terms of representations of so_{10}.

Their charges verify the trace condition as

$$\mathbf{27} = \mathbf{1}_{-\frac{4}{3}} \oplus \mathbf{10}_{+\frac{2}{3}} \oplus \mathbf{16}_{-\frac{1}{3}} \tag{3.129}$$

We can deduce that the L-operator $\mathcal{L}_{\mathbf{27}}^{\mu_1}(z)$ will be a 27×27 matrix with three sub-blocks in one to one with the representations (4.160). The states of the fundamental **27** are actually as represented in the weight diagram of Figure 3.30.

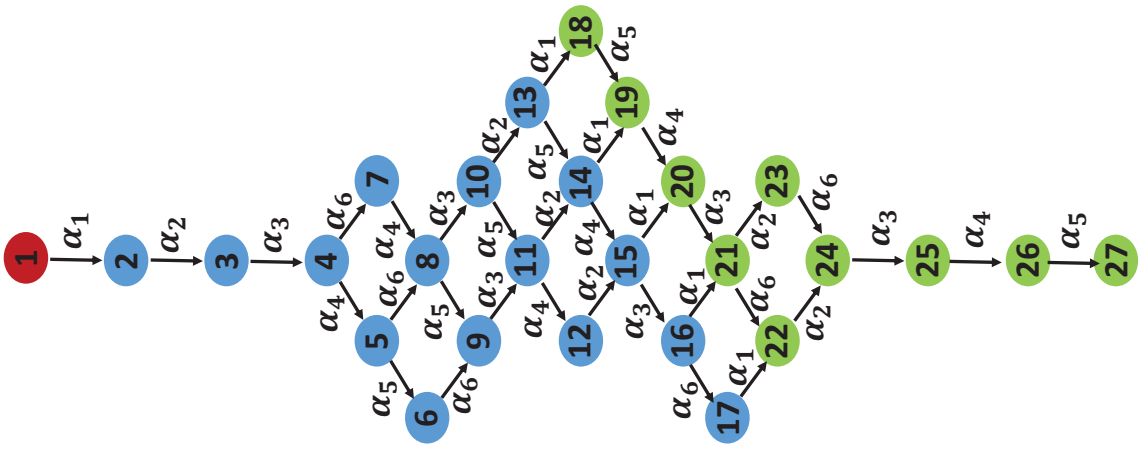

Figure 3.30: The weight diagram of the representation 27 of the exceptional Lie algebra e_6 where every state $|\xi_A\rangle$ is simply represented by the node carrying its number. The states 1+16+10 of the SO_{10} sub-representations of e_6 are represented by different colors.

We label these states as $|\xi_A\rangle$ such that

$$\begin{array}{lll} |\mathbf{1}\rangle & |\xi_1\rangle_{-4/3} & = |\omega_1\rangle \\ \downarrow & & \\ |i\rangle_{2\leq i\leq 17} & |\xi_\alpha\rangle_{+1/3} & \\ \downarrow & & \\ |\beta\rangle_{18\leq\beta\leq 27} & |\xi_i\rangle_{-2/3} & \end{array} \tag{3.130}$$

This basis verifies the orthogonality $\langle 0|i\rangle = \langle 0|\beta\rangle = \langle i|\beta\rangle = 0$, in addition to the closure $\varrho_{\mathbf{1}} + \varrho_{\mathbf{10}} + \varrho_{\mathbf{16}} = I_{\mathbf{27}}$ where

$$\varrho_{\mathbf{1}} = |1\rangle\langle 1|\,, \qquad \varrho_{\mathbf{10}} = \sum_{l=2}^{11} |i\rangle\langle i|\,, \qquad \varrho_{\mathbf{16}} = \sum_{\beta=12}^{27} |\beta\rangle\langle\beta| \tag{3.131}$$

From (4.160), we write the adjoint action of μ_1 as

$$\mu_1 = -\frac{4}{3}\varrho_{\underline{\mathbf{1}}} + \frac{2}{3}\varrho_{\underline{\mathbf{10}}} - \frac{1}{3}\varrho_{\underline{\mathbf{16}}} \tag{3.132}$$

The generators of the nilpotents $n_\pm$ can be read from the weight diagram 3.30 such that they link the three subspaces by help of tensors Gamma allowing to transit between the vector and spinor labels of the orthogonal subalgebra. In fact, since we have $\dim n_+ = \dim n_- = 16$, one can deduce that the expansions of $X \in n_+$ and $Y \in n_-$ depend on the label β

$$X = \sum_{\beta=1}^{16} b^\beta X_\beta, \qquad Y = \sum_{\beta=1}^{16} c_\beta Y^\beta \tag{3.133}$$

The expression 3.133 involves 16 couples of oscillator degrees of freedom $\{b^\gamma, c_\beta\} = \delta^\gamma_\beta$, and the generators

$$X_\beta = \left(\Gamma^i\right)_{\beta\gamma} |i\rangle\langle\gamma| + |\beta\rangle\langle 1|\,, \quad Y^\beta = |1\rangle\langle\beta| + (\Gamma_i)^{\beta\gamma} |\gamma\rangle\langle i| \tag{3.134}$$

The 10 Gammas Γ are 16×16 matrices characterizing the orthogonal so_{10} algebraic structure, they satisfy the Clifford algebra

$$\Gamma_i\Gamma_j + \Gamma_j\Gamma_i = 2\delta_{ij} \tag{3.135}$$

The Levi constraints are verified

$$\begin{array}{rcl} [\mu, X_\beta] & = & (-\frac{1}{3} + \frac{4}{3})\,|\beta\rangle\langle 1| + (\frac{2}{3} + \frac{1}{3})\left(\Gamma^i\right)_{\beta\gamma} |i\rangle\langle\gamma| = X_\beta \\ \left[\mu, Y^\beta\right] & = & -Y^\beta \end{array} \tag{3.136}$$

and we have

$$\begin{array}{lcl} X^2 = V^i\,|i\rangle\langle 1| & , & Y^2 = W_i\,|1\rangle\langle i| \\ V^i = b^\alpha\left(\Gamma^i\right)_{\alpha\beta} b^\beta & , & W_i = c_\alpha\left(\Gamma_i\right)^{\alpha\beta} c_\beta \\ X^3 = 0 & , & Y^3 = 0 \end{array} \tag{3.137}$$

We moreover define the tensors

$$B^i_\beta = b^\gamma \Gamma^i_{\gamma\beta} \qquad , \qquad C^\alpha_i = c_\gamma \Gamma_i^{\gamma\alpha} \tag{3.138}$$

in order to simplify the expressions

$$\begin{array}{llll} e^X & = I + X + \frac{1}{2}X^2 & = I + B^i_\gamma\,|i\rangle\langle\gamma| + b^\beta\,|\beta\rangle\langle 1| + \frac{1}{2}V^i\,|i\rangle\langle 1| \\ e^Y & = I + Y + \frac{1}{2}Y^2 & = I + c_\beta\,|1\rangle\langle\beta| + C^\gamma_i\,|\gamma\rangle\langle i| + \frac{1}{2}W_i\,|1\rangle\langle i| \end{array} \tag{3.139}$$

The three factors appearing in the L-operator formula $\mathcal{L}^{\mu_1}_{\mathbf{27}}(z) = e^X z^{\mu_1} e^Y$ are represented in the basis (3.130) as

$$e^X = \begin{pmatrix} 1 & 0 & 0 \\ V^i & \delta^i_j & B^i_\beta \\ b^\alpha & 0 & \delta^\alpha_\beta \end{pmatrix}, \qquad z^\mu = \begin{pmatrix} z^{-\frac{4}{3}} & 0 & 0 \\ 0 & z^{\frac{2}{3}}\delta^i_j & 0 \\ 0 & 0 & z^{-\frac{1}{3}}\delta^\alpha_\beta \end{pmatrix}, \qquad e^Y = \begin{pmatrix} 1 & W_j & c_\beta \\ 0 & \delta^i_j & 0 \\ 0 & C^\alpha_j & \delta^\alpha_\beta \end{pmatrix} \tag{3.140}$$

Thus leading to the Lax matrix

$$\mathcal{L}^{\mu_1}_{\mathbf{27}} = \begin{pmatrix} z^{-\frac{4}{3}} & z^{-\frac{4}{3}}W_j & z^{-\frac{4}{3}}c_\beta \\ z^{-\frac{4}{3}}V^i & z^{\frac{2}{3}}\delta^i_j + z^{-\frac{4}{3}}V^iW_j + z^{-\frac{1}{3}}B^i_\alpha C^\alpha_j & z^{-\frac{4}{3}}V^ic_\beta + z^{-\frac{1}{3}}B^i_\beta \\ z^{-\frac{4}{3}}b^\alpha & z^{-\frac{4}{3}}b^\alpha W_j + z^{-\frac{1}{3}}C^\alpha_j & z^{-\frac{1}{3}}\delta^\alpha_\beta + z^{-\frac{4}{3}}b^\alpha c_\beta \end{pmatrix} \tag{3.141}$$

Concerning the minuscule L-operator $\mathcal{L}^{\mu_5}_{\mathbf{27}}$ corresponding to the magnetic coweight μ_5, it can be deduced by taking advantage of the result (3.141). As mentioned before, these two coweights are linked in the DD_{E_6} to the fundamental $\mathbf{27}_+$ and anti-fundamental $\mathbf{27}_-$ minuscule representations, and are exchanged by a $\mathbb{Z}_2$ symmetry. On the level of the Lie algebra, their associated Levi decompositions read the same 3.124, but their actions on the fundamental representation are opposed since we have $\mu_5 = -\mu_1$. From 3.132, one can directly write

$$\mu_5 = \frac{4}{3}\varrho_{\mathbf{1}} - \frac{2}{3}\varrho_{\mathbf{10}} + \frac{1}{3}\varrho_{\mathbf{16}} \tag{3.142}$$

For the nilpotents elements, we use the notations $\bar{X} \in n_+$ and $\bar{Y} \in n_-$ to avoid confusion. These matrices are realized as by a simple sign change of (3.134) to verify

$$\left[\mu_5, \bar{X}_\beta\right] = \bar{X}_\beta \qquad ; \qquad \left[\mu_5, \bar{Y}^\beta\right] = -\bar{Y}^\beta \tag{3.143}$$

We obtain

$$\begin{aligned} \bar{X} &= \sum_{\beta=1}^{16} b^\beta \bar{X}_\beta, \qquad \bar{Y} = \sum_{\beta=1}^{16} c_\beta \bar{Y}^\beta \\ \bar{X}_\beta &= |1\rangle\langle\beta| + (\Gamma_i)^{\beta\gamma}|\gamma\rangle\langle i|, \quad \bar{Y}^\beta = \left(\Gamma^i\right)_{\beta\gamma}|i\rangle\langle\gamma| + |\beta\rangle\langle 1| \end{aligned} \tag{3.144}$$

The L-operator reads in this case as

$$\mathcal{L}^{\mu_5}_{\mathbf{27}} = \begin{pmatrix} z^{\frac{4}{3}} & z^{-\frac{4}{3}}W_j & z^{\frac{4}{3}}c_\beta \\ z^{\frac{4}{3}}V^i & z^{-\frac{2}{3}}\delta^i_j + z^{\frac{4}{3}}V^iW_j + z^{\frac{1}{3}}B^i_\alpha C^\alpha_j & z^{\frac{4}{3}}V^ic_\beta + z^{\frac{1}{3}}B^i_\beta \\ z^{\frac{4}{3}}b^\alpha & z^{\frac{4}{3}}b^\alpha W_j + z^{\frac{1}{3}}C^\alpha_j & z^{-\frac{1}{3}}\delta^\alpha_\beta + z^{\frac{4}{3}}b^\alpha c_\beta \end{pmatrix} \tag{3.145}$$

3.5.2 Topological quiver of E6 type

Now, we build the topological gauge quivers associated to the L-matrices (3.141) and (3.145). We begin by thinking of these matrices in the projector basis as

$$\mathcal{L}^{\mu_{1,5}}_{\mathbf{27}} = \begin{pmatrix} \varrho_{\mathbf{1}}\mathcal{L}^{\mu_{1,5}}_{\mathbf{27}}\varrho_{\mathbf{1}} & \varrho_{\mathbf{1}}\mathcal{L}^{\mu_{1,5}}_{\mathbf{27}}\varrho_{\mathbf{10}} & \varrho_{\mathbf{1}}\mathcal{L}^{\mu_{1,5}}_{\mathbf{27}}\varrho_{\mathbf{16}} \\ \varrho_{\mathbf{10}}\mathcal{L}^{\mu_{1,5}}_{\mathbf{27}}\varrho_{\mathbf{1}} & \varrho_{\mathbf{10}}\mathcal{L}^{\mu_{1,5}}_{\mathbf{27}}\varrho_{\mathbf{10}} & \varrho_{\mathbf{10}}\mathcal{L}^{\mu_{1,5}}_{\mathbf{27}}\varrho_{\mathbf{16}} \\ \varrho_{\mathbf{16}}\mathcal{L}^{\mu_{1,5}}_{\mathbf{27}}\varrho_{\mathbf{1}} & \varrho_{\mathbf{16}}\mathcal{L}^{\mu_{1,5}}_{\mathbf{27}}\varrho_{\mathbf{10}} & \varrho_{\mathbf{16}}\mathcal{L}^{\mu_{1,5}}_{\mathbf{27}}\varrho_{\mathbf{16}} \end{pmatrix} \tag{3.146}$$

We can associate to their sub-blocks elements of topological quiver diagrams representing the behaviour of internal gauge field bundles in the subspaces $\mathbf{1}, \mathbf{10}$ and $\mathbf{16}$. These quivers are denoted as $\mathrm{Q}^{\mu_{1,5}}_{\mathbf{27}}$, and are formed by three nodes describing self-dual topological matter of $SO(2) \times SO(10)$

$$\mathcal{N}_{\mathbf{1}_{\mp 4/3}} \sim \varrho_{\mathbf{1}}\mathcal{L}^{\mu_{1,5}}_{\mathbf{27}}\varrho_{\mathbf{1}} \qquad , \qquad \mathcal{N}_{\mathbf{10}_{\pm 2/3}} \sim \varrho_{\mathbf{10}}\mathcal{L}^{\mu_{1,5}}_{\mathbf{27}}\varrho_{\mathbf{10}} \qquad , \qquad \mathcal{N}_{\mathbf{16}_{\mp 1/3}} \sim \varrho_{\mathbf{16}}\mathcal{L}^{\mu_{1,5}}_{\mathbf{27}}\varrho_{\mathbf{16}} \tag{3.147}$$

The connection between these three nodes is guaranteed by six oriented links giving by the off-diagonal blocks and carrying bi-fundamental matter in terms of the oscillators b,c.

link	Repres	bi-matter	link	Repres	bi-matter
$L_{1\to 2}$	$\mathbf{16}_{-\frac{1}{3}} \times \mathbf{10}_{-\frac{2}{3}}$	$\mathbf{b}$, $\mathbf{b}^2c$	$L_{2\to 1}$	$\mathbf{10}_{\frac{2}{3}} \times \mathbf{16}_{\frac{1}{3}}$	$\mathbf{c}$, $\mathbf{bc}^2$
$L_{2\to 3}$	$\mathbf{1}_{-\frac{4}{3}} \times \mathbf{16}_{+\frac{1}{3}}$	$\mathbf{b}$	$L_{2\to 1}$	$\mathbf{16}_{-\frac{1}{3}} \times \mathbf{1}_{\frac{4}{3}}$	$\mathbf{c}$
$L_{1\to 3}$	$\mathbf{1}_{-\frac{4}{3}} \times \mathbf{10}_{-\frac{2}{3}}$	$\mathbf{b}^2$	$L_{3\to 1}$	$\mathbf{10}_{\frac{2}{3}} \times \mathbf{1}_{+\frac{4}{3}}$	$\mathbf{c}^2$

(3.148)

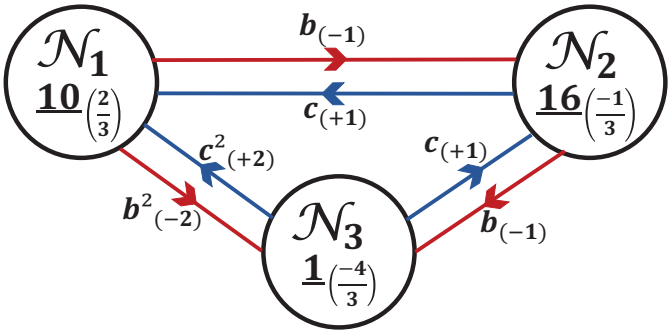

Figure 3.31: $\mathcal{L}^{\mu}_{\mathbf{27}}$ as a topological quiver with 3 nodes and 6 links. The nodes are given by the self-dual $R_i \otimes \bar{R}_i$ and the links by bi-matter $R_i \otimes \bar{R}_j$. In addition to SO_{10} representations, the Darboux coordinates b^α, c_α carry SO_2 charges given by $q = \pm 1$. The fundamental vector-like matter V^i and W_i carry -2 and $+2$.

We begin by drawing the quiver $\mathrm{Q}^{\mu_1}_{\mathbf{27}}$ in the Figure 3.31.
Regarding the $\mathrm{Q}^{\mu_5}_{\mathbf{27}}$ drawn in Figure 3.32, it has similar nodes with opposite charges to $\mathrm{Q}^{\mu_1}_{\mathbf{27}}$; to preserve the charges circulation, the links should be oriented oppositely to the first quiver.

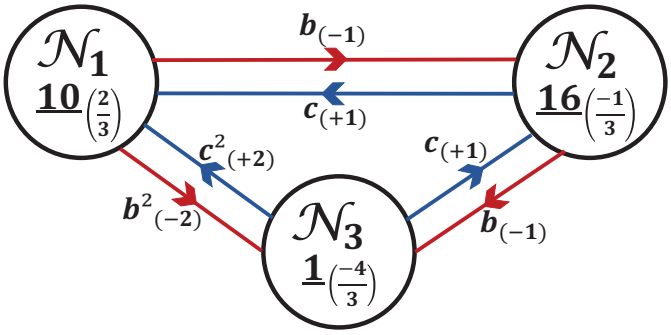

Figure 3.32: $\mathcal{L}^{\mu}_{\mathbf{27}}$ as a topological quiver with 3 nodes and 6 links. The nodes are given by the self-dual $R_i \otimes \bar{R}_i$ and the links by bi-matter $R_i \otimes \bar{R}_j$. In addition to SO_{10} representations, the Darboux coordinates b^α, c_α carry SO_2 charges given by $q = \pm 1$. The fundamental vector-like matter V^i and W_i carry -2 and $+2$.

3.6 E7 type

To conclude the list of minuscule L-operators concerning bosonic spin chains, we treat now the integrable spin chain with exceptional e_7 Lie algebra. We take advantage of its only minuscule coweight μ_1 to explicitly build an RLL solution missing in the spin chain literature, in the framework of the 4D Chern-Simons theory. This concerns the minuscule L-operator $\mathcal{L}^{\mu_1}_{\mathbf{56}}$ realized in the fundamental representation **56** and corresponding to the minuscule magnetic charge μ_1. We will see that this particular L-matrix reveals interesting internal structure involving 54 oscillators of the phase space, that we translate into the topological quiver $\mathrm{Q}^{\mu_1}_{\mathbf{56}}$.

3.6.1 L-operator of E7 type

We begin by recalling some general aspects of the rich structure of the the exceptional e_7 symmetry. As a Lie algebra of rank 7, its Dynkin diagram drawn in Figure 3.33 contains 7

simple roots reading in terms of the $\mathbb{R}^8$ basis vectors as

$$\begin{aligned} \alpha_1 &= \frac{1}{2}(\epsilon_1 - \epsilon_2 - \epsilon_3 - \epsilon_4 - \epsilon_5 - \epsilon_6 - \epsilon_7 + \epsilon_8) \\ \alpha_i &= \epsilon_i - \epsilon_{i-1} \qquad 2 \leq i \leq 6 \end{aligned} \tag{3.149}$$

These are in one to one with 7 Cartan generators H_i with $1 \leq i \leq 7$. The remaining 126

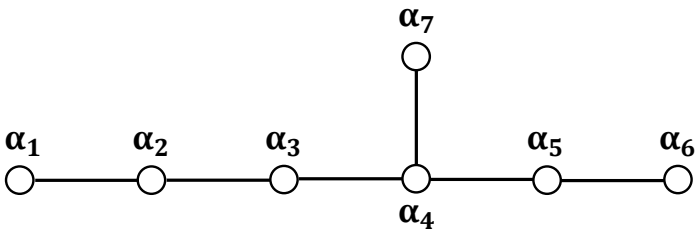

Figure 3.33: The Dynkin Diagram of E_7 having seven nodes labeled by the simple roots α_i. The cross ($\times$) indicates the roots used in the Levi decomposition with Levi subgroup $SO(2) \times E_6$.

from the total 133 dimensions are divided into two subsets consisting of 63 positive and 63 negative step roots. The latter are realized as combinations of simple roots 3.149 and define step operators $E\alpha$.
This e_7 Lie algebra admits only one minuscule coweight μ_1 corresponding to the fundamental representation **56** and verifying $\mu_1.\alpha_i = \delta_{i1}$ with $1 \leq i \leq 7$. The Levi decomposition with respect to this coweight reads as

$$\boldsymbol{e}_7 \to so(2) \oplus e_6 \oplus n_{\pm} \tag{3.150}$$

It can be deduced from the DD_{E_7} by omitting the node α_1 as depicted in Figure 3.34.

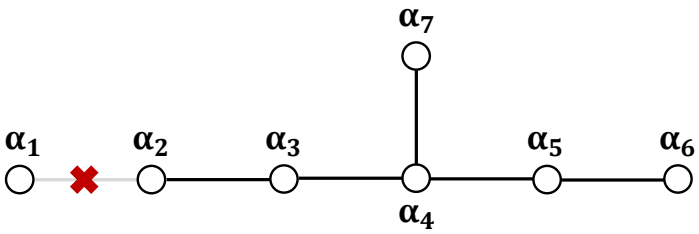

Figure 3.34: If we cut the node α_1 from the Dynkin Diagram of the e_7 Lie algebra, we obtain two sub-Dynkin diagrams corresponding to the algebra e_6 and the node so_2.

The Levi subalgebra is given by

$$l_{\mu_6} = so(2) \oplus e_6 \tag{3.151}$$

where the exceptional e_6 is generated by the simple roots $\alpha_2, \alpha_3, \alpha_4, \alpha_5, \alpha_6$ and α_7. The nilpotents corresponding to the root sub-system $\Phi_{\boldsymbol{e}_7} \backslash \Phi_{\boldsymbol{e}_6}$) are given by the fundamental and anti-fundamental representations of the e_6, i.e.

$$n_{\pm} = \mathbf{27}_{\pm} \tag{3.152}$$

The simplest electric-magnetic crossing to be considered in the E_7 Chern Simons theory involves a minuscule 't Hooft with magnetic charge μ_1 and a Wilson line carrying the fundamental

representation **56**. This representation splits following the Levi decomposition 3.151 as

$$\begin{array}{rcl} \mathbf{56} \rightarrow \mathbf{28}_{+} \oplus \mathbf{28}_{-} & & \\ \mathbf{28}_{\pm 1} & = & \mathbf{1}_{\pm 3/2} \oplus \mathbf{27}_{\pm 1/2} \end{array} \tag{3.153}$$

generating two singlets $\mathbf{1}_{\pm 3/2}$ corresponding to so_2 and the $\mathbf{27}_{\pm 1/2}$ of e_6. We can therefore assimilate to **56** the basis

$$\left\{ \begin{array}{c} |1_+\rangle \\ |\beta_+\rangle_{2_+ \leq \beta_+ \leq 28_+} \\ |\beta_-\rangle_{28_- \leq \beta_+ \leq 2_-} \\ |1_-\rangle \end{array} \right\} \tag{3.154}$$

The states $\left\{|l_+\rangle_{1_+ \leq l_+ \leq 28_+}\right\}$ belong to $\mathbf{28}_+$ and $\left\{|l_-\rangle_{28_- \leq l_- \leq 1_-}\right\}$ to $\mathbf{28}_-$ with $l_- = 56 + 1 - l$ which manifests the self-duality and pseudo-reality properties of **56**. This states splitting is visualized in Figure 3.35 In this basis, the adjoint action of μ_6 reads in terms of projectors as

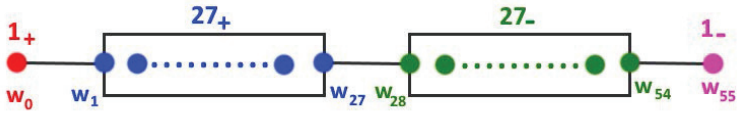

Figure 3.35: The decomposition of the **56** representation of E_7 in terms of representations of E_6. We have $\mathbf{56} = \mathbf{28}_{+q} \oplus \mathbf{28}_{-q}$ with $\mathbf{28}_{\pm q}$ reducible like $\mathbf{1}_{\pm 3/2} \oplus \mathbf{27}_{\pm 1/2}$.

$$\mu = \frac{3}{2}\varrho_{\mathbf{1}_+} + \frac{1}{2}\varrho_{\mathbf{27}_+} - \frac{1}{2}\varrho_{\mathbf{27}_-} - \frac{3}{2}\varrho_{\mathbf{1}_-} \tag{3.155}$$

where

$$\begin{array}{lcl} \varrho_{\mathbf{1}_+} = |1_+\rangle\langle 1_+| & , & \varrho_{\mathbf{1}_-} = |1_-\rangle\langle 1_-| \\ \varrho_{\mathbf{27}_+} = \sum\limits_{l_+=2_+}^{28_+} |\beta_+\rangle\langle\beta_+| & , & \varrho_{\mathbf{27}_-} = \sum\limits_{l_+=28_-}^{2_-} |\beta_-\rangle\langle\beta_-| \end{array} \tag{3.156}$$

Now concerning the realization of the nilpotents, it can be built following a similar rationale to the e_6 case. Here, we have 27 couples of oscillators that should be labeled by the β

$$X = b^\beta X_\beta \in \mathbf{27}_+ \quad , \quad Y = c_\beta Y^\beta \in \mathbf{27}_- \tag{3.157}$$

Moreover, the four subspaces that should be connected by the generators of X_β and Y^β, which demands the introduction of tensor matrices transporting from the space $\mathbf{27}_+$ to $\mathbf{27}_-$ such that

$$\begin{array}{rcl} X_\beta & = & |1_+\rangle\langle\beta_+| + |\delta_+\rangle\Gamma_\beta^{\delta_+\gamma_-}\langle\gamma_-| + |\beta_-\rangle\langle 1_-| \\ Y^\beta & = & |1_-\rangle\langle\beta_-| + |\gamma_-\rangle\Gamma^\beta_{\gamma_-\delta_+}\langle\delta_+| + |\beta_+\rangle\langle 1_+| \end{array} \tag{3.158}$$

These realizations can be checked by verification of the Levi commutation conditions. The tensors $\Gamma_\beta^{\delta_+\gamma_-}$ and $\Gamma^\beta_{\gamma_-\delta_+}$ are coupling tensors of three 27 representations of E_6. They are respectively given by

$$\langle\omega^{\delta_+}|X_\beta|\omega^{\gamma_-}\rangle \tag{3.159}$$

and

$$\langle\omega_{\gamma_-}|Y^\beta|\omega_{\delta_+}\rangle \tag{3.160}$$

They also verify

$$\Gamma_\beta^{\delta_+\gamma_-}\Gamma^\beta_{\gamma_-\eta_+} = \frac{4}{3}\delta_\beta^{\delta_+}\delta^\beta_{\eta_+} \tag{3.161}$$

Computing the powers of the X and Y indicates a particular structure for the Lax operator $\mathcal{L}^{\mu_6}_{\mathbf{56}}$ because of the nilpotency of $n_\pm$ of order 4, i.e. $X^4 = Y^4 = 0$. We have

$$\begin{array}{rcl} X^2 & = & 2S^{\beta_-}\left|\omega_{0_+}\right\rangle\left\langle\omega_{\beta_-}\right| + 2S^{\beta_+}\left|\omega_{\beta_+}\right\rangle\left\langle\omega_{0_-}\right| \\ Y^2 & = & 2R_{\alpha_+}\left|\omega_{0_-}\right\rangle\left\langle\omega^{\alpha_+}\right| + 2R_{\alpha_-}\left|\omega^{\alpha_-}\right\rangle\left\langle\omega_{0_+}\right| \end{array} \tag{3.162}$$

with

$$\begin{array}{rclcrcl} S^{\beta_-} & = & \frac{1}{2}b^\gamma\Gamma^{\beta_-}_{\gamma_+\delta}b^\delta & , & R_{\alpha_-} & = & \frac{1}{2}c_\gamma\Gamma^{\gamma\delta_+}_{\alpha_-}c_\delta \\ S^{\beta_+} & = & \frac{1}{2}b^\gamma\Gamma^{\beta_+}_{\gamma\delta_-}b^\delta & , & R_{\alpha_+} & = & \frac{1}{2}c_\gamma\Gamma^{\gamma_-\delta}_{\alpha_+}c_\delta \end{array} \tag{3.163}$$

and

$$\begin{array}{rclcrcl} X^3 & = & 6\mathcal{E}\left|\omega_{0_+}\right\rangle\left\langle\omega_{0_-}\right| & , & \mathcal{E} & = & \frac{1}{3}b_{\beta_+}S^{\beta_+} \\ Y^3 & = & 6\mathcal{F}\left|\omega_{0_-}\right\rangle\left\langle\omega_{0_+}\right| & , & \mathcal{F} & = & \frac{1}{3}R_{\alpha_-}c^{\alpha_-} \end{array} \tag{3.164}$$

By combining these relations, we can begin by representing the exponentials e^X and e^Y in the basis 3.154

$$e^X = \begin{pmatrix} 1 & b^{\beta_+} & S^{\beta_-} & \mathcal{E} \\ 0 & \delta^{\beta_+}_{\alpha_+} & T^{\beta_-}_{\alpha_+} & S_{\alpha_+} \\ 0 & 0 & \delta^{\beta_-}_{\alpha_-} & b_{\alpha_-} \\ 0 & 0 & 0 & 1 \end{pmatrix}, \qquad e^Y = \begin{pmatrix} 1 & 0 & 0 & 0 \\ z^{\frac{1}{2}}c_{\alpha_+} & \delta^{\beta_+}_{\alpha_+} & 0 & 0 \\ z^{-\frac{1}{2}}S_{\alpha_-} & z^{-\frac{1}{2}}J^{\beta_+}_{\alpha_-} & \delta^{\beta_-}_{\alpha_-} & 0 \\ z^{-\frac{3}{2}}\mathcal{F} & z^{-\frac{3}{2}}R^{\beta_+} & z^{-\frac{3}{2}}c^{\beta_-} & 1 \end{pmatrix} \tag{3.165}$$

with z^{μ_6} as

$$z^{\mu_6} = \begin{pmatrix} z^{\frac{3}{2}} & 0 & 0 & 0 \\ 0 & z^{\frac{1}{2}} & 0 & 0 \\ 0 & 0 & z^{-\frac{1}{2}} & 0 \\ 0 & 0 & 0 & z^{-\frac{3}{2}} \end{pmatrix} \tag{3.166}$$

The resulting L-operator is represented by a 56×56 matrix in the projector basis

$$\mathcal{L}^{\mu_6}_{\mathbf{56}} = \begin{pmatrix} L^{0_+}_{0_+} & L^{\beta_+}_{0_+} & L^{\beta_-}_{0_+} & z^{-\frac{3}{2}}\mathcal{E} \\ L^{0_+}_{\alpha_+} & L^{\beta_+}_{\alpha_+} & L^{\beta_-}_{\alpha_+} & z^{-\frac{3}{2}}S_{\alpha_+} \\ L^{0_+}_{\alpha_-} & L^{\beta_+}_{\alpha_-} & L^{\beta_-}_{\alpha_-} & z^{-\frac{3}{2}}b_{\alpha_-} \\ z^{-\frac{3}{2}}\mathcal{F} & z^{-\frac{3}{2}}R^{\beta_+} & z^{-\frac{3}{2}}c^{\beta_-} & z^{-\frac{3}{2}} \end{pmatrix} \tag{3.167}$$

Its characterized by a rich content as given below

$$\begin{array}{rcl} L^{0_+}_{0_+} & = & z^{\frac{3}{2}} + z^{\frac{1}{2}}b^{\beta_+}c_{\alpha_+} + z^{-\frac{1}{2}}S^{\alpha_-}S_{\alpha_-} + z^{-\frac{3}{2}}\mathcal{E}\mathcal{F} \\ L^{\beta_+}_{\alpha_+} & = & z^{\frac{1}{2}}\delta^{\beta_+}_{\alpha_+} + z^{-\frac{1}{2}}T^{\gamma_-}_{\alpha_+}J^{\beta_+}_{\gamma_-} + z^{-\frac{3}{2}}S_{\alpha_+}R^{\beta_+} \\ L^{\beta_-}_{\alpha_-} & = & z^{-\frac{1}{2}}\delta^{\beta_-}_{\alpha_-} + z^{-\frac{3}{2}}b_{\alpha_-}c^{\beta_-} \end{array} \tag{3.168}$$

$$\begin{array}{rclcrcl} L^{\beta_+}_{0_+} & = & z^{\frac{1}{2}}b^{\beta_+} + z^{-\frac{1}{2}}S^{\alpha_-}J^{\beta_+}_{\alpha_-} + z^{-\frac{3}{2}}\mathcal{E}R^{\beta_+} & , & L^{0_+}_{\alpha_-} & = & z^{-\frac{1}{2}}S_{\alpha_-} + z^{-\frac{3}{2}}b_{\alpha_-}\mathcal{F} \\ L^{\beta_-}_{0_+} & = & z^{-\frac{1}{2}}S^{\beta_-} + z^{-\frac{3}{2}}\mathcal{E}c^{\beta_-} & , & L^{\beta_-}_{\alpha_+} & = & z^{-\frac{1}{2}}T^{\beta_-}_{\alpha_+} + z^{-\frac{3}{2}}S_{\alpha_+}c^{\beta_-} \\ L^{0_+}_{\alpha_+} & = & z^{\frac{1}{2}}c_{\alpha_+} + z^{-\frac{1}{2}}T^{\gamma_-}_{\alpha_+}S_{\gamma_-} + z^{-\frac{3}{2}}S_{\alpha_+}\mathcal{F} & , & L^{\beta_+}_{\alpha_-} & = & z^{-\frac{1}{2}}J^{\beta_+}_{\alpha_-} + z^{-\frac{3}{2}}b_{\alpha_-}R^{\beta_+} \end{array} \tag{3.169}$$

3.6.2 Topological quiver of E_7 type

The minuscule L-matrix (3.167) concerning the e_7 spin chain system manifests a special and rich inner structure. It is divided by four sub-blocks corresponding to $\mathbf{1}_{+3/2}$, $\mathbf{27}_{+1/2}$, $\mathbf{27}_{-1/2}$ and $\mathbf{1}_{-3/2}$. Hence quiver diagram $\mathrm{Q}^{\mu_6}_{\mathbf{56}}$ has four nodes in one to one with the subspaces carrying charges $\pm 1/2$ and $\pm 3/2$.

$$\begin{array}{rclcrcl} \mathcal{N}_{\mathbf{1}_{+3/2}} & \simeq & \varrho_{\mathbf{1}_+}\mathcal{L}^{\mu_6}_{\mathbf{56}}\varrho_{\mathbf{1}_+} & , & \mathcal{N}_{\mathbf{27}_{+1/2}} & \simeq & \varrho_{\mathbf{27}_+}\mathcal{L}^{\mu_6}_{\mathbf{56}}\varrho_{\mathbf{27}_+} \\ \mathcal{N}_{\mathbf{1}_{-3/2}} & \simeq & \varrho_{\mathbf{1}_-}\mathcal{L}^{\mu_6}_{\mathbf{56}}\varrho_{\mathbf{1}_-} & , & \mathcal{N}_{\mathbf{27}_{-1/2}} & \simeq & \varrho_{\mathbf{27}_-}\mathcal{L}^{\mu_6}_{\mathbf{56}}\varrho_{\mathbf{27}_-} \end{array} \tag{3.170}$$

The other sub-blocks are translated into 12 links representing fundamental bi-matter carrying integer $SO(2)$ charges with value up to 3; these provide transition between the $\mathcal{N}_{\mathbf{1}_{+3/2}}$ and $\mathcal{N}_{\mathbf{1}_{-3/2}}$ for example. In general, the links are given by polynomials of the oscillators b^β and c_β extracted from the off-diagonal blocks of $\mathcal{L}^{\mu 6}_{\mathbf{56}}$. In particular, the upper triangle contains negatively charged links

Link	Bi-matter	Charge	link	bi-matter	Charge
$L_{\mathbf{1}_{+3/2}\to\mathbf{27}_{-1/2}}$	b^α	-1	$L_{\mathbf{27}_{+1/2}\to\mathbf{27}_{-1/2}}$	b^α	-1
$L_{\mathbf{1}_{+3/2}\to\mathbf{1}_{-3/2}}$	$\mathcal{B}^\alpha$	-2	$L_{\mathbf{27}_{+1/2}\to\mathbf{1}_{-3/2}}$	$\mathcal{B}^\alpha$	-2
$L_{\mathbf{1}_{+3/2}\to\mathbf{27}_{+1/2}}$	$\mathcal{B}_\alpha b^\alpha$	-3	$L_{\mathbf{27}_{-1/2}\to\mathbf{1}_{-3/2}}$	b_α	-1

(3.171)

while the lower blocks carry positive $SO(2)$ charges

Link	Bi-matter	Charge	link	bi-matter	Charge
$L_{\mathbf{27}_{-1/2}\to\mathbf{1}_{+3/2}}$	c_α	$+1$	$L_{\mathbf{27}_{-1/2}\to\mathbf{27}_{+1/2}}$	c^α	$+1$
$L_{\mathbf{1}_{-3/2}\to\mathbf{1}_{+3/2}}$	$\mathcal{C}_\alpha$	$+2$	$L_{\mathbf{1}_{-3/2}\to\mathbf{27}_{+1/2}}$	$\mathcal{C}^\alpha$	$+2$
$L_{\mathbf{27}_{+1/2}\to\mathbf{1}_{+3/2}}$	$c_\alpha\mathcal{C}^\alpha$	$+3$	$L_{\mathbf{1}_{-3/2}\to\mathbf{27}_{-1/2}}$	c_α	$+1$

(3.172)

This quiver diagram is drawn in Figure 3.36.

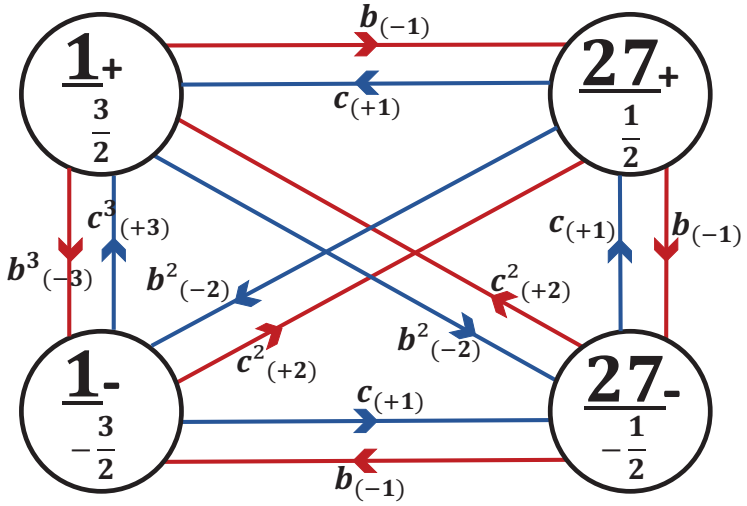

Figure 3.36: The topological quiver $\mathrm{Q}^{\mu}_{\mathbf{56}}$ representing $\mathcal{L}^{\mu}_{\mathbf{56}}$. It has 4 nodes and 12 links. The nodes describe self-dual topological matter. The links describe bi-matter in $\left(R_i, \bar{R}_j\right)$ of E_6 charged under $SO\,(2)$ with charges $\pm 1, \pm 2, \pm 3$.

CHAPTER 4

MINUSCULE SUPER LAX OPERATORS FOR ABCD SUPERSPIN CHAINS

In the last chapter, we investigated integrable spin chain systems of bosonic nature, i.e. with spins valued in a Lie algebra representation. We showed that the correspondence with a 4D Chern-Simons theory having the gauge symmetry G_{bos} allows to construct minuscule Lax operators solving the RLL equations of a spin chain system with internal symmetry g_{bos}. One may wonder if we can extend the power of this duality to obtain solutions for superspin chain systems. These are defined similarly to bosonic spin chains but with spins valued in representations of Lie superalgebras [212]; their study is of great interest in theoretical physics [213]-[218] because they allow to understand dynamics of complicated models of condensed matter physics [219]-[222], and make interesting appearances in different contexts such as six-dimensional supersymmetric gauge and string theories [223]-[226].

However, due to the complexity of their internal symmetry structure, the study and characterization of superspin chain systems is still challenging by relying on "traditional" techniques of the integrability literature such as the Algebraic Bethe Ansatz, and graded Yangian realizations of the Yang Baxter Equation. In the present study, we will take a shortcut by generalizing the 4D CS/ Integrability correspondence to the case of super symmetries. We will first show that a superspin system associated to the super Lie algebra g_{BF} can be realized in the framework of a four dimensional Chern-Simons theory equipped with the super gauge group G_{BF} corresponding to g_{BF}. This is done in analogy to the bosonic case [123], by assimilating the one-dimensional integrable super lattice to a super line defects lattice in 4D CS. We then propose a general super Lax operator formula as the crossing of a super Wilson line with a super 't Hooft line defect. For that purpose, we use the diagrammatic interpretation of Levi decompositions presented before, in order to generalize of the notion of minuscule coweight and Levi decompositions to super symmetries.

We focus in the first section on the simple linear $sl(m|n)$ super symmetry to introduce the super analog of the 4D CS theory and properties of its super line defects, and show that they allow to recover degrees of freedom of integrable superspin chain systems. Based on this model, we set up a general demarche for the realization of minuscule-like super Lax operators, by direct exploitation of special Levi-like decompositions of any Lie superalgebra. We first check this demarche in the second section for the linear $A(m-1|n-1)$ symmetry whose solutions are computed in superspin chain literature. Then, we apply the same rationale to give new solutions concerning orthosymplectic superspin chains with internal $B(m|n)$, $C(n)$ and $D(m|n)$ symmetries.

4.1 Super Integrability/ 4D CS Correspondence

In order to extend the power of the Integrability/ Gauge correspondence to super symmetries, we need to first build a 4D Chern-Simons theory with gauge symmetry given by a super group, and hosting super electric and magnetic line defects that carry bosonic, as well as fermioinc degrees of freedom. A lattice construction of these lines in the four dimensions should serve as a higher dimensional realization of a one dimensional chain system of superspins evaluated in a representation of a Lie superalgebra $\tilde{g}$ of $\tilde{G}$. This interpretation offers a general formula to be used to compute super oscillator Lax operators for Lie superalgebras with special 3-gradings.

4.1.1 Super 4D CS gauge theory with $SL(m|n)$ symmetry

As a starting point, we can begin by considering a super gauge potential valued in a Lie superalgebra defined on a $\mathbb{Z}_2$ -graded space $\mathbb{R}^{m|n}$. This field connexion expands in terms of graded generators $\mathcal{E}_{\rm AB}$ labeled by vectors of the $\mathbb{R}^{m|n}$ as

$$\mathcal{A} = \sum_{\rm AB} A^{\rm AB} \mathcal{E}_{\rm AB} \tag{4.1}$$

such that vectors of this graded space can be either bosonic or fermioinc depending on their even or odd $\mathbb{Z}_2$ degree.

$$\begin{array}{rcll} & & \text{BOSONIC} & \rightarrow \quad \deg {\rm A} = |{\rm A}| = \bar{\mathbf{0}} \\ {\rm A} & = & & \\ & & \text{FERMIOINC} & \rightarrow \quad \deg {\rm A} = |{\rm A}| = \bar{\mathbf{1}} \end{array} \tag{4.2}$$

and hence, the degree of the generators $\mathcal{E}_{\rm AB}$ is defined as

$$|\mathcal{E}_{\rm AB}| \equiv \deg \mathcal{E}_{\rm AB} = |{\rm A}| + |{\rm B}| \tag{4.3}$$

By taking the Lie superalgebra as the linear $sl(m|n)$, the generators should verify super commutation relations

$$[\mathcal{E}_{\rm AB}, \mathcal{E}_{\rm CD}\} = \delta_{\rm BC} \mathcal{E}_{\rm AD} - (-)^{|\mathcal{E}_{\rm AB}||\mathcal{E}_{\rm CD}|} \delta_{\rm DA} \mathcal{E}_{\rm CB} \tag{4.4}$$

that boil down to the usual commutators

$$[\mathcal{E}_{\rm AB}, \mathcal{E}_{\rm CD}] = \mathcal{E}_{\rm AB}\mathcal{E}_{\rm CD} - \mathcal{E}_{\rm CD}\mathcal{E}_{\rm AB} \tag{4.5}$$

if $\mathcal{E}_{\rm AB}$ and $\mathcal{E}_{\rm CD}$ have of the same $\mathbb{Z}_2$ degree, or to the anti-commutators

$$\{\mathcal{E}_{\rm AB}, \mathcal{E}_{\rm CD}\} = \mathcal{E}_{\rm AB}\mathcal{E}_{\rm CD} + \mathcal{E}_{\rm CD}\mathcal{E}_{\rm AB} \tag{4.6}$$

if else. The $\mathbb{Z}_2$ graduation reads for the Lie superalgebra $sl(m|n)$ as

$$sl(m|n) = sl(m|n)_{\bar{\mathbf{0}}} \oplus sl(m|n)_{\bar{\mathbf{1}}} \tag{4.7}$$

where the even subspace is given by the adjoint representations of $sl(m)$ and $sl(n)$, and the odd subspace is given by bi-fundamental of $sl(m) \oplus sl(n)$

$$\begin{array}{rcl} sl(m|n)_{\bar{\mathbf{0}}} & = & (\mathbf{m}, \bar{\mathbf{m}}) \oplus (\mathbf{n}, \bar{\mathbf{n}}) \\ sl(m|n)_{\bar{\mathbf{1}}} & = & (\mathbf{m}, \bar{\mathbf{n}}) \oplus (\bar{\mathbf{m}}, \mathbf{n}) \end{array}$$

We can moreover distinguish the labels (4.2) of $\mathbb{R}^{m|n}$ into bosonic labels a,b$\in \mathbb{R}^m$ ($|{\rm a}| = |{\rm b}| = \bar{\mathbf{0}}$), and fermioinc ones i,j$\in \mathbb{R}^n$ with $|{\rm i}| = |{\rm j}| = \bar{\mathbf{1}}$, the development (4.1) becomes

$$\mathcal{A} = A^{\rm ab}\mathcal{E}_{\rm ab} + A'^{\rm ij}\mathcal{E}'_{\rm ij} + \tilde{A}^{\rm ai}\tilde{\mathcal{E}}_{\rm ai} + \tilde{A}'^{\rm ia}\tilde{\mathcal{E}}'_{\rm ia} \tag{4.8}$$

This is represented by the $(m+n)\times(m+n)$ matrix

$$\mathcal{A}=\left(\begin{array}{cc} A^{\mathrm{ab}}\mathcal{E}_{\mathrm{ab}} & \tilde{A}^{\mathrm{ai}}\tilde{\mathcal{E}}_{\mathrm{ai}} \\ \tilde{A}'^{\mathrm{ia}}\tilde{\mathcal{E}}'_{\mathrm{ia}} & A'^{\mathrm{ij}}\tilde{\mathcal{E}}_{\mathrm{ij}} \end{array}\right) \tag{4.9}$$

where the diagonal $A^{\mathrm{ab}}=tr\left(\mathcal{E}^{\mathrm{ab}}\mathcal{A}\right)$ and $A'^{\mathrm{ij}}=-tr\left(\mathcal{E}'^{\mathrm{ij}}\mathcal{A}\right)$ are of bosonic nature and are respectively contained in the adjoints of $sl(m)$ and $sl(n)$ in agreement with the $\mathbb{Z}_2$ graduation of the $sl(m|n)$ Lie superalgebra; while the components $\tilde{A}^{\mathrm{ai}}=tr\left(\tilde{\mathcal{E}}^{\mathrm{ai}}\mathcal{A}\right)$ and $\tilde{A}'^{\mathrm{ia}}=-tr\left(\tilde{\mathcal{E}}'^{\mathrm{ia}}\mathcal{A}\right)$ are fermioinc potentials with mixed labels, corresponding to the bi-representations.
Finally, notice that for such graded matrix (4.9), the supertrace is defined by

$$str\left(\begin{array}{cc} A^{\mathrm{ab}} & \tilde{A}^{\mathrm{ai}} \\ \tilde{A}'^{\mathrm{ia}} & A'^{\mathrm{ij}} \end{array}\right)=tr(A^{\mathrm{ab}})-tr(A'^{\mathrm{ij}}) \tag{4.10}$$

We define here the super 4D Chern-Simons theory with $SL\left(m|n\right)$ gauge symmetry by the following action describing the configuration of the gauge field (4.1) in the manifold $M_4=\Sigma\times\mathbb{C}$

$$S_{4DCS}^{SL(m|n)}=\int_{M_4}dz\wedge str\left[\mathcal{A}\wedge d\mathcal{A}+\frac{2}{3}\mathcal{A}\wedge\mathcal{A}\wedge\mathcal{A}\right] \tag{4.11}$$

Similarly to (2.18), this action is obtained from the Chern-Simons 3-form whose trace is lifted here to the supertrace expanding as

$$str\left(\mathcal{A}\wedge d\mathcal{A}+\frac{2}{3}\mathcal{A}\wedge\mathcal{A}\wedge\mathcal{A}\right)=g_{\mathrm{ABCD}}A^{\mathrm{AB}}dA^{\mathrm{CD}}+\frac{2}{3}f_{\mathrm{ABCDEF}}A^{\mathrm{AB}}A^{\mathrm{CD}}A^{\mathrm{EF}} \tag{4.12}$$

The constant structures read in terms of graded generators as

$$g_{\mathrm{ABCD}}=str(\mathcal{E}_{\mathrm{AB}}\mathcal{E}_{\mathrm{CD}})\qquad,\qquad f_{\mathrm{ABCDEF}}=str(\mathcal{E}_{\mathrm{AB}}\mathcal{E}_{\mathrm{CD}}\mathcal{E}_{\mathrm{EF}}) \tag{4.13}$$

The partial gauge connexion A^{AB} expands in space as

$$A^{\mathrm{AB}}=dxA_x^{\mathrm{AB}}+dyA_y^{\mathrm{AB}}+d\bar{z}A_{\bar{z}}^{\mathrm{AB}} \tag{4.14}$$

The equation of the fields motion in absence of external sources is given by $\delta S\left[\mathcal{A}\right]=0$, i.e.

$$\mathcal{F}=d\mathcal{A}+\mathcal{A}\wedge\mathcal{A}=0 \tag{4.15}$$

To introduce charges to this theory, we implement line defects and their observables in analogy to the bosonic theory. We will name these as super lines to refer to their super internal symmetry properties. Their definition can be simply motivated by the lifting from the bosonic Wilson line $W_{\xi_z}^{\mathbf{m}}$ of the $SL\left(m\right)$ theory by using the embedding properties

$$\begin{array}{rcl} sl\left(m\right) & \subset & sl(m|n)_{\bar{0}}\subset sl(m|n) \\ \mathbf{rep}_{sl_m} & \subset & \mathbf{rep}_{sl(m|n)_{\bar{0}}}\subset\mathbf{rep}_{sl(m|n)} \end{array} \tag{4.16}$$

This extension is performed as follows

gauge symmetry	$SL(m)$	$\rightarrow$	$SL(m\|n)$
fund representation	$\boldsymbol{R}=\mathbf{m}$	$\rightarrow$	$\boldsymbol{R}=\mathbf{m}\|\mathbf{n}$
Wilson line	$W_{\xi_z}^{\mathbf{m}}$	$\rightarrow$	$W_{\xi_z}^{\mathbf{m}\|\mathbf{n}}$
Observable	tr	$\rightarrow$	str

(4.17)

where $\mathbf{m}|\mathbf{n}$ is the fundamental representation of $sl(m|n)$ and where the extrinsic properties stay intact. A super Wilson line is therefore associated to a curve ξ_z in the 4D CS expanding in $\mathbb{R}^2$, and located at the point $z \in C$ similarly to the bosonic case. Its formal observable is given by

$$W_{\xi_z}^{\boldsymbol{m}|\boldsymbol{n}} = str_{\boldsymbol{m}|\boldsymbol{n}} \left[P \exp \left(\oint_{\xi_z} \mathcal{A} \right) \right] \tag{4.18}$$

In general, the electrical charge of a super Wilson line is given by a highest weight $\omega_{\boldsymbol{R}}$ of a super gauge group; it carries bosonic and fermionic states valued in the representation $\mathbf{R}$.
On the other hand , magnetically charged 't Hooft line defects are characterized by coweights of the super gauge group. We denote a super 't Hooft line in the $SL\left(m|n\right)$ 4D CS as $\mathrm{tH}^{\mu}_{\gamma_{z'}}$ where $\gamma_{z'}$ in a curve of $\mathbb{R}^2$ sitting in the point z' of $\mathbb{CP}^1$, and μ its magnetic charge whch is given by a coweight of the super $SL\left(m|n\right)$ symmetry. This magnetic super line defect is defined such that its presence in the $SL\left(m|n\right)$ 4D CS creates a Dirac like singularity in the field configuration and the gauge curvature (4.15) takes the form of a Dirac monopole of 4D Yang Mills theory. And so this singularity leads to the dispersion of the surrounding field bundles in the super 4D CS, exactly like the action of a bosonic magnetic line on bosonic gauge fields (2.24).
This disorder observable is described by the L-operator which by taking $\gamma_{z'} = \{y = 0, z' = 0\}$, reads as

$$\mathcal{L}^{\mu}(z) = P \exp \left(\int_{y<0}^{y>0} \mathcal{A}_y(z) \right) \tag{4.19}$$

Recall that in the bosonic case, the explicit calculation of this operator in the framework of 4D CS theory was worked out by choosing the magnetic charge as a minuscule coweight μ, and then identifying the splitting of gauge fields (2.27) with the Levi decomposition of the Lie algebra with respect to μ. The complication for the case of super line defects is the that minuscule coweights and Levi decompositions are not known for Lie superalgebras. Our purpose for the next subsection is to generalize these notions to graded symmetries, and elaborate a formula allowing to construct super L-operators in 4D CS for generic superalgebras.

4.1.2 Super L-operators from 4D Chern-Simons

To fix ideas, we consider a superspin chain of $sl(m|n)$ type and of lenght L. The internal symmetry of each super atom Υ^l with $1 \leq l \leq L$ can be described by a highest weight vector λ^l associated to the representation $R^l\left(\lambda^l\right)$ of $sl(m|n)$ in which the superspins take values. This weight vector expands in the basis of unit weight vectors ϵ_{A} of $R^{m|n}$ as

$$\lambda^l = \sum_{\mathrm{A}=1}^{m+n} \lambda^l_{\mathrm{A}} \epsilon_{\mathrm{A}} \tag{4.20}$$

This graded basis is defined with the inner product $\langle \epsilon_A, \epsilon_B \rangle = (-)^{|A|} \delta_{AB}$ with $|A| = \{\bar{0}, \bar{1}\}$. Notice here that for the full superspin chain, the total quantum state transforms in a tensor product representation with highesst weight $\mathbf{\Lambda}$, where we have

$$\mathbf{R}\left(\mathbf{\Lambda}\right) = \prod_{l=1}^{L} \mathbf{R}^l \quad , \quad \mathbf{\Lambda} = \sum_{l=1}^{L} \lambda^l \tag{4.21}$$

$$\mathbf{\Lambda} = \sum_{\mathrm{A}=1}^{m+n} \Lambda_{\mathrm{A}} \epsilon_{\mathrm{A}} \quad , \quad \Lambda_{\mathrm{A}} = \sum_{l=1}^{L} \lambda^l_{\mathrm{A}} \tag{4.22}$$

These degrees of freedom will be realized in the framework of a 4D Chern-Simons with a super gauge group $SL(m|n)$, such that the internal symmetry of a super atom Υ^l is encoded in the

gauge fields carried by a super Wilson line with electric charge λ^l.
By taking the super atoms in the same fundamental representation $\mathbf{m}|\mathbf{n}$ of $sl(m|n)$, we illustrate in Figure 4.1 the associated XXX superspin chain by placing L super Wilson lines $W_{\xi_z^l}^{\boldsymbol{m|n}}$ in positions $x_l \in \mathbf{R}$ of the chain nodes, and in the same position z in C. We have

$$\xi_z^l = \{x_l = cte, z_l = z\} \tag{4.23}$$

These neighboring electrically charged super atoms create a magnetic field modeled by the super 't Hooft line $\mathrm{tH}_{\gamma_0}^{\mu}$ at

$$\gamma_0 = \{y = 0, z' = 0\} \tag{4.24}$$

The 't Hooft line acts as a transfer matrix carrying the auxiliary space of the spin chain, hence each Wilson /'t Hooft coupling in this Figure is interpreted as a super Lax operator which is nothing but the L-operator measuring the transport of gauge fields carried by the Wilson past the 't Hooft. Notice that the lines intersect in $\mathbb{R}^2$ but are distinct in $\mathbb{C}$, and so can be freely

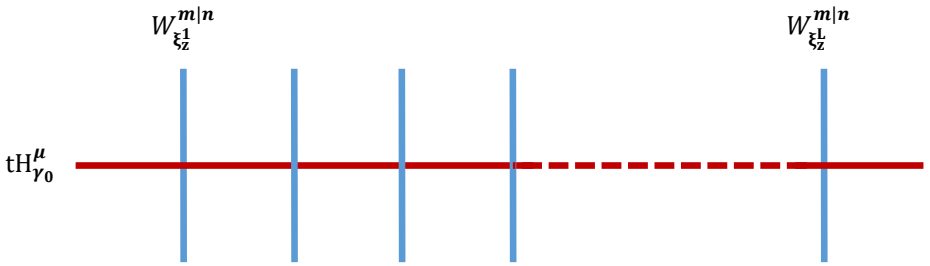

Figure 4.1: Realization of an $sl(m|n)$ superspin chain of L nodes in the fundamental representation using super line defects in the 4D Chern Simons.

moved in four dimensions.
This diffeomorphism invariance allows to draw the equivalence of Figure 4.2 where two electric Wilson lines and a magnetic 't Hooft line cross each other in different orders. This image is

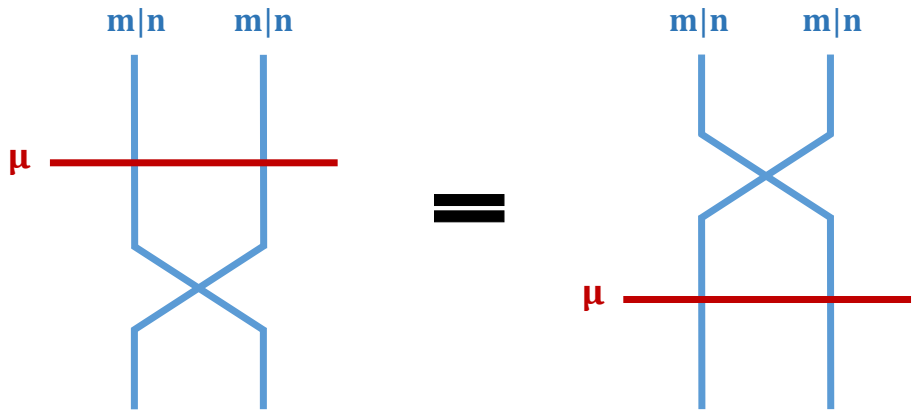

Figure 4.2: Graphic representation of the RLL equation in terms of intersecting line defects in $SL(m|n)$ 4D CS theory.

equivalent to the RLL equation of integrability reading as

$$R_{rs}^{ik}(z-w)\, L_j^r(z)\, L_l^s(w) = L_r^i(w)\, L_s^k(z)\, R_{jl}^{rs}(z-w) \tag{4.25}$$

Note here that the R-matrix R^{ik}_{rs} verifies the Yang Baxter equation and refers to the crossing of two Wilson lines with incoming graded sates $|r\rangle$ and $|s\rangle$ and outgoing graded states $|i\rangle$ and $|k\rangle$. Just like in the bosonic case, these "super" R-matrices can be directly calculated in dual 4D CS from Feynman diagrams amplitudes of lines' crossing.
In general, a superspin chain system characterised by superspin representations of a graded Lie superalgebra denoted as,

$$g_{\text{BF}} \equiv g_{\text{BOSE/FERMI}} \qquad , \qquad g_{\text{BF}} = g_{\bar{0}} \oplus g_{\bar{1}} \tag{4.26}$$

with $g_{\bar{0}}$ its even part and $g_{\bar{1}}$ its odd part, is realized as a lattice of Wilson and 't Hooft super line defects in the dual four-dimensional Chern-Simons theory with the graded gauge symmetry

$$G_{\text{BF}} \equiv G_{\text{BOSE/FERMI}} \qquad , \qquad G_{\text{BF}} = G_{\bar{0}} \oplus G_{\bar{1}} \tag{4.27}$$

In the present thesis, we will use this dulaity to study the integrable superspin chain systems defined by the basic Lie superalgebras as given in the following table [227, 229]

g_{BF}	even part $g_{\bar{0}}$	odd part $g_{\bar{1}}$
$A(m\|n)$	$A_m \oplus A_n \oplus U(1)$	$(\bar{m}, n) \oplus (m, \bar{n})$
$B(m\|n)$	$B_m \oplus C_n$	$(2m+1, 2n)$
$C(n)$	$C_{n-1} \oplus U(1)$	$(2n-2) \oplus (2n-2)$
$D(m\|n)$	$D_m \oplus C_n$	$(2m, 2n)$

(4.28)

However, notice that for a superalgebra g_{BF}, one has different varieties of superspin chains that can be labeled by the distinct super Dynkin diagrams $\mathfrak{D}[\mathbf{g}_{\text{BF}}]^{(\kappa)}$ of g_{BF}. This is due to the grading of the vector space $\mathbb{R}^{m|n}$ leading to different possible choices of the ordering of the unit basis in which the weight λ^l is defined as in (4.20). In what follows, we will label the two kinds of fundamental unit weight vectors ϵ_{A} as ε_i for the bosonic unit vectors having the metric $\langle \varepsilon_i, \varepsilon_j \rangle = \delta_{ij}$, and δ_a for the fermionic ones with $\langle \delta_a, \delta_b \rangle = -\delta_{ab}$. This leads to different graduations of the graded simple roots of g_{BF}, which for the example of $sl(m|n)$ can be of three types: fermionic simple roots of the form

$$\alpha_{\text{A}} = \delta_{\text{A}} - \varepsilon_{\text{A}+1} \qquad or \qquad \alpha_{\text{A}} = \varepsilon_{\text{A}} - \delta_{\text{A}+1} \qquad , \qquad \alpha^2_{\text{A}} = 0 \tag{4.29}$$

or bosonic simple roots with two possible forms

$$\begin{array}{rclcrcl} \alpha_{\text{A}} & = & \varepsilon_i - \varepsilon_{i+1} & , & \alpha^2_{\text{A}} & = & +2 \\ \alpha_{\text{A}} & = & \delta_a - \delta_{a+1} & , & \alpha^2_{\text{A}} & = & -2 \end{array} \tag{4.30}$$

Thus, in contrary to bosonic Lie algebras $\mathbf{g}_{\text{BOSE}}$, a superalgebra $\mathbf{g}_{\text{BF}}$ admits several realizations of the set of simple roots, and hence several different Dynkin super diagrams $\mathfrak{D}[\mathbf{g}_{\text{BF}}]^{(\kappa)}$ labeled by κ

$$\mathfrak{D}[\mathbf{g}_{\text{BF}}]^{(1)}, \quad \mathfrak{D}[\mathbf{g}_{\text{BF}}]^{(2)}, \quad \mathfrak{D}[\mathbf{g}_{\text{BF}}]^{(3)}, \quad .... \quad , \quad \mathfrak{D}[\mathbf{g}_{\text{BF}}]^{(\mathbf{n}_{\text{BF}})} \tag{4.31}$$

where n_{BF} is the number of these possibilities. As an illustration, we give in **Figure 4.3** examples of super Dynkin diagrams $\mathfrak{D}[sl_{(3|4)}]^{(\kappa)}$ concerning the $sl(3|4)$ superalgebra that actually has

$$\mathbf{n}_{sl_{(3|4)}} = \frac{7!}{4! \times 3!} = 35 \tag{4.32}$$

possible Dynkin representations. In this Figure, the fermionic simple roots are represented by green nodes, the bosonic simple roots with $\alpha^2 = -2$ are represented in blue, and the bosonic simple roots with $\alpha^2 = 2$ in red.

The simplest basis choice, and the most studied in the literature of Lie superalgebras, is called

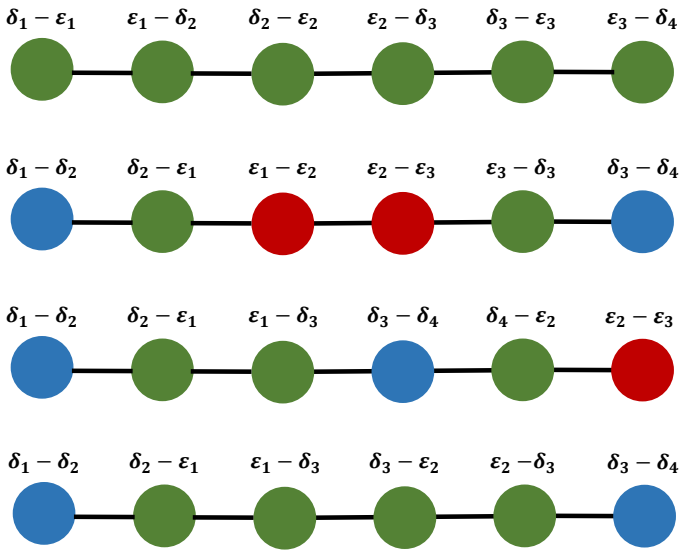

Figure 4.3: Graded Dynkin diagrams of the $sl(3|4)$ superalgebra. The green nodes represent fermionic simple roots, blue nodes represent bosonic roots with $\alpha^2 = -2$ and red nodes represent bosonic roots with $\alpha^2 = 2$.

the distinguished basis. In this case, the basis vectors of $\mathbb{R}^{m|n}$ are ordered such that the m bosonic weight vectors are distinguished from the n fermionic ones like

$$\epsilon_{A=1,\dots,m+n} = \{\delta_1, \dots, \delta_n, \varepsilon_1, \dots, \varepsilon_m\} \tag{4.33}$$

The super Dynkin diagram associated to such basis is referred to as the distinguished Dynkin diagram, and has only one fermionic simple root with the rest of bosonic type. The distinguished Dynkin diagram of the $sl(m|n)$ Lie superalgebra is depicted in Figure 4.4. For simplicity, we will mainly choose this type of basis for the study of basic superspin chains, especially the orthosymplectic families.

Now in order to realize solutions for these superspin chain systems, we need to generalize

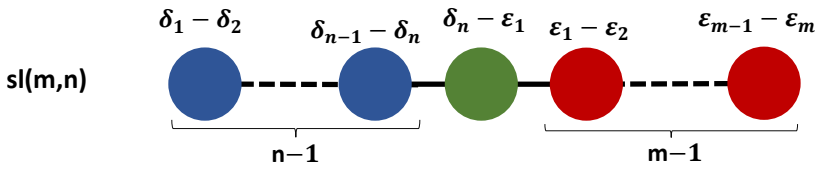

Figure 4.4: Distinguished Dynkin diagrams for the $sl(m|n)$ superalgebra. The green node represents the only fermionic node, blue and red nodes are bosonic.

the L-operator formula (4.49) for super symmetries, which requires the generalization of the Levi decomposition to super Lie algebras. However, since this type of decompositions, as well as minuscule coweights, are not known in the literature of superalgebras, we propose here to exploit their graphical interpretation on the level of super Dynkin diagrams. In general, the cutting (or deletion) of nodes from the Dynkin diagrams of a Lie algebras allows to classify their regular subalgebras [230] and decompositions as studied in [231]-[233]. In the special case where the cut node corresponds to a minuscule coweight, one obtains a Levi decomposition of the Lie algebra, which can be directly read from the Dynkin diagram, and exploited to calculate a minuscule Lax operator associated to a minuscule magnetic charge.

The same rationale can be applied to Lie superalgebras to investigate their different possible decompositions. In fact, the nodes' cutting operation in a super Dynkin diagram of the Lie superalgebra g_{BF} leads in general to a 5-grading of the form [234]- [236]

$$\mathbf{g}_{\text{BF}} = \mathbf{g}_{-2} \oplus \mathbf{g}_{-1} \oplus \mathbf{g}_0 \oplus \mathbf{g}_{+1} \oplus \mathbf{g}_{+2} \tag{4.34}$$

The g_0 here is a regular subalgebra of g_{BF}, and $\mathbf{g}_{\pm 1,2}$ are g_0-modules such that

$$\mathbf{g}_{j+k} = [\mathbf{g}_j, \mathbf{g}_k\} \tag{4.35}$$

and

$$w(\mathbf{g}_{+k}) = \mathbf{g}_{-k} \tag{4.36}$$

where $j, k = 0, \pm 1, 2$ and w is the standard antilinear anti-involutive mapping of the Lie superalgebra g_{BF}. The particular decompositions that interest us verify $\mathbf{g}_{\pm 2} = 0$, i.e.

$$\mathbf{g}_{\text{BF}} = \mathbf{g}_{-1} \oplus \mathbf{g}_0 \oplus \mathbf{g}_{+1} \tag{4.37}$$

These 3-gradings are equivalent to Levi decompositions with subspaces $\mathbf{g}_{\pm 1}$ of oscillator nature. They will be exploited here to build super minuscule Lax operators by interpreting the indices carried by subspaces $\mathbf{g}_{0,\pm 1}$ as Levi charges with respect to the cut node acting as a minuscule coweight. For the families of basic Lie superalgebras of table (4.28), the possible 3-gradings of the form (4.37) read as follows

$\mathbf{g}_{\text{BF}}$	$\mathbf{g}_0$	$\dim \mathbf{g}_{-1} = \dim \mathbf{g}_{+1}$
$A(m-1\|n-1)$	$sl(k\|l) \oplus sl(m-k\|n-l) \oplus U(1)$	$(k+l)(m-k+n-l)$
$B(m\|n)$	$B(m-1\|n) \oplus U(1)$	$2m+2n-1$
$C(n)$	$C_{n-1} \oplus U(1)$	$2\,(n-1)$
	$sl(1\|n-1) \oplus U(1)$	$\frac{n(n+1)}{2} - 1$
$D(m\|n)$	$D(m-1\|n) \oplus U(1)$	$2\,(m+n-1)$
	$sl(m\|n) \oplus U(1)$	$\frac{(m+n)(m+n+1)}{2} - m$

(4.38)

with $0 \leq k \leq m$ and $0 \leq l \leq n$. For each of these 3-gradings, we will build an associated oscillator super Lax operator by extending the Levi decomposition -based formula (2.37). This general construction is described as follows

A) *3-grading of the superalgebra* $\mathbf{g}_{\text{BF}}$

We consider the Lie superalgebra $\mathbf{g}_{\text{BF}}$ with a 3-grading of the type (4.37) that we can write for convenience as

$$\mathbf{g}_{\text{BF}} = \mathbf{N}_+ \oplus \boldsymbol{l}_\mu \oplus \mathbf{N}_- \tag{4.39}$$

The three algebraic subspaces are interpreted as described below:

• The $\boldsymbol{l}_\mu$ is a regular Lie sub-(super)algebra of g_{BF} with elements carrying charge 0 with respect to the coweight μ. It plays the role of a Levi subalgebra

$$[\mu, \boldsymbol{l}_\mu] = 0 \tag{4.40}$$

which is actually given by a direct sum

$$\boldsymbol{l}_\mu = \mathfrak{l}_\mu \oplus \mathbb{C}\mu \tag{4.41}$$

of a subalgebra $\mathfrak{l}_\mu$ with the $\mathbb{C}\mu$ associated to the cut node acting as a minuscule coweight.

• The remaining elements of the decomposition ($\mathbf{N} = \mathbf{g}_{\text{BF}} \backslash \boldsymbol{l}_\mu$) are nilpotent. They are given by $\boldsymbol{l}_\mu$-modules that carry charges ± 1 with respect to the μ.

$$\left[\mu, \mathbf{N}_\pm\right] = \pm \mathbf{N}_\pm \tag{4.42}$$

The two graded subspaces $\mathbf{N}_\pm$ mutually super-commute

$$[\mathbf{N}_+, \mathbf{N}_+\} = 0 \qquad , \qquad [\mathbf{N}_-, \mathbf{N}_-\} = 0 \tag{4.43}$$

and verify the generalized Levi-like constraint

$$\big[\mathbf{N}_+, \mathbf{N}_-\big\} \subset \boldsymbol{l}_\mu \tag{4.44}$$

B) *Branching of representations of* $\mathbf{g}_{\text{BF}}$

Following from the decomposition (4.39), a representation $\mathbf{R}$ of the $\mathbf{g}_{\text{BF}}$ splits into a direct sum of irreducible representations $\mathfrak{R}_{q_i}$ of the superalgebras in $\boldsymbol{l}_\mu = \mathfrak{l}_\mu + \mathbb{C}\mu$. These subspaces $\mathfrak{R}_{q_i}$ carry charges q_i with respect to μ,

$$\mathbf{R} = \sum_i \mathfrak{R}_{q_i} \qquad , \qquad [\mu, \mathfrak{R}_{q_i}] = q_i \mathfrak{R}_{q_i} \tag{4.45}$$

The adjoint action of the coweight μ on the representation $\mathbf{R}$ can be therefore written as

$$\mu = \sum_i q_i \Pi_i \qquad , \qquad \sum_i \Pi_i = I_{id} \tag{4.46}$$

where Π_i is the projector on the subspace $\mathfrak{R}_{q_i}$ and q_i is represents the Levi-charge carried by super states in $\mathfrak{R}_{q_i}$. In the superalgebra case, these charges are identified, in absence of branching rules, by the condition

$$q_i - q_{i+1} = \pm 1 \tag{4.47}$$

in addition to the vanishing of the super-trace,

$$str\,(\mu) = \sum_i q_i str\,(\Pi_i) = 0 \tag{4.48}$$

C) *Super Lax operator* $\mathcal{L}^\mu_{\mathbf{R}}$

The super L-operator describing the coupling of the representation $\mathbf{R}$ with the magnetic coweight μ leading to the superalgebra decomposition (4.39), is calculated by the formula

$$\mathcal{L}^\mu_{\mathbf{R}} = e^X z^\mu e^Y \tag{4.49}$$

In what follows, we will simply label it as $\mathcal{L}^\mu$, since we will take $\mathbf{R}$ as the fundamental representation for every ABCD superalgebra. In (4.49), the operator z^μ is calculated from the action of μ on $\mathbf{R}$ as in (4.46), while operators X and Y are nilpotent matrices belonging to $\mathbf{N}_+$ and $\mathbf{N}_-$ and expanding as

$$X = \sum_{i=1}^{\dim \mathbf{N}_+} b^i X_i \qquad , \qquad Y = \sum_{i=1}^{\dim \mathbf{N}_-} c_i Y^i \tag{4.50}$$

The graded basis generators X_i and Y^i are determined as corresponding to graded roots of $\mathbf{g}_{\text{BF}}$ that are not contained in the $\boldsymbol{l}_\mu = \mathfrak{l}_\mu \oplus \mathbb{C}\mu$. In analogy to the bosnic case (2.45), by cutting the node corresponding to the graded simple root β, the root system $\Phi_{\mathbf{g}_{\text{BF}}}$ splits as

$$\Phi_{\mathbf{g}_{\text{BF}}} = \{\pm\beta\} \cup \Phi_{\boldsymbol{l}_\mu} \cup \Phi_{\mathbf{N}_\pm} \qquad , \qquad \Phi'_{\mathbf{g}_{\text{BF}}} = \Phi_{\boldsymbol{l}_\mu} \cup \Phi_{\mathbf{N}_\pm} \tag{4.51}$$

where $\Phi_{\mathbf{N}_\pm}$ contains graded roots in $\Phi'_{\mathbf{g}_{\text{BF}}}$ that depend on β, i.e.

$$\Phi_{\mathbf{N}_\pm} = \left\{ \pm\alpha_{\text{BF}} \in \Phi'_{\mathbf{g}_{\text{BF}}}, \quad \frac{\partial \alpha_{\text{BF}}}{\partial \beta} \neq 0 \right\} \tag{4.52}$$

$$\Phi_{\boldsymbol{l}_\mu} = \left\{ \pm\alpha_{\text{BF}} \in \Phi'_{\mathbf{g}_{\text{BF}}}, \quad \frac{\partial \alpha_{\text{BF}}}{\partial \beta} = 0 \right\} \tag{4.53}$$

The sign of roots in each of the nilpotent subspaces is defined by the condition (4.42), such that μ acts on roots of $\mathbf{N}_\pm$ with ± 1. The (b^i, c_i) are graded Darboux coordinates of the phase space of the L-operator. They are given by bosonic and fermionic oscillators with Poisson bracket as

$$\left\{b^i, c_j\right\}_{PB} = \delta^i_j \tag{4.54}$$

which lifts to the super-commutator in the quantum level

$$\left[b^i, c_j\right\} = \delta^i_j \tag{4.55}$$

4.2 Super L-operators for all $sl(m|n)$ superspin chains

In this section, we will apply the general super Lax operator construction based on the formula (4.49) for the case of the linear $sl(m|n)$ superspin chain. We will compute its RLL solutions based on Levi-like decompositions generated from the Dynkin diagrams of $sl(m|n)$, and compare them to graded Lax matrices of the superspin chain literature. Thanks to the simplicity of this linear supersymmetry and its resemblance with the bosonic A-type symmetry, we will be able to generate all RLL solutions for all superspin chains associated to the

$$\mathbf{n}_{sl(m|n)} = \frac{(m+n)!}{(m!n!)} \tag{4.56}$$

Dynkin diagrams of $sl(m|n)$. These solutions $\mathcal{L}^\mu$ are labeled by magnetic charges μ given by coweights of $SL(m|n)$. These coweights correspond to different nodes of different Dynkin diagrams $\mathfrak{D}[sl(m|n)]^{(\kappa)}$ of $sl(m|n)$. Therefore, we will be considering here the general 3-grading of $A(m-1|n-1)$ as given in table (4.38). For the detailed analysis of decompositions obtained by nodes cutting in the distinguished Dynkin diagram 4.4, see [237] where the same approach is used to construct minuscule super Lax operators for the nodes of the distinguished $sl(m|n)$ superspin chain from the 4D CS, and where the purely fermionic super Lax operator corresponding to the fermionic node is also studied. Note that those particular solutions are included among those built here for an arbitrary minuscule coweight of $sl(m|n)$.
We begin by recalling that the Lie superalgebra $A(m-1|n-1) = sl(m|n)$ with $n \neq m$ is of rank $m+n-1$ and $(m+n)^2 - 1$ dimensions. Its even sector reads as

$$sl(m|n)_{\bar{0}} = sl(m) \oplus sl(n) \tag{4.57}$$

and its odd sector $sl(m|n)_{\bar{1}}$ is given by the module $m|\bar{n} \oplus \bar{m}|n$ that can be simply denoted below as $2mn$.
If we consider an arbitrary super Dynkin diagram of this superalgebra of linear type like those of Figures 4.3,4.4, and cut one of the nodes that can correspond to a fermionic or a bosonic simple root, we will always end up with subalgebras also of linear type in addition to $sl(1)$ standing for the isolated node. In fact, all the $(m+n-1) \times \frac{(m+n)!}{(m!n!)}$ act like minuscule coweights a lead to a 3-grading of $sl(m|n)$ that reads in the general case as

$$\begin{array}{ccc} sl(m|n) & \rightarrow & l_\mu \oplus sl(1) \oplus \mathbf{N}_+ \oplus \mathbf{N}_- \\ \boldsymbol{l}_\mu & = & sl(k|l) \oplus sl(m-k|n-l) \end{array} \tag{4.58}$$

with nilpotents

$$\dim \mathbf{N}_+ = \dim \mathbf{N}_- = (k+l)\,(m-k+n-l) \tag{4.59}$$

and $0 \leq k \leq m$, $0 \leq l \leq n$. This means that every 't Hooft line defined with a magnetic charge μ of $SL(m|n)$ allows to calculate a minuscule super Lax operator $\mathcal{L}^\mu$ by fixing the representation

carried by the Wilson super line. We will consider here the fundamental $\mathbf{m}|\mathbf{n}$ of $sl(m|n)$ which under the action of μ splits into irreducible representations of $sl(k|l)$ and $sl(m-k|n-l)$ like

$$\mathbf{m}|\mathbf{n} \to \mathbf{k}|\mathbf{l}_{1+\frac{l-k}{m-n}} \oplus (\mathbf{m}-\mathbf{k}|\mathbf{n}-\mathbf{l})_{\frac{l-k}{m-n}} \tag{4.60}$$

These representations carry four types of states that we will represent as follows :
(i) Bosonic states in the basis $|a\rangle$ with $1 \leq a \leq k$ of the fundamental $\underline{\mathbf{k}}$ of $sl(k)$ with the projector $\Pi_{\mathbf{k}}$,
(ii) Fermionic states in the basis $|i\rangle$ with $k+1 \leq i \leq m$ of the fundamental $\underline{\mathbf{l}}$ of $sl(l)$ with the projector $\Pi_{\mathbf{l}}$,
(iii) Bosonic states in the basis $|\alpha\rangle$ with $m+1 \leq \alpha \leq m+l$ of the fundamental $\underline{\mathbf{m}-\mathbf{k}}$ of $sl(m-k)$ with projector $\Pi_{\mathbf{m-k}}$,
(iv) Fermionic states in the basis $|\lambda\rangle$ with $m+l+1 \leq \lambda \leq m+n$ of the fundamental $\underline{\mathbf{n}-\mathbf{l}}$ of $sl(n-l)$ with projector $\Pi_{\mathbf{n-l}}$.
Working in the basis $\{|a\rangle, |i\rangle, |\alpha\rangle, |\lambda\rangle\}$ of $\mathbf{m}|\mathbf{n}$, we can write the adjoint action of the coweight μ as

$$\mu = \left(1+\frac{l-k}{m-n}\right)(\Pi_{\mathbf{k}}+\Pi_{\mathbf{l}}) + \left(\frac{l-k}{m-n}\right)(\Pi_{\mathbf{m-k}}+\Pi_{\mathbf{n-l}}) \tag{4.61}$$

The vanishing of the super trace justifying the charges of the subspaces appearing in (4.61) reads as

$$str\,(\mu) = \left(\frac{m-n+l-k}{m-n}\right)(k-l) + \frac{l-k}{m-n}(m-n+l-k) = 0 \tag{4.62}$$

The generators of the nilpotents (4.59) are realised as elements of the bi-representations $\underline{\mathbf{k}} \times \underline{\mathbf{m}-\mathbf{k}}$, $\underline{\mathbf{k}} \times \underline{\mathbf{n}-\mathbf{l}}$, $\underline{\mathbf{l}} \times \underline{\mathbf{m}-\mathbf{k}}$ and $\underline{\mathbf{l}} \times \underline{\mathbf{n}-\mathbf{l}}$. We write

$$X = b^{ai}|a\rangle\langle i| + \beta^{a\lambda}|a\rangle\langle\lambda| + \beta^{\alpha i}|\alpha\rangle\langle i| + b^{\alpha\lambda}|\alpha\rangle\langle\lambda| \tag{4.63}$$

$$Y = c_{ia}|i\rangle\langle a| + \gamma_{\lambda a}|\lambda\rangle\langle a| + \gamma_{i\alpha}|i\rangle\langle\alpha| + c_{\lambda\alpha}|\lambda\rangle\langle\alpha| \tag{4.64}$$

in terms of coordinates that form couples of oscillators such that (b^{ai}, c_{ia}) and $\left(b^{\alpha\lambda}, c_{\lambda\alpha}\right)$ are of bosonic nature and $\left(\beta^{a\lambda}, \gamma_{\lambda a}\right)$ and $(\beta^{\alpha i}, \gamma_{i\alpha})$ are fermioinc, thus the resulting super Lax matrices will carry graded oscillatory phase spaces.
By replacing in the formula (4.49), and using the following properties of the nilpotent operators

$$\begin{array}{lcl} X^2 = 0 & , & Y^2 = 0 \\ X\Pi_{\mathbf{k}} = X\Pi_{\mathbf{l}} = 0 & , & \Pi_{\mathbf{k}}Y = \Pi_{\mathbf{l}}Y = 0 \\ X\Pi_{\mathbf{m-k}} = X\Pi_{\mathbf{n-l}} = X & , & \Pi_{\mathbf{m-k}}Y = \Pi_{\mathbf{n-l}}Y = Y \end{array} \tag{4.65}$$

we find

$$\begin{aligned} \mathcal{L}^{\mu} = {} & z^{1+\frac{l-k}{m-n}}\Pi_{\mathbf{k}} + z^{1+\frac{l-k}{m-n}}\Pi_{\boldsymbol{l}} + z^{\frac{l-k}{m-n}}\Pi_{\mathbf{m-k}} + z^{\frac{l-k}{m-n}}\Pi_{\mathbf{n-}\boldsymbol{l}} \\ & + X\left(z^{\frac{l-k}{m-n}}\Pi_{\mathbf{m-k}} + z^{\frac{l-k}{m-n}}\Pi_{\mathbf{n-}\boldsymbol{l}}\right) + \left(z^{\frac{l-k}{m-n}}\Pi_{\mathbf{m-k}} + z^{\frac{l-k}{m-n}}\Pi_{\mathbf{n-}\boldsymbol{l}}\right)Y \\ & + X\left(z^{\frac{l-k}{m-n}}\Pi_{\mathbf{m-k}} + z^{\frac{l-k}{m-n}}\Pi_{\mathbf{n-}\boldsymbol{l}}\right)Y \end{aligned} \tag{4.66}$$

In matrix language, we have

$$\mathcal{L}^{\mu}_{sl_{m|n}} = z^{\frac{l-k}{m-n}} \begin{pmatrix} z\delta^a_b + \left(b^{ai}c_{ib} + \beta^{a\lambda}\gamma_{\lambda b}\right) & \left(b^{ai}\gamma_{i\alpha} + \beta^{a\lambda}c_{\lambda\alpha}\right) & b^{aj}\delta_{ji} & \beta^{a\rho}\delta_{\rho\lambda} \\ \left(\beta^{\alpha i}c_{ib} + b^{\alpha\lambda}\gamma_{\lambda b}\right) & z\delta^{\alpha}_{\eta} + \left(\beta^{\alpha i}\gamma_{i\eta} + b^{\alpha\lambda}c_{\lambda\eta}\right) & \beta^{\alpha j}\delta_{ji} & b^{\alpha\rho}\delta_{\rho\lambda} \\ c_{ia} & \gamma_{i\alpha} & \delta^j_i & 0 \\ \gamma_{\lambda a} & c_{\lambda\alpha} & 0 & \delta^{\rho}_{\lambda} \end{pmatrix} \tag{4.67}$$

By comparing with matrices obtained in [61] based on degenerate solutions of the graded Yang Baxter equation, the approach proposed here is proven to yield the desired RLL solutions of oscillator type.

4.3 Super L-operators of $B(m|n)$ type

Now, we will rely on the strength of the super Lax operator construction proposed in 4.1.2 and tested in 4.2, in order to build novel graded Lax matrices that are still missing in the superspin chain literature. These concern the orthosymplectic superspin chain systems with internal symmetry given by the basic Lie superalgebra

$$B(m|n) = osp(2m+1|2n), \qquad m,n>0 \tag{4.68}$$

of rank $m+n$, and dimension equal to $2(m+n)^2+m+3n$. Its even subspace

$$\begin{array}{rcl} B(m|n)_{\bar{0}} & = & B_m \oplus C_n \\ & \simeq & so(2m+1)\oplus sp\,(2n) \end{array} \tag{4.69}$$

is formed of $2m^2+2n^2$ roots realized as

$$\begin{array}{rcccll} \Phi_{\bar{0}} & : & \pm(\varepsilon_i \pm \varepsilon_j) & , & \pm\varepsilon_i & , \qquad i\neq j=1,...,m \\ & & \pm(\delta_a \pm \delta_b) & , & \pm 2\delta_a & , \qquad a\neq b=1,...,n \end{array} \tag{4.70}$$

and its odd subspace is given by the bi-fundamental representation of $so(2m+1)\oplus sp\,(2n)$

$$B(m|n)_{\bar{1}} = (2m+1,2n) \tag{4.71}$$

with $2n+2mn$ elements like

$$\Phi_{\bar{1}} \quad : \quad \pm\delta_a \quad , \qquad \pm(\varepsilon_i \pm \delta_a) \tag{4.72}$$

The total root system $\Phi_{B_{m|n}} = \Phi_{\bar{0}} \oplus \Phi_{\bar{1}}$ sums up to $2(m+n)^2+2n$ graded root.
Such orthosymplectic chain system can be realized in the framework of a four-dimensional Chern-Simons theory with gauge symmetry $OSP(2m+1|2n)$ by means of super Wilson and 't Hooft lines. This line defects construction will not be detailed for this case since it is similar to the case of the $SL(m|n)$ super symmetry. We will directly exploit the 3-grading of table (4.38) in order to compute the associated super Lax operator $\mathcal{L}^{\mu}_{B_{m|n}}$ by using the formula (4.49). However, notice that this 3-grading is obtained from the distinguished Dynkin diagram of $B(m|n)$, i.e. we will be focusing on the distinguished superspin chain of $B(m|n)$ type defined on the particular basis of unit weight vectors reading as in (4.20)

$$\delta_1, \quad \delta_2, \quad ... \quad \delta_{n-1}, \quad \delta_n, \quad \varepsilon_1, \quad \varepsilon_2, \quad ... \quad \varepsilon_{m-1}, \quad \varepsilon_m \tag{4.73}$$

The simple roots generated in this weight vectors basis contain only one fermionic node γ with length $\gamma^2=0$, and $m+n-1$ fermionic root.

$$\delta_a-\delta_{a+1} \qquad , \qquad \gamma=\delta_n-\varepsilon_1 \qquad , \qquad \varepsilon_i-\varepsilon_{i+1} \qquad , \qquad \varepsilon_m \tag{4.74}$$

The associated super Cartan matrix reads in this case as

$$\alpha_A.\alpha_B = \begin{pmatrix} -2 & 1 & \cdots & & & & & & \\ 1 & -2 & 1 & & & & & & \\ & \ddots & \ddots & & & & & & \\ & & 1 & -2 & 1 & & & & \\ & & & 1 & 0 & -1 & & & \\ & & \cdots & & -1 & 2 & -1 & & \\ & & & & & \ddots & \ddots & \ddots & \\ & & & & & & -1 & 2 & -1 \\ & & & & & & & -1 & 1 \end{pmatrix} \tag{4.75}$$

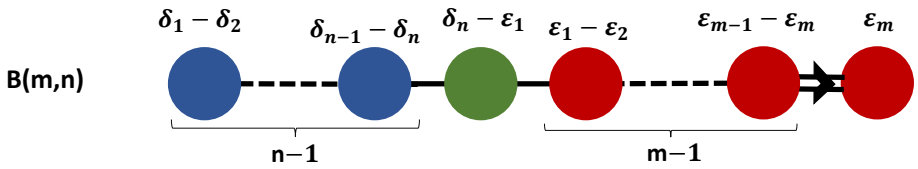

Figure 4.5: The distinguished super Dynkin diagram of the $B(m|n)$ superalgebra having one fermionic simple root represented in Green color. Notice that the $B(m|n)$ superalgebra has $\frac{(n+m-1)!}{n!\times(m-1)!}$ possible super Dynkin diagrams

and allows to draw the distinguished super Dynkin diagram given in **Figure 4.5**. We recall now the only possible 3-grading of this superalgebra (4.38)

$$B(m|n) \to A_1 \oplus B(m-1|n) \oplus \mathbf{N}_+ \oplus \mathbf{N}_- \tag{4.76}$$

or also

$$osp(2m+1|2n) \to so(2) \oplus osp(2m-1|2n) \oplus \mathbf{N}_+ \oplus \mathbf{N}_- \tag{4.77}$$

where

$$\mathbf{N}_\pm = 2m+2n-1 \tag{4.78}$$

Thus, we have one minuscule super L-operator that we realize in the fundamental representation splitting as

$$(\mathbf{2m+1|2n})_0 \to \mathbf{1}_+ \oplus (\mathbf{2m-1|2n})_0 \oplus \mathbf{1}_- \tag{4.79}$$

We will represent the two singlets $\mathbf{1}_\pm$ by the states $|\pm\rangle$, the bosonic states of the fundamental $\underline{\mathbf{2m-1}}$ of $so(2m+1)$ as $|i\rangle$, and the fermionic states of the fundamental $\underline{\mathbf{2n}}$ of $sp(2n)$ by $|\alpha\rangle$. Thus we have the basis

$$\{|+\rangle\,, \quad |i\rangle\,, \quad |-\rangle\,, \quad |\alpha\rangle\} \tag{4.80}$$

We write the adjoint action of the minuscule coweight μ_{n+1} associated to the decomposition (4.77) is written as in terms of the projectors on the basis (4.80)

$$\varrho_\pm = |\pm\rangle\langle\pm|\,, \qquad \Pi_1 = \sum_{i=1}^{2m+1} |i\rangle\langle i|\,, \qquad \Pi_2 = \sum_{\alpha=1}^{2n} |\alpha\rangle\langle\alpha| \tag{4.81}$$

as follows

$$\mu_{n+1} = \varrho_+ + q_1\Pi_1 - \varrho_- + q_2\Pi_2 \tag{4.82}$$

with charges $q_1 = q_2 = 0$. This means we have

$$z^{\mu_{n+1}} = z\varrho_+ + \Pi_1 + z^{-1}\varrho_- + \Pi_2 \tag{4.83}$$

Concerning the operators X and Y, they are be generated by antisymmetric matrices as

$$\begin{array}{rcll} X_i & = & |+\rangle\langle i| - |i\rangle\langle -| & ; \qquad \mathcal{X}_\alpha = |+\rangle\langle\alpha| - |\alpha\rangle\langle -| \\ Y^i & = & |i\rangle\langle +| - |-\rangle\langle i| & ; \qquad \mathcal{Y}^\alpha = |\alpha\rangle\langle +| - |-\rangle\langle\alpha| \end{array} \tag{4.84}$$

verifying the Levi -like conditions (4.42) such that

$$[\mu,X_i] = X_i, [\mu,X_\alpha] = X_\alpha, \quad [\mu,Y^i] = -Y^i, \quad [\mu,Y^\alpha] = -Y^\alpha \tag{4.85}$$

in addition to

$$[X_i,Y^i] = [\mathcal{X}_\alpha,\mathcal{Y}^\alpha] = \mu \tag{4.86}$$

The X and Y also expand in terms of coordinates of the phase space of the L-operator as

$$X = b^i X_i + \beta^\alpha X_\alpha \qquad , \qquad Y = c_i Y^i + \gamma_\alpha Y^\alpha \tag{4.87}$$

These $2(2m+2n-1)$ parameters form couples of oscillators such that (b^i, c_i) are bosonic oscillators and $(\beta^\alpha, \gamma_\alpha)$ are fermionic oscillators.
We calculate the quantities

$$\begin{array}{rcl} X^2 & = & -\mathbf{b}^2 \left|+\right\rangle \left\langle -\right| - \boldsymbol{\beta}^2 \left|+\right\rangle \left\langle -\right| \\ Y^2 & = & -\mathbf{c}^2 \left|-\right\rangle \left\langle +\right| - \boldsymbol{\gamma}^2 \left|-\right\rangle \left\langle +\right| \end{array} \tag{4.88}$$

where we have set

$$\begin{array}{rcl} \mathbf{b}^2 & = & b^i \delta_{ij} b^j \\ \mathbf{c}^2 & = & c_i \delta^{ij} c_j \\ \boldsymbol{\beta}^2 & = & \beta^\alpha \delta_{\alpha\beta} \beta^\beta \\ \boldsymbol{\gamma}^2 & = & \gamma_\alpha \delta^{\alpha\beta} \gamma_\beta \end{array} \tag{4.89}$$

and

$$X^3 = 0 \qquad , \qquad Y^3 = 0 \tag{4.90}$$

leading to

$$e^X = 1 + X + \frac{1}{2} X^2 \qquad , \qquad e^Y = 1 + Y + \frac{1}{2} Y^2 \tag{4.91}$$

We also have

$$\begin{array}{llll} X \varrho_+ & = \varrho_+ Y & = 0 \\ X^2 \varrho_+ & = X^2 \Pi_1 & = 0 \\ \varrho_+ Y^2 & = \Pi_1 Y^2 & = 0 \\ X^2 \Pi_2 & = \Pi_2 Y^2 & = 0 \end{array} \tag{4.92}$$

Thus the super L-operator

$$\mathcal{L}^{\mu_{n+1}} = \left(1 + X + \frac{1}{2} X^2\right) z^{\mu_{n+1}} \left(1 + Y + \frac{1}{2} Y^2\right) \tag{4.93}$$

expands like

$$\begin{array}{rcl} \mathcal{L}^{\mu_{n+1}} & = & z\varrho_+ + \Pi_1 + z^{-1}\varrho_- + \Pi_2 + X\left(\Pi_1 + z^{-1}\varrho_- + \Pi_2\right) + \\ & & \left(\Pi_1 + z^{-1}\varrho_- + \Pi_2\right) Y + X\left(\Pi_1 + z^{-1}\varrho_- + \Pi_2\right) Y \\ & & + \frac{1}{2} X^2 z^{-1} \varrho_- + \frac{1}{2} z^{-1} \varrho_- Y^2 + \frac{1}{2} X^2 z^{-1} \varrho_- Y \\ & & + \frac{1}{2} X z^{-1} \varrho_- Y^2 + \frac{1}{4} X^2 z^{-1} \varrho_- Y^2 \end{array} \tag{4.94}$$

In matrix language we finally have

$$\mathcal{L}^{\mu_{n+1}}_{B_{m|n}} = \begin{pmatrix} \varrho_+ L \varrho_+ & \varrho_+ L \Pi_1 & \varrho_+ L \varrho_- & \varrho_+ L \Pi_2 \\ \Pi_1 L \varrho_+ & \Pi_1 L \Pi_1 & \Pi_1 L \varrho_- & \Pi_1 L \Pi_2 \\ \varrho_- L \varrho_+ & \varrho_- L \Pi_1 & \varrho_- L \varrho_- & \varrho_- L \Pi_2 \\ \Pi_2 L \varrho_+ & \Pi_2 L \Pi_1 & \Pi_2 L \varrho_- & \Pi_2 L \Pi_2 \end{pmatrix} \tag{4.95}$$

with blocks reading explicitly as

$$\begin{array}{rcl} \varrho_+ L \varrho_+ & = & z + \left(b^i \delta^j_i c_j + \beta^\alpha \delta^\beta_\alpha \gamma_\beta\right) + \frac{1}{4} z^{-1} \left(\mathbf{b}^2 + \beta^2\right)\left(\mathbf{c}^2 + \gamma^2\right) \\ \varrho_+ L \Pi_1 & = & b^i + \frac{1}{2} z^{-1} \left(\mathbf{b}^2 + \beta^2\right) c_i \\ \varrho_+ L \varrho_- & = & -\frac{1}{2} z^{-1} \left(\mathbf{b}^2 + \beta^2\right) \\ \varrho_+ L \Pi_2 & = & b^\alpha + \frac{1}{2} z^{-1} \left(\mathbf{b}^2 + \beta^2\right) \gamma_\alpha \end{array} \tag{4.96}$$

and

$$\begin{array}{lcl} \Pi_1 L \varrho_+ & = & c_i + \frac{1}{2} z^{-1} b^i \left(\mathbf{c}^2 + \gamma^2\right) \\ \Pi_1 L \Pi_1 & = & \delta^i_j + z^{-1} b^i c_j \\ \Pi_1 L \varrho_- & = & -z^{-1} b^i \\ \Pi_1 L \Pi_2 & = & z^{-1} b^i \gamma_\beta \end{array} \tag{4.97}$$

and

$$\begin{array}{lcl} \varrho_- L \varrho_+ & = & -\frac{1}{2} z^{-1} \left(\mathbf{c}^2 + \gamma^2\right) \\ \varrho_- L \Pi_1 & = & -z^{-1} c_i \\ \varrho_- L \varrho_- & = & z^{-1} \\ \varrho_- L \Pi_2 & = & -z^{-1} \gamma_\alpha \end{array} \tag{4.98}$$

and

$$\begin{array}{lcl} \Pi_2 L \varrho_+ & = & \gamma_\alpha + \frac{1}{2} z^{-1} \beta^\alpha \left(\mathbf{c}^2 + \gamma^2\right) \\ \Pi_2 L \Pi_1 & = & z^{-1} \beta^\alpha c_j \\ \Pi_2 L \varrho_- & = & -z^{-1} \beta^\alpha \\ \Pi_2 L \Pi_2 & = & \delta^\beta_\alpha + \beta^\alpha \delta^\beta_\alpha \gamma_\beta \end{array} \tag{4.99}$$

4.4 Super L-operators of $C(n)$ type

We focus in this section on the family of integrable superspin chain systems defined by spins in representations of the basic orthosymplectic superalgebra

$$C(n) = D(1|n-1) = osp(2|2n-2) \tag{4.100}$$

with $n > 1$. This graded algebra of rank n and dimension $2n^2 + n - 2$ splits into an even subalgebra reading as

$$C(n)_{\bar{0}} = u(1) \oplus C_{n-1} = so(2) \oplus sp(2n-2) \tag{4.101}$$

and an odd graded subspace

$$C(n)_{\bar{1}} = (2n-2) \oplus (2n-2) \tag{4.102}$$

Similarly to the previous orthosymplectic superspin system, we will focus here on the particular distinguished superspin chain system that emerges in the framework of 4D Chern-Simons gauge theory with $OSP(2|2n-2)$ gauge supersymmetry as a super line defects lattice. To calculate the RLL solutions, we will use the possible 3-gradings reported in table (4.38). These two decompositions are obtained by nodes' cutting from the distinguished super Dynkin diagram of the $C(n)$ superalgebra depicted in **Figure 4.6**. The associated super Cartan matrix is

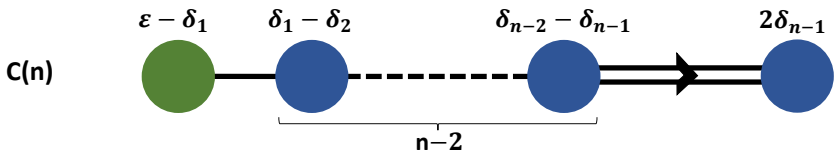

Figure 4.6: Distinguished Dynkin diagram of the $C(n)$ superalgebra, the only fermionic node is represented in green.

$$\alpha_A . \alpha_B = \begin{pmatrix} 0 & -1 & & & \\ -1 & 2 & -1 & & \\ & \ddots & \ddots & \ddots & \\ & & -1 & 2 & -2 \\ & & & -2 & 4 \end{pmatrix} \tag{4.103}$$

where we have only one fermionic simple root of length $\alpha_1^2 = 0$.

4.4.1 The super L-operator $\mathcal{L}^{\mu_1}_{C(n)}$

By considering the distinguished super Dynkin diagram of **Figure 4.6**, and cutting the fermionic node $\alpha_1 = \delta - \varepsilon_1$, one obtains the following 3-grading of the $C(n)$ superalgebra with respect to μ_1 acting as a minuscule coweight

$$osp(2|2n-2) \quad \rightarrow \quad so(2) \oplus sp(2n-2) \oplus N_+ \oplus N_- \tag{4.104}$$

with nilpotent subspaces of dimensions

$$N_\pm = 2\,(n-1) \tag{4.105}$$

To draw the difference with the other possible 3-grading, notice here that the $2n^2+n-2$ dimensions are decomposed like

$$\begin{array}{ccc} 2n^2+n-2 & \rightarrow & 1 \;\oplus\; (n-1)\,[2(n-1)+1] \;\oplus \\ & & N_+ \;\oplus\; N_- \end{array} \tag{4.106}$$

and the fundamental representation $\mathbf{2|2n-2}$ splits as

$$(\mathbf{2|2n-2}) \quad \rightarrow \quad \mathbf{1}_+ \oplus (\mathbf{2n-2})_0 \oplus \mathbf{1}_- \tag{4.107}$$

The two singlets $\mathbf{1}_\pm$ correspond to the $so(2)$ of the cut node with projectors $\varrho_\pm = |\pm\rangle\langle\pm|$, while the subspace $\underline{\mathbf{2n-2}}$ corresponds to the fundamental of $sp(2n-2)$ with projector $\Pi = \sum_{i=1}^{2n-2} |i\rangle\langle i|$. For convenience, we denote the basis states as

$$|2n\rangle \rightarrow |+\rangle \oplus |i\rangle \oplus |-\rangle \tag{4.108}$$

with $1 \leq i \leq 2n-2$ labeling the bosonic states carrying charge 0 with respect to μ_1. We deduce

$$\mu_1 = \varrho_+ + q\Pi - \varrho_- \tag{4.109}$$

with $q = 0$, and therefore

$$z^{\mu_1} = z\varrho_+ + \Pi + z^{-1}\varrho_- \tag{4.110}$$

The nilpotents are generated by the antisymmetric matrices

$$\begin{array}{rcl} X_i & = & |+\rangle\langle i| - |i\rangle\langle -| \\ Y^i & = & |i\rangle\langle +| - |-\rangle\langle i| \end{array} \tag{4.111}$$

that are all of bosonic nature and verify

$$[\mu_1, X_i] = X_i, \qquad [\mu_1, Y^i] = -Y^i, \qquad [X_i, Y^j] = \delta_i^j \mu_1 \tag{4.112}$$

Thus, the oscillator coordinates appearing in the expansions of X and Y

$$\begin{array}{rcccl} X & = & b^i X_i & \in & N_+ \\ Y & = & c_i Y^i & \in & N_- \end{array} \tag{4.113}$$

are also bosonic, and verify the Poisson bracket

$$\{b^i, c_j\}_{PB} = \delta^i_j \tag{4.114}$$

To substitute into the super Lax operator formula (4.49), we moreover calculate the quantities

$$\begin{array}{rclcrcl} X^2 & = & -\mathbf{b}^2 \left|+\right\rangle \left\langle -\right| & , & \mathbf{b}^2 & = & b^i \delta_{ij} b^j \\ Y^2 & = & -\mathbf{c}^2 \left|-\right\rangle \left\langle +\right| & , & \mathbf{c}^2 & = & c_i \delta^{ij} c_j \end{array} \tag{4.115}$$

and

$$X^3 = 0 \quad , \quad Y^3 = 0 \tag{4.116}$$

to write

$$e^X = 1 + X + \frac{1}{2} X^2 \quad , \quad e^Y = 1 + Y + \frac{1}{2} Y^2 \tag{4.117}$$

leading to

$$\mathcal{L}^{\mu_1} = \left(1 + X + \frac{1}{2} X^2 \right) \left(z \varrho_+ + \Pi + z^{-1} \varrho_- \right) \left(1 + Y + \frac{1}{2} Y^2 \right) \tag{4.118}$$

This factorized formula expands in terms of the projectors basis as

$$\begin{array}{rcl} \mathcal{L}^{\mu_1} & = & z \varrho_+ + \Pi + z^{-1} \varrho_- + X \left(\Pi + z^{-1} \varrho_- \right) + \\ & & \left(\Pi + z^{-1} \varrho_- \right) Y + X \left(\Pi + z^{-1} \varrho_- \right) Y + \\ & & \frac{1}{2} X^2 z^{-1} \varrho_- + \frac{1}{2} z^{-1} \varrho_- Y^2 + \frac{1}{2} X^2 z^{-1} \varrho_- Y + \\ & & \frac{1}{2} X z^{-1} \varrho_- Y^2 + \frac{1}{4} X^2 z^{-1} \varrho_- Y^2 \end{array} \tag{4.119}$$

In matrix form, the super L-operator associated to the node μ_1 of $C(n)$ reads in terms of bosonic oscillator coordinates as

$$\mathcal{L}^{\mu_1} = \begin{pmatrix} z + b^i c_i + \frac{1}{4} z^{-1} \mathbf{b}^2 \mathbf{c}^2 & b^i + \frac{1}{2} z^{-1} \mathbf{b}^2 c_i & -\frac{1}{2} z^{-1} \mathbf{b}^2 \\ c_i + \frac{1}{2} z^{-1} \mathbf{c}^2 b^i & \delta^i_j + z^{-1} b^i c_i & -z^{-1} b^i \\ -\frac{1}{2} z^{-1} \mathbf{c}^2 & -z^{-1} c_i & z^{-1} \end{pmatrix} \tag{4.120}$$

4.4.2 The super L-operator $\mathcal{L}^{\mu_n}_{C(n)}$

The second 3-grading of the Lie superalgebra $C(n)$ is associated to the minuscule -like coweight μ_n which is dual to α_n. We can read this specific decomposition by cutting the bosonic node $2\delta_{n-1}$ from the distinguished super Dynkin diagram of Figure 4.6. This yields

$$osp(2|2n-2) \quad \rightarrow \quad A_1 \oplus sl(1|n-1) \oplus N_+ \oplus N_- \tag{4.121}$$

with

$$N_\pm = \frac{n(n+1)}{2} - 1 \tag{4.122}$$

In this case, the fundamental representation of $osp(2|2n-2)$ splits into the fundamental and anti-fundamental of $sl(1|n-1)$ with opposite charges

$$(\mathbf{2}|\mathbf{2n-2}) \quad \rightarrow \quad (\mathbf{1}|\mathbf{n-1})_{+\frac{1}{2}} \oplus (\mathbf{1}|\mathbf{n-1})_{-\frac{1}{2}} \tag{4.123}$$

To distinguish the bosonic and fermionic states, we can moreover write $(\mathbf{2}|\mathbf{2n-2})$ as the sum of four subspaces

$$(\mathbf{2}|\mathbf{2n-2}) \quad \rightarrow \quad (\mathbf{1}|\mathbf{0})_{+\frac{1}{2}} \oplus (\mathbf{0}|\mathbf{n-1})_{+\frac{1}{2}} \oplus (\mathbf{0}|\mathbf{n-1})_{-\frac{1}{2}} \oplus (\mathbf{1}|\mathbf{0})_{-\frac{1}{2}} \tag{4.124}$$

corresponding to the following decomposed basis

$$|2n\rangle \quad \rightarrow \quad |0\rangle \oplus |i\rangle \oplus |\bar{i}\rangle \oplus |\bar{0}\rangle \tag{4.125}$$

with $1 \leq i \leq n-1$ and $\overline{n-1} \leq \bar{\imath} \leq \bar{1}; \bar{\imath} = 2n-1-i$ labeling fermionic states, and the singlets of bosonic nature. In this basis, we realize the adjoint action of the μ_n as

$$\mu_n = \frac{1}{2}\varrho + \frac{1}{2}\Pi - \frac{1}{2}\bar{\Pi} - \frac{1}{2}\bar{\varrho} \tag{4.126}$$

with

$$\varrho = |0\rangle\langle 0|\,, \qquad \Pi = \sum_{i=1}^{n-1} |i\rangle\langle i|\,, \qquad \bar{\Pi} = \sum_{\bar{\imath}=2n-2}^{n} |\bar{\imath}\rangle\langle\bar{\imath}|\,, \qquad \bar{\varrho} = |\bar{0}\rangle\langle\bar{0}| \tag{4.127}$$

The elements of the nilpotents $N_\pm = (n-1) + \frac{(n-1)n}{2}$ are realized by means of two types of generators like

$$\begin{array}{rcl} X & = & b^i X_i + b^{\{i\bar{j}\}} X_{\{i\bar{j}\}} \\ Y & = & c_{\bar{\imath}} Y^{\bar{\imath}} + c_{\{\bar{\imath}j\}} Y^{\{\bar{\imath}j\}} \end{array} \tag{4.128}$$

where

$$\begin{array}{rcl} X_i & = & |0\rangle\langle\bar{\imath}| - |i\rangle\langle\bar{0}| \\ Y^{\bar{\imath}} & = & |\bar{0}\rangle\langle i| - |\bar{\imath}\rangle\langle 0| \end{array} \tag{4.129}$$

are of fermionic nature, while

$$\begin{array}{rcl} X_{\{i\bar{j}\}} & = & |i\rangle\langle\bar{j}| - |j\rangle\langle\bar{\imath}| \\ Y^{\{\bar{\imath}j\}} & = & |\bar{\imath}\rangle\langle j| - |\bar{j}\rangle\langle i| \end{array} \tag{4.130}$$

are bosonic. These generators verify

$$\begin{array}{rcl} [\mu_n, X_i] = X_i & , & [\mu_n, Y^{\bar{\imath}}] = Y^{\bar{\imath}} \\ \left[\mu_n, X_{\{i\bar{j}\}}\right] = X_{\{i\bar{j}\}} & , & \left[\mu_n, Y^{\{\bar{\imath}j\}}\right] = Y^{\{\bar{\imath}j\}} \end{array} \tag{4.131}$$

Using properties of this realisation such as $X^2 = Y^2 = 0$ and

$$X\Pi = X\varrho = 0 \qquad , \qquad \varrho Y = \Pi Y = 0, \tag{4.132}$$

the L-operator $\mathcal{L}^{\mu_n}$ is simplified as

$$\begin{array}{rcl} \mathcal{L}^{\mu_n} & = & (1+X)\left(z^{\frac{1}{2}}\varrho + z^{\frac{1}{2}}\Pi + z^{-\frac{1}{2}}\bar{\Pi} + z^{-\frac{1}{2}}\bar{\varrho}\right)(1+Y) \\ & = & z^{\frac{1}{2}}\varrho + z^{-\frac{1}{2}}\Pi + z^{\frac{1}{2}}\bar{\Pi} + z^{-\frac{1}{2}}\bar{\varrho} + z^{-\frac{1}{2}}X\left(\bar{\varrho} + \bar{\Pi}\right) + \\ & & z^{-\frac{1}{2}}\left(\bar{\varrho} + \bar{\Pi}\right)Y + z^{-\frac{1}{2}}X\bar{\Pi}Y \end{array} \tag{4.133}$$

where we have also used

$$z^{\mu_n} = z^{\frac{1}{2}}\varrho + z^{\frac{1}{2}}\Pi + z^{-\frac{1}{2}}\bar{\Pi} + z^{-\frac{1}{2}}\bar{\varrho} \tag{4.134}$$

The matrix representation reads as

$$\mathcal{L}^{\mu_n} = \begin{pmatrix} z^{\frac{1}{2}} - z^{-\frac{1}{2}} b^i c_i & z^{-\frac{1}{2}} b^i c_{ij} & z^{-\frac{1}{2}} b^i & 0 \\ -z^{-\frac{1}{2}} b^{ij} c_i & z^{\frac{1}{2}}\mathbf{1}_{n-1} + z^{-\frac{1}{2}}\Phi\Psi & z^{-\frac{1}{2}}\Phi & -z^{-\frac{1}{2}} b^i \\ z^{-\frac{1}{2}} c_i & z^{-\frac{1}{2}}\Psi & z^{-\frac{1}{2}}\mathbf{1}_{n-1} & 0 \\ 0 & -z^{-\frac{1}{2}} c_i & 0 & z^{-\frac{1}{2}} \end{pmatrix} \tag{4.135}$$

where (b^i, c_i) are couples of fermionic oscillators and $\Phi = b^{\{i\bar{j}\}} X_{\{i\bar{j}\}}$ and $\Psi = c_{\{\bar{\imath}j\}} Y^{\{\bar{\imath}j\}}$ are symmetric $(n-1)(n-1)$ matrices carrying bosonic oscillator coordinates as

$$\Phi = \begin{pmatrix} b^{1\bar{1}} & \dots & b^{1\overline{(n-1)}} \\ \vdots & \ddots & \vdots \\ b^{(n-1)\bar{1}} & \dots & b^{(n-1)\overline{(n-1)}} \end{pmatrix} \tag{4.136}$$

and

$$\Psi = \begin{pmatrix} c_{\bar{1}1} & \dots & c_{\bar{1}(n-1)} \\ \vdots & \ddots & \vdots \\ c_{\overline{(n-1)}1} & \dots & c_{\overline{(n-1)}(n-1)} \end{pmatrix} \tag{4.137}$$

Their product is given by

$$\Phi\Psi = \begin{pmatrix} b^{1\bar{i}}c_{\bar{i}1} & \dots & b^{1\bar{i}}c_{\bar{i}(n-1)} \\ \vdots & \ddots & \vdots \\ b^{(n-1)\bar{i}}c_{\bar{i}1} & \dots & b^{(n-1)\bar{i}}c_{\bar{i}(n-1)} \end{pmatrix} \tag{4.138}$$

4.5 Super L-operators of D-type

To complete the list of orthosymplectic minuscule super Lax operators, we investigate in this section solutions for the family of superspin chains defined by the internal symmetry of type

$$D(m|n) = osp(2m|2n), \qquad m \geq 3, n \geq 1 \tag{4.139}$$

Recall that this Lie superalgebra is characterized by a rank equal to $m+n$ and $2(m+n)^2-m+n$ dimensions that split into even dimensions of the subalgebra

$$D(m|n)_{\bar{0}} = D_m \oplus C_n = so(2m) \oplus sp(2n) \tag{4.140}$$

and odd dimensions of the bi-representation

$$D(m|n)_{\bar{1}} = (2m, 2n) \tag{4.141}$$

Among the different varieties of superspin chains of $D(m|n)$ type in one to one with the

$$\mathbf{n}_{D(m|n)} = \frac{(n+m)!}{n! \times m!} \tag{4.142}$$

possible super Dynkin diagrams $\left\{\mathfrak{D}[D(m|n)]^{(\kappa)}, \kappa = 1, ..., \mathbf{n}_{D(m|n)}\right\}$ of this superalgebra, we focus here on the distinguished superspin chain associated to the simple roots

$$\delta_a - \delta_{a+1}, a = 1, ..., n-1 \quad ; \quad \gamma = \delta_n - \varepsilon_1 \quad ; \quad \varepsilon_i - \varepsilon_{i+1}, i = 1, ..., m-1 \quad ; \quad \varepsilon_{m-1} + \varepsilon_m \tag{4.143}$$

This roots set containing one only fermionic root γ, emerges from the choice of the weight basis as in (4.20). The distinguished super Dynkin diagram depicted in **Figure 4.7** is behind the 3-gradings reported in Table (4.38) where we have three minuscule -like coweights

$$\mu_{n+1} \quad , \quad \mu_{n+m-1} \quad , \quad \mu_{n+m} \tag{4.144}$$

By considering in the four-dimensional Chern-Simons theory with $OSP(2m|2n)$ super gauge symmetry the crossing of a super Wilson line is in the fundamental representation $\boldsymbol{R} = \mathbf{2m|2n}$, and a 't Hooft line having one of the minuscule magnetic charges (4.144), we can calculate three families of minuscule super Lax operators as solutions to the RLL equations for the $D(m|n)$ superspin chain system. We will begin here below by applying the nodes' cutting based approach for the node α_{n+1} to compute $\mathcal{L}^{\mu_{n+1}}_{D_{m|n}}$. Than, we will see that the two last nodes μ_{n+m-1} and μ_{n+m} act similarly on the level of the Lie superalgebra, and the solutions $\mathcal{L}^{\mu_{m+n-1}}_{D_{m|n}}, \mathcal{L}^{\mu_{m+n}}_{D_{m|n}}$ can be treated collectively.

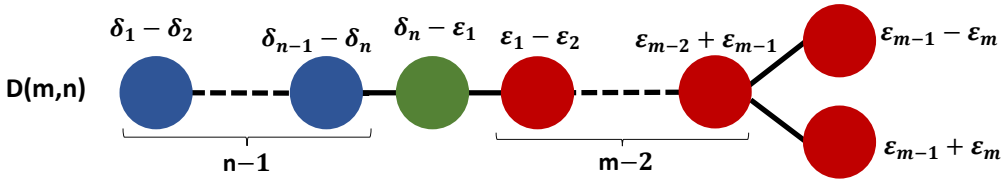

Figure 4.7: Distinguished Dynkin diagram of the $D(m|n)$ superalgebra having one fermionic simple root in Green color. Here, we have $\varepsilon_i^2=1$ and $\delta_a^2=-1$.

4.5.1 The super L-operator $\mathcal{L}^{\mu_{n+1}}_{D_{m|n}}$

The first Levi -like decomposition of the Lie superalgebra $osp(2m|2n)$ given in Table (4.38) reads as

$$osp(2m|2n) \quad \rightarrow \quad N_+ \oplus so(2) \oplus osp(2m-2|2n) \oplus N_- \tag{4.145}$$

with nilpotent -like subspaces

$$\dim N_\pm = \left[2\left(m+n-1\right)\right]_\pm$$

Following from this 3-grading, the representation $\mathbf{2m|2n}$ should also split like

$$(\mathbf{2m|2n}) \quad \rightarrow \quad (\mathbf{1}|0)_+ \oplus (\mathbf{2m-2|2n})_0 \oplus (\mathbf{1|0})_- \tag{4.146}$$

Accordingly, we will choose the basis states as follows

$$|A\rangle \quad \rightarrow \quad |+\rangle \oplus |i\rangle \oplus |\alpha\rangle \oplus |-\rangle \tag{4.147a}$$

where $i=1,\ldots,2m-2$ labels bosonic the states of $\mathbf{2m-2}$, and $\alpha=1,\ldots,2n$ labels the fermionic states of $\mathbf{2n}$; the $|\pm\rangle$ concern singlets of the $so(2)$. The adjoint action of the minuscule coweight reads as

$$\mu_{n+1}=\Pi_+ + q\left(\Pi_i+\Pi_\alpha\right)-\Pi_- \tag{4.147b}$$

with $q=0$, and the projectors

$$\begin{array}{rclcrcl} \Pi_+ &=& |+\rangle\langle+| & ; & \Pi_- &=& |-\rangle\langle-| \\ \Pi_i &=& \sum\limits_{i=1}^{2m-2} |i\rangle\langle i| & ; & \Pi_\alpha &=& \sum\limits_{\alpha=1}^{2n} |\alpha\rangle\langle\alpha| \end{array} \tag{4.148}$$

Hence, we have

$$z^{\mu_{n+1}} = z\Pi_+ + \Pi_i + \Pi_\alpha + z^{-1}\Pi_- \tag{4.149}$$

The operators X and Y expand in terms of two types of matrix generators and space coordinates as

$$\begin{array}{rclcrcl} X &=& \mathcal{B}^{\mathrm{A}}\boldsymbol{X}_{\mathrm{A}} &=& b^i X_i + \beta^\alpha \mathcal{X}_\alpha & \in & N_+ \\ Y &=& \mathcal{C}_{\mathrm{A}}\boldsymbol{Y}^{\mathrm{A}} &=& c_i Y^i + \gamma_\alpha \mathcal{Y}^\alpha & \in & N_- \end{array} \tag{4.150}$$

where the (b^i,c_i) form $2m-2$ couples of bosonic oscillators and $(\beta^\alpha,\gamma_\alpha)$ form $2n$ fermionic oscillators because we have

$$\begin{array}{rclcrcl} X_i &=& |+\rangle\langle i| - |i\rangle\langle-| & , & \mathcal{X}_\alpha &=& |+\rangle\langle\alpha| - |\alpha\rangle\langle-| \\ Y^i &=& |i\rangle\langle+| - |-\rangle\langle i| & & \mathcal{Y}^\alpha &=& |\alpha\rangle\langle+| - |-\rangle\langle\alpha| \end{array} \tag{4.151}$$

In order to substitute to the formula $\mathcal{L}^{\mu_{n+1}}=e^X z^{\mu_{n+1}} e^Y$(4.49), we define the quantities

$$\begin{array}{rclcrcl} X^2 &=& -\mathcal{B}^2\,|+\rangle\langle-| & , & \mathcal{B}^2 &=& (\mathbf{b}^2+\beta^2) \\ Y^2 &=& -\mathcal{C}^2\,|-\rangle\langle+| & & \mathcal{C}^2 &=& (\mathbf{c}^2+\gamma^2) \end{array} \tag{4.152}$$

with

$$\begin{array}{rclcrcl} \mathbf{b}^2 & = & b^i\delta_{ij}b^j & , & \beta^2 & = & \beta^\alpha\delta_{\alpha\beta}\beta^\beta \\ \mathbf{c}^2 & = & c_i\delta^{ij}c_j & , & \gamma^2 & = & \gamma_\alpha\delta^{\alpha\beta}\gamma_\beta \end{array} \tag{4.153}$$

Thus we have

$$\mathcal{L}^{\mu_1} = (1 + X + \frac{X^2}{2})\left(z\Pi_+ + \Pi_0 + z^{-1}\Pi_-\right)(1 + Y + \frac{Y^2}{2}) \tag{4.154}$$

which yields the graded matrix solution (4.155) where we have multiplied by the factor z. Recall that the Yang Baxter as well as the RLL equations are invariant by the multiplication by a function of the spectral parameter z [1].

$$\mathcal{L}^{\mu_{n+1}}_{D_{m|n}} = \begin{pmatrix} z^2+z(b^ic_i + b^\alpha c_\alpha)+\frac{(\mathbf{b}^2+\beta^2)(\mathbf{c}^2+\gamma^2)}{4} & zb^i+c_i\frac{\mathbf{b}^2+\beta^2}{2} & z\beta^\alpha+\frac{\left(\mathbf{b}^2+\beta^2\right)}{2}\gamma_\alpha & \frac{-(\mathbf{b}^2+\beta^2)}{2} \\ zc_i + \frac{(\mathbf{c}^2+\gamma^2)}{2}b^i & z\delta^i_j + b^ic_j & b^i\gamma_\beta & -b^i \\ z\gamma_\alpha + \frac{(\mathbf{c}^2+\gamma^2)}{2}\beta^\alpha & \beta^\alpha c_j & z\delta^\alpha_\beta + \beta^\alpha\gamma_\beta & -\beta^\alpha \\ -\frac{(\mathbf{c}^2+\gamma^2)}{2} & -c_i & -\gamma^\alpha & 1 \end{pmatrix} \tag{4.155}$$

4.5.2 The super L-operator $\mathcal{L}^{\mu_{m+n}}_{D_{m|n}}$

The super Lax operator $\mathcal{L}^{\mu_{n+1}}_{D_{m|n}}$ calculated in the previous subsection can be referred to as a vectorial solution in analogy to the bosonic $\mathcal{L}^{\mu_1}_{D_N}$ having a similar matrix structure emerging from a similar action of the minuscule coweight. The minuscule coweights μ_{m+n-1} and μ_{m+n} of $D(m|n)$ that we will be focusing on here are of spinorial nature as can be observed in the distinguished Dynkin diagram **Figure 4.7**. These are exchanged by a $\mathbb{Z}_2$ automorphism on graphical level and their associated coweights have equivalent actions on elements of the Lie superalgebra $osp(2m|2n)$. In fact, if we cut any of these two nodes, we obtain a sub-diagram corresponding to the $sl(m|n)$ sub- superalgebra. This is the 3-grading given in Table (4.38) as follows

$$osp(2m|2n) \quad \longrightarrow \quad so\,(2) \oplus sl(m|n) \oplus N_+ \oplus N_- \tag{4.156}$$

with

$$\dim N_+ = \dim N_- = \frac{(m+n)^2 + n - m}{2} \tag{4.157}$$

Since these coweights lead to the same Levi-like decomposition, the resulting minuscule super Lax operators are equivalent

$$\mathcal{L}^{\mu_{m+n-1}}_{D_{m|n}} \qquad \simeq \qquad \mathcal{L}^{\mu_{m+n}}_{D_{m|n}} \tag{4.158}$$

We can focus in what follows on the explicit computation of the solution $\mathcal{L}^{\mu_{m+n}}_{D_{m|n}}$, i.e. by considering the super 't Hooft line with magnetic charge μ_{m+n} acting on the representation $\mathbf{R} = 2m|2n$ of a super Wilson line as

$$(\mathbf{2m}|\mathbf{2n}) = (\mathbf{m}|\mathbf{n})_{+\frac{1}{2}} \oplus (\bar{\mathbf{m}}|\bar{\mathbf{n}})_{-\frac{1}{2}} \tag{4.159}$$

where $(\mathbf{m}|\mathbf{n})_{\pm\frac{1}{2}}$ represent the fundamnetal and anti-fundamental of $sl(m|n)$, we will associate to their states the following basis vectors

$$\begin{array}{ll} |i\rangle & 1 \leq i \leq m \\ |\alpha\rangle & m+1 \leq \alpha \leq m+n \\ |\bar{\imath}\rangle & n+m+1 \leq \bar{\imath} \leq n+2m \\ |\bar{\alpha}\rangle & 2m+n+1 \leq \bar{\alpha} \leq 2n+2m \end{array} \tag{4.160}$$

In this basis, the adjoint action of μ_{m+n} is

$$\mu_{m+n}=\frac{1}{2}\left[\sum_{i=1}^{m}|i\rangle\langle i| + \sum_{\alpha=m+1}^{m+n}|\alpha\rangle\langle\alpha|\right] - \frac{1}{2}\left[\sum_{\bar{\imath}=n+m+1}^{n+2m}|\bar{\imath}\rangle\langle\bar{\imath}| + \sum_{\bar{\alpha}=n+2m+1}^{2m+2n+1}|\bar{\alpha}\rangle\langle\bar{\alpha}|\right] \tag{4.161}$$

Now for the realization of X and Y as elements of N_+ and N_-, one can see that their dimensions split as

$$\dim N_\pm = \frac{m(m-1)}{2} + \frac{n(n+1)}{2} + mn \tag{4.162}$$

and are thus generated by three types of matrices that we denote as

$$\begin{array}{lcl;{\quad}lcl} X_{[i\bar{j}]} & = & |i\rangle\langle\bar{j}| - |j\rangle\langle\bar{i}| & Y^{[\bar{j}i]} & = & |\bar{j}\rangle\langle i| - |\bar{i}\rangle\langle j| \\ X_{\left(\alpha\bar{\beta}\right)} & = & |\alpha\rangle\left\langle\bar{\beta}\right| + |\beta\rangle\langle\bar{\alpha}| & Y^{\left(\bar{\beta}\alpha\right)} & = & \left|\bar{\beta}\right\rangle\langle\alpha| + |\bar{\alpha}\rangle\langle\beta| \\ \mathcal{X}_{i\bar{\alpha}} & = & |i\rangle\langle\bar{\alpha}| & \mathcal{Y}^{\bar{\alpha}i} & = & |\bar{\alpha}\rangle\langle i| \end{array} \tag{4.163}$$

We introduce $2[m(m-1)/2 + n(n+1)/2]$ bosonic oscillators $(b^{[ij]}, c_{[\bar{j}\bar{i}]})$, $(\mathrm{f}^{\left(\alpha\bar{\beta}\right)}, \mathrm{g}_{\left(\bar{\beta}\alpha\right)})$ and $2mn$ fermionic ones $(\beta^{i\bar{\alpha}}, \gamma_{\bar{\alpha}i})$ in order to write the expansions

$$X = b^{[i\bar{j}]} X_{[i\bar{j}]} + \mathrm{f}^{(\alpha\bar{\beta})} X_{\left(\alpha\bar{\beta}\right)} + \beta^{i\bar{\alpha}} \mathcal{X}_{i\bar{\alpha}} \tag{4.164}$$

and

$$Y = c_{[\bar{j}i]} Y^{[\bar{j}i]} + \mathrm{g}_{(\bar{\beta}\alpha)} Y^{(\alpha\bar{\beta})} + \gamma_{\bar{\alpha}i} \mathcal{Y}^{\bar{\alpha}i} \tag{4.165}$$

In this case we have $X^2 = Y^2 = 0$ and thus $e^x = I + X$ and $e^Y = I + Y$ which simplifies the super Lax operator formula (4.49) to

$$\mathcal{L}^{\mu_{m+n}} = z^{\mu_{m+n}} + z^{\mu_{m+n}} Y + X z^{\mu_{m+n}} + X z^{\mu_{m+n}} Y \tag{4.166}$$

where

$$z^{\mu_{m+n}} = z^{\frac{1}{2}} \left[\sum_{i=1}^{m} |i\rangle\langle i| + \sum_{\alpha=m+1}^{m+n} |\alpha\rangle\langle\alpha| \right] + z^{-\frac{1}{2}} \left[\sum_{\bar{\imath}=n+m+1}^{n+2m} |\bar{\imath}\rangle\langle\bar{\imath}| + \sum_{\bar{\alpha}=n+2m+1}^{2m+2n+1} |\bar{\alpha}\rangle\langle\bar{\alpha}| \right] \tag{4.167}$$

We obtain after calculations

$$\begin{array}{rcl} \mathcal{L}^{\mu_{m+n}} & = & z^{\mu_{m+n}} + z^{-\frac{1}{2}} X + z^{-\frac{1}{2}} Y \\ & & + z^{-\frac{1}{2}} (\Phi\Psi + \Lambda\Gamma + \mathrm{f}^{\left(\alpha\bar{\beta}\right)} \gamma_{\bar{\alpha}i} X_{\left(\alpha\bar{\beta}\right)} \mathcal{Y}^{\bar{\alpha}i} + \beta^{i\bar{\alpha}} \mathrm{g}_{\left(\bar{\beta}\alpha\right)} \mathcal{X}_{i\bar{\alpha}} Y^{\left(\bar{\beta}\alpha\right)}) \\ & & + z^{-\frac{1}{2}} \beta^{i\bar{\alpha}} \gamma_{\bar{\alpha}i} \mathcal{X}_{i\bar{\alpha}} \mathcal{Y}^{\bar{\alpha}i} \end{array}$$

we define the matrices

$$\begin{array}{lcl} \Phi = b^{[i\bar{j}]} X_{[i\bar{j}]} & , & \Psi = c_{[\bar{j}i]} Y^{[\bar{j}i]} \\ \Lambda = \mathrm{f}^{\left(\alpha\bar{\beta}\right)} X_{\left(\alpha\bar{\beta}\right)} & , & \Gamma = \mathrm{g}_{\left(\bar{\beta}\alpha\right)} Y^{\left(\bar{\beta}\alpha\right)} \end{array} \tag{4.168}$$

IN matrix language, this is equivalent, after multiplication by an overall factor $z^{\frac{1}{2}}$, to

$$\mathcal{L}^{\mu_{m+n}}_{D(m|n)} = \begin{pmatrix} z + \Phi\Psi + \beta^{i\bar{\alpha}}\gamma_{\bar{\alpha}i} & \beta^{i\bar{\alpha}} c_{\left\{\bar{\beta}\alpha\right\}} & \beta^{i\bar{\alpha}} & \Phi \\ \mathrm{b}^{\left(\alpha\bar{\beta}\right)}\gamma_{\bar{\alpha}i} & z + \Lambda\Gamma & \Lambda & 0 \\ \gamma_{\bar{\alpha}i} & \Gamma & z & 0 \\ \Psi & 0 & 0 & z \end{pmatrix} \tag{4.169}$$

with

$$\Phi = \begin{pmatrix} 0 & \dots & b^{1\overline{m}} \\ \vdots & \ddots & \vdots \\ b^{m\bar{1}} & \dots & 0 \end{pmatrix} \quad ; \quad \Psi = \begin{pmatrix} 0 & \dots & c_{\bar{1}m} \\ \vdots & \ddots & \vdots \\ c_{\overline{m}1} & \dots & 0 \end{pmatrix} \tag{4.170}$$

and

$$\Lambda = \begin{pmatrix} b^{1\bar{1}} & \dots & b^{1\overline{n}} \\ \vdots & \ddots & \vdots \\ b^{n\bar{1}} & \dots & b^{n\overline{n}} \end{pmatrix} \quad ; \quad \Gamma = \begin{pmatrix} c_{\bar{1}1} & \dots & c_{\bar{1}n} \\ \vdots & \ddots & \vdots \\ c_{\overline{n}1} & \dots & c_{\overline{n}n} \end{pmatrix} \tag{4.171}$$

CHAPTER 5

BRANE REALISATION OF SUPERSPIN CHAINS

For the last chapter, we refuge to string theory for a better scope and understanding of the Gauge/ Integrability correspondence. We show how the lower-dimensional superspin chain system can be represented in brane language by taking advantage of dualities. We focus on the $sl(m|n)$ Lie superalgebra and show how its Z_2-grading leads to exotic features of the associated superspin chain, and how it affects the brane realization in Type IIA strings and M-theory.
We begin by recalling some basic features and of these integrable systems translated into an algebraic setup. Then, we give a generalization of the Algebra/ Homology correspondence to the super case in order to motivate and justify the brane realization given later on.

5.1 Superspin Chain : Algebraic setup

As a first step towards the string realization, we first need to determine the degrees of freedom and symmetries characterizing a superspin chain system, that should be translated in terms of branes. We begin by giving an overview of these features for a general superspin chain with internal symmetry g_{BF}, then we closely examine the $sl(3|2)$ model of A-type superspin chains that we will focus on for the rest of this chapter.

5.1.1 Degrees of freedom and symmetries

We recall that a closed XXX Heisenberg superspin chain of length L and internal symmetry g_{BF} is defined by :

- A set of L nodes labeled by $1 \leq l \leq L$ positioned along one space direction.
- A set of L identical "Super" atoms Υ_l sitting on chain nodes, in the sense that their internal quantum states are valued in the same representation $\mathbf{R}$ of a Lie superalgebra g_{BF}. This is what distinguishes a superspin chain from a bosonic spin chain system.
- A twisted boundary condition $\Upsilon_{L+1} \equiv \Upsilon_1$ leading to a closed chain with a space dimension that can be identified with the circle $\mathbb{S}^1_\theta = \{\Upsilon_l\}_{1\leq l\leq L}$.

In this image, each super atom is characterized by :

- The extrinsic degree of freedom ξ given by its position in the real space space $\mathbb{S}^1_\theta$.

- Internal quantum states characterized by the highest weight vector λ_A of the representation $\mathbf{R}$ of $\mathbf{g}$. Here, the label A corresponds to the graded space of the Lie superalgebra
- The spectral parameter z appearing as the parameter of the Yangian, also interpreted as the rapidity of the super atom.

We can therefore write the quantum state of a super atom $|\Upsilon\rangle$ using these parameters as

$$|\Psi_A\rangle = |\xi; \lambda_A, z\rangle \tag{5.1}$$

which denotes the ground state of Υ. For the full superspin chain of super atoms $\Upsilon_1, \Upsilon_2, ..., \Upsilon_L$, we should have L copy of the parameters (5.1), we add the label l such that $1 \leq l \leq L$ in order to write the ground state or the pseudo-vacuum of the chain as the combination

$$|\Psi[\varrho]\rangle = \sum_{A,l} \varrho_l^A \left|\Psi_A^l\right\rangle \tag{5.2}$$

with

$$\left|\Psi_A^l\right\rangle = \left|\xi^l; \lambda_A^l, z^l\right\rangle \tag{5.3}$$

Here as well, the ξ^l play the role of extrinsic degrees of freedom of the chain while the intrinsic ones are given by the spectral parameters z^l, and the weight vectors λ_A^l as introduced in (4.22). These elements as well as their associated symmetries are analyzed here below. In fact, we have two types of symmetries

A) Flavour symmetry

The classical variable position ξ_l can be replaced by a unitary symmetry parameter allowing to distinguish between the L different positions and therefore super atoms. This is achieved by the flavour symmetry group

$$U(L) = U(1) \times SU(L) \tag{5.4}$$

This symmetry has weight vectors $\{\mathbf{e}_l\}$ in one to one with the parameters $\{\xi_l\}$. Equation (5.3) therefore becomes

$$\left|\Psi_A^l\right\rangle = \left|\mathbf{e}_l; \lambda_A^l, z_l\right\rangle \tag{5.5}$$

B) Internal super symmetry

Concerning the internal superspin states of the chain, we will chooseto focus here as well as in the rest of this study on the simple example of states in the fundamental representation $m|n$ of the linear $sl(m|n)$ Lie superalgebra. The internal characteristics linked to such superspin chain are as introduced in the previous chapter, see (4.22). We will further analyze here some relevant internal symmetry properties for the brane realization. In these regards, notice that the weight vectors λ_A of $m|n$ are identified with the unit weight vectors ϵ_A as

$$\lambda_A = \epsilon_A \qquad , \qquad A = 1, ..., m+n \tag{5.6}$$

where the fundamental $m|n$ corresponds to $R(\epsilon_1)$. In terms of this basis vectors, the $m+n-1$ simple roots

$$\alpha_1, ..., \alpha_{m+n-1} \tag{5.7}$$

are written like

$$\alpha_{A,A+1} = \epsilon_A - \epsilon_{A+1} \tag{5.8}$$

These roots can be bosonic or fermioinc depending on the grading of the labels, where we have in general

$$|\alpha_{A,A+1}| = |\epsilon_A| + |\epsilon_{A+1}| = |A| + |A+1| \tag{5.9}$$

In total, the symmetry of the superspin chain system is given by the product of the internal and external symmetries

$$U(L) \times \mathbf{g} \tag{5.10}$$

The quantum representation of the pseudo-vacuum (5.5) can be written as the factorization

$$\left|\Psi_A^l\right\rangle \quad = \quad |\mathbf{e}_l\rangle \otimes \left|\lambda_A^l\right\rangle \tag{5.11}$$

Notice here that the $|z_l\rangle$ in fact correspond to the $Y_{SL(m|n)}$, but are linked here to $sl(m|n)$ for simplicity.

5.1.2 Varieties of the A- type Superspin Chain

We exploit now the simple $sl(3|2)$ model as a representative of the $sl(m|n)$ family with $m > n$ (or equivalently $m \neq n$), we focus on the Lie super algebraic properties of $sl(3|2)$ to explain the nature of such superspin chains and the existence of different varieties due to the Z_2-grading of the internal space. For the $sl(3|2)$ superspin chain, one has 10 varieties in one to one with the possible Dynkin diagrams. This diversity emerges from the graded nature of the vector space which is given for the $sl(3|2)$ Lie superalgebra by the space $\mathbb{R}^{3|2}$ generated by the weight sates

$$\epsilon_1, \quad \epsilon_2, \quad \epsilon_3, \quad \epsilon_4, \quad \epsilon_5 \tag{5.12}$$

This basis contains three even-graded weight vectors and two odd-graded, it differs depending on the ordering of these weight vectors. We have here 10 possible permutations of the (5.12), and therefore 10 basis for the fundamental $\mathbf{3|2}$. These are listed in 5.13a where we labeled the three bosonic as ε_i $(i = 1, 2, 3)$ and the two fermioinic as δ_a $(a = 1, 2)$

basis I	$(\varepsilon_1, \varepsilon_2, \varepsilon_3, \delta_1, \delta_2)$	basis VI	$(\delta_1, \varepsilon_1, \varepsilon_2, \delta_2, \varepsilon_3)$
basis II	$(\varepsilon_1, \varepsilon_2, \delta_1, \delta_2, \varepsilon_3)$	basis VII	$(\delta_1, \delta_2, \varepsilon_1, \varepsilon_2, \varepsilon_3)$
basis III	$(\delta_1, \varepsilon_1, \varepsilon_2, \varepsilon_3, \delta_2)$	basis VIII	$(\varepsilon_1, \delta_1, \delta_2, \varepsilon_2, \varepsilon_3)$
basis IV	$(\varepsilon_1, \varepsilon_2, \delta_1, \varepsilon_3, \delta_2)$	basis IX	$(\delta_1, \varepsilon_1, \delta_2, \varepsilon_2, \varepsilon_3)$
basis V	$(\varepsilon_1, \delta_1, \varepsilon_2, \delta_2, \varepsilon_3)$	basis X	$(\varepsilon_1, \delta_1, \varepsilon_2, \varepsilon_3, \delta_2)$

(5.13a)

As a result, the four simple roots of the $sl(3|2)$ Lie superalgebras can be of one of three types

$\alpha_A = \epsilon_A - \epsilon_{A+1}$	Degree	Length
$\varepsilon_i - \varepsilon_{i+1}$	0	2
$\varepsilon_i - \delta_a$	1	0
$\delta_a - \delta_{a+1}$	0	-2

(5.14)

The length here is linked to the super Cartan matrices

$$\mathcal{K}_{AB}^{sl_{3|2}} = \alpha_A.\alpha_B \tag{5.15}$$

which take exotic values that do not occur for bosonic Lie algebras; in particular the negative -2 length. In consequence, the Cartan matrix for a Lie superalgebra is not unique; it depends on the basis choice (5.13a). Moreover, in order to distinguish these different types of simple roots in the Dynkin diagram description of any superalgebra, we will have to introduce "colored" Dynkin super diagrams. These are characterised by a number of fermioinc nodes and a number of bosonic nodes that can be associated to roots with vanishing or non-vanishing length. As these Dynkin diagrams will play a major role in the brane realisation of the internal symmetry, we will draw them here below for the different possible non-redundant cases of the $sl(3|2)$ superalgebra. We will also give the list of Cartan matrices that allow to directly read the lengths for the four simple roots.

- **Basis I :**
  For the basis I of (5.13a), the four simple roots read like

$$\alpha_1 = \varepsilon_1 - \varepsilon_2, \quad \alpha_2 = \varepsilon_2 - \varepsilon_3, \quad \alpha_3 = \varepsilon_3 - \delta_1, \quad \alpha_4 = \delta_1 - \delta_2 \tag{5.16}$$

  The associated super Cartan matrix denoted as $\mathcal{K}^I_{sl_{3|2}}$ is given by the following

$$\mathcal{K}^I_{sl_{3|2}} = \begin{pmatrix} 2 & -1 & 0 & 0 \\ -1 & 2 & -1 & 0 \\ 0 & -1 & 0 & +1 \\ 0 & 0 & +1 & -2 \end{pmatrix} \tag{5.17}$$

  from which we can deduce that the corresponding Dynkin super diagram DSD_I has three bosonic simple roots $\alpha_1, \alpha_2, \alpha_4$ and one fermionic α_3 as
  (**a**) Two bosonic simple roots with length $\alpha_1^2 = \alpha_2^2 = 2$ given by red nodes in the Dynkin diagram description.
  (**b**) One bosonic simple root with $\alpha_4^2 = -2$ given by the blue node.
  (**c**) One fermionic simple root remarkably having the property $\alpha_3^2 = 0$, and represented by the green node.
  The corresponding Dynkin super diagram is given in **Figure** 5.1.

Figure 5.1: The Dynkin super diagram corresponding to the basis I of $sl(3|2)$.

- **Basis II :**
  The four simple roots are given by

$$\alpha_1 = \varepsilon_1 - \varepsilon_2, \quad \alpha_2 = \varepsilon_2 - \delta_1, \quad \alpha_3 = \delta_1 - \delta_2, \quad \alpha_4 = \delta_2 - \varepsilon_3 \tag{5.18}$$

  The Cartan matrix $\mathcal{K}^{II}_{sl_{3|2}}$ corresponding to the second basis reads as

$$\mathcal{K}^{II}_{sl_{3|2}} = \begin{pmatrix} 2 & -1 & 0 & 0 \\ -1 & 0 & +1 & 0 \\ 0 & +1 & -2 & +1 \\ 0 & 0 & +1 & 0 \end{pmatrix} \tag{5.19}$$

  The associated Dynkin super diagram has four nodes: two bosonic and two fermionic. The two bosonic roots obey $\alpha_1^2 = 2$ and $\alpha_3^2 = -2$, while the fermionic one obeys $\alpha_1^2 = 0$. These are represented in Figure 5.2

Figure 5.2: The Dynkin super diagram corresponding to the basis II of $sl(3|2)$.

- **Basis III :**
  The simple roots are realised by

$$\alpha_1 = \delta_1 - \varepsilon_1, \quad \alpha_2 = \varepsilon_1 - \varepsilon_2, \quad \alpha_3 = \varepsilon_2 - \varepsilon_3, \quad \alpha_4 = \varepsilon_3 - \delta_2 \tag{5.20}$$

  such that the Cartan matrix $\mathcal{K}^{III}_{sl_{3|2}}$ reads as

$$\mathcal{K}^{III}_{sl_{3|2}} = \begin{pmatrix} 0 & -1 & 0 & 0 \\ -1 & 2 & -1 & 0 \\ 0 & -1 & 2 & -1 \\ 0 & 0 & -1 & 0 \end{pmatrix} \tag{5.21}$$

  The Dynkin super diagram for this basis is given by **Figure** 5.3.

Figure 5.3: The Dynkin super diagram corresponding to the basis III of $sl(3|2)$.

- **Basis IV :**
  In this case, we have

$$\alpha_1 = \varepsilon_1 - \varepsilon_2, \quad \alpha_2 = \varepsilon_2 - \delta_1, \quad \alpha_3 = \delta_1 - \varepsilon_3, \quad \alpha_4 = \varepsilon_3 - \delta_2 \tag{5.22}$$

  with the Cartan matrix $\mathcal{K}^{IV}_{sl_{3|2}}$

$$\mathcal{K}^{IV}_{sl_{3|2}} = \begin{pmatrix} 2 & -1 & 0 & 0 \\ -1 & 0 & +1 & 0 \\ 0 & +1 & 0 & -1 \\ 0 & 0 & -1 & 0 \end{pmatrix} \tag{5.23}$$

  and the Dynkin super diagram as in **Figure** 5.4

Figure 5.4: The Dynkin super diagram corresponding to the basis IV of $sl(3|2)$.

- **Basis V :**
  We have for the fifth basis

$$\alpha_1 = \delta_1 - \varepsilon_1, \quad \alpha_2 = \varepsilon_1 - \varepsilon_2, \quad \alpha_3 = \varepsilon_2 - \delta_2, \quad \alpha_4 = \delta_2 - \varepsilon_3 \tag{5.24}$$

  meaning that the Cartan matrix $\mathcal{K}^{V}_{sl_{3|2}}$ reads as

$$\mathcal{K}^{V}_{sl_{3|2}} = \begin{pmatrix} 0 & -1 & 0 & 0 \\ -1 & 2 & -1 & 0 \\ 0 & -1 & 0 & +1 \\ 0 & 0 & +1 & 0 \end{pmatrix} \tag{5.25}$$

  and the corresponding Dynkin super diagram is as drawn in **Figure** 5.5.

Figure 5.5: The Dynkin super diagram corresponding to the basis V of $sl(3|2)$.

- **Basis VI :**
  This case is very special, it corresponds to the distinguished basis. In particular, all its weight vectors are arranged in such a way that all the four simple roots are fermionic

$$\alpha_1 = \varepsilon_1 - \delta_1, \quad \alpha_2 = \delta_1 - \varepsilon_2, \quad \alpha_3 = \varepsilon_2 - \delta_2, \quad \alpha_4 = \delta_2 - \varepsilon_3 \tag{5.26}$$

  Its associated super Cartan matrix also has a unique form where all the diagonal values vanish.

$$\mathcal{K}^{VI}_{sl_{3|2}} = \begin{pmatrix} 0 & +1 & 0 & 0 \\ +1 & 0 & -1 & 0 \\ 0 & -1 & 0 & +1 \\ 0 & 0 & +1 & 0 \end{pmatrix} \tag{5.27}$$

  The distinguished Dynkin super diagram (*DDSD* for short) has all nodes in green as depicted in **Figure** 5.6.

Figure 5.6: The distinguished Dynkin super diagram corresponding to the basis VI of $sl(3|2)$.

Regarding the other basis VII, VIII, IX and X, they are actually equivalent to I, II, III and IV due to the mirror symmetry associated with the reflection

$$\boldsymbol{r} : \alpha_A \to -\alpha_{5-A} \qquad , \qquad \boldsymbol{r}^2 = I_{id} \tag{5.28}$$

This property also manifests in the Dynkin super diagrams of these basis that are reflections of the ones given here. Their associated Cartan matrices should also have the same values of diagonal entries, but in opposite order.

5.2 Super Algebra/ Homology

In this section, we make a further step towards the brane realization of the systems symmetries by focusing on the super internal symmetry. We take advantage of the known results on complex surfaces with ADE singularities, and investigate their extension to complex manifolds with super singularity given by $sl(m|n)$, that will be useful for the string compactification in the the brane theory. Mainly, we will exploit here the exotic properties of the colored Dynkin super diagrams in order to translate simple roots to 2-cycles of the complex manifolds.

5.2.1 Bosonic geometry

By comparing algebraic properties of the bosonic $sl(5)$ and the super $sl(3|2)$ symmetry, we begin here by constructing the 2-cycle homology for singularity related to superalgebras, and

Figure 5.7: On the left, the Dynkin super diagram of the distinguished $sl(3|2)$. On the right, the Dynkin diagram of $sl(5)$.

propose a complex super geometry. Starting from the graphical descriptions of $sl(5)$ and $sl(3|2)$ (**Figure 5.7**) that look similar due to their linear form, we observe that the the superalgebra is characterized by colored roots verifying

$$\alpha_3^2 = 0 \quad , \quad \alpha_4^2 = -2 \quad , \quad \alpha_3.\alpha_4 = +1 \tag{5.29}$$

in contrast to the $sl\,(5)$ roots that obey

$$\tilde{\alpha}_a^2 = +2 \quad , \quad \tilde{\alpha}_a.\tilde{\alpha}_{a+1} < 0 \tag{5.30}$$

These values allow to interpret the complex ALE surfaces $\tilde{\mathcal{S}}$ with $sl\,(5)$ geometry in terms of intersecting 2-cycles $\tilde{\mathfrak{C}}_a$, with the intersection matrix reading as

$$\mathcal{I}_{ab}^{sl_5} = \tilde{\mathfrak{C}}_a.\tilde{\mathfrak{C}}_b \tag{5.31}$$

This is actually the opposite of the Cartan

$$\mathcal{I}_{ab}^{sl_5} = -\mathcal{A}_{ab}^{sl_5} \begin{pmatrix} -2 & 1 & 0 & 0 \\ 1 & -2 & 1 & 0 \\ 0 & 1 & -2 & 1 \\ 0 & 0 & 1 & -2 \end{pmatrix} \tag{5.32}$$

The 2-cycles hence verify

$$\tilde{\mathfrak{C}}_a^2 = -2 \quad , \quad \tilde{\mathfrak{C}}_a.\tilde{\mathfrak{C}}_{a+1} = 1 \tag{5.33}$$

and we deduce that they are given by complex projective lines $\mathbb{CP}_a^1$ (2-spheres) that intersect transversally according to the bosonic Dynkin diagram of $sl(5)$. The four simple roots $\tilde{\alpha}_a = \tilde{\varepsilon}_a - \tilde{\varepsilon}_{a+1}$ $(a = 1, 2, 3, 4)$ of $sl\,(5)$ are in one to one with four 2-cycles $\tilde{\mathfrak{C}}_a$ in the resolved ALE surface $\tilde{\mathcal{S}}^{sl_5}$. The Algebra/Homology correspondence used here is represented by

Lie algebra $sl(5)$	homology of ALE surfaces $\tilde{\mathcal{S}}^{sl_5}$
$\tilde{\alpha}_a^2 = 2$	$\tilde{\mathfrak{C}}_a^2 = -2$
$\tilde{\varepsilon}_a^2 = 1$	$\tilde{E}_a^2 = -1$

(5.34)

This bosonic correspondence is used first to geometrize the superspin chain bosonic flavor symmetry, and then to generalize to the super internal symmetry by analogy. The corresponding cycles realizations are given by:

Flavor symmetry $U\,(L) = U\,(1) \times SU\,(L)$

For the bosonic $su\,(L)$ Lie algebra contained in the $sl\,(L)$, the Algebra/ Homology correspondence is directly applied and yields $L-1$ intersecting 2-spheres $\tilde{\mathfrak{C}}_a$ with $a = 1, ..., L-1$, and self intersection

$$\tilde{\mathfrak{C}}_a^2 = -2 \tag{5.35}$$

These should have large volumes, since they are associated with a flavor symmetry and not a gauge invariance.

Graded $SL(3|2)$ invariance

As a generalization of the Algebra/ Homology correspondence, we propose here a Super Algebra/Homology that should have the form

Lie superalgebra $sl(3\|2)$	graded surfaces $\mathcal{S}^{sl_{3\|2}}$
graded roots α_A	graded cycles $\mathfrak{C}_A$
graded weights ϵ_A	graded divisors E_A

(5.36)

To define these graded geometries for the super symmetry, we begin by recalling here below the singular surfaces associated to the bosonic case and then turn to treating the $SL(m|n)$ super symmetry by focusing on the $SL(3|2)$ case. In general, the complex surfaces with Du Val singularities, regarding complex surfaces V/Γ with orbifold symmetry given by finite groups Γ contained in $GL(2)$, can be defined by local equations

$$f(x,y,z)=0 \tag{5.37}$$

These singularity equations are embedded in $\mathbb{C}^3$ with local coordinates (x,y,z). They are resolved according to Dynkin diagrams of the simply laced ADE symmetries as classifies in Table **5.1**

Geometry	$f(x,y,z)$	Γ	Cartan	Resolution graph and 2-cycles
A_{n-1}	$x^2+y^2+z^n$	Z_n	$A[A_{n-1}]$	
D_n	$x^2+y^2z+z^{n-1}$	BD_{4n-8}	$A[D_n]$	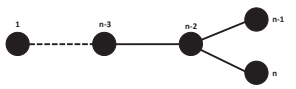
E_6	$x^2+y^3+z^4$	BT_{24}	$A[E_6]$	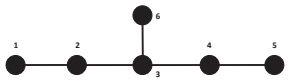
E_7	$x^2+y^3+yz^3$	BO	$A[E_7]$	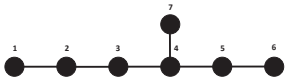
E_8	$x^2+y^3+z^5$	BIcosa	$A[E_8]$	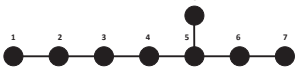

Table 5.1: The defining equations of the complex surfaces with ADE geometries. The 2-cycle homology of the surface is given by the ADE Dynkin diagrams with roots describing the 2-cycles.

Here, BD_{4n-8} refers to the Binary- Dihedral group, BT_{24} to the Binary-Tetrahedral group, BO is the Binary-Octahedral group and BIcosa represents the Binary Icosahedral. For the simplest example of A_1, (5.37) is written as

$$x^2+y^2+z^2=0 \tag{5.38}$$

which describes a sphere vanishing at $(x,y,z)=(0,0,0)$. Moreover, by writing $u=i(x+iy), v=i(x-iy)$, this singularity simply becomes

$$uv=z^2 \tag{5.39}$$

For the larger $SU(n)$ family, we have

$$uv = z^n \tag{5.40}$$

In terms of weights $\tilde{\varepsilon}_a$ and roots $\tilde{\alpha}_a = \tilde{\varepsilon}_a - \tilde{\varepsilon}_{a+1}$, the resolution of the $SU(n)$ singularity is described by

$$\tilde{\varepsilon}_1 - \tilde{\varepsilon}_N = \sum \tilde{\alpha}_a \tag{5.41}$$

For the $sl(5)$ singularity, we write

$$\tilde{\varepsilon}_1 - \tilde{\varepsilon}_5 = \tilde{\alpha}_1 + \tilde{\alpha}_2 + \tilde{\alpha}_3 + \tilde{\alpha}_4 \tag{5.42}$$

which by using the Algebra /Homology correspondence, is equivalent to

$$\tilde{E}_1 - \tilde{E}_5 = \tilde{\mathfrak{C}}_1 + \tilde{\mathfrak{C}}_2 + \tilde{\mathfrak{C}}_3 + \tilde{\mathfrak{C}}_4 \tag{5.43}$$

For the other ADE singularities, the homology of their resolved singularities involves 2-spheres intersecting according to the shape of their Dynkin diagrams.

5.2.2 Super $sl(3|2)$ geometry

Now, we exploit the Algebra/ Homology correspondence in order to propose surfaces with super symmetry, by focusing on the $SL(3|2)$ as the leading model of the $SL(m|n)$. We begin by writing the weights in terms of super roots as

$$\epsilon_1 - \epsilon_5 = \alpha_1 + \alpha_2 + \alpha_3 + \alpha_4 \tag{5.44}$$

where we have used the expressions of ϵ_2, ϵ_3 and ϵ_4

$$\epsilon_1 - \epsilon_5 = (\epsilon_1 - \epsilon_2) + (\epsilon_2 - \epsilon_3) + (\epsilon_3 - \epsilon_4) + (\epsilon_4 - \epsilon_5) \tag{5.45}$$

By interpreting this as a blowing up of the singularity, we can translate (5.44) in terms of the graded divisors E_A and cycles $\mathfrak{C}_A$

$$E_1 - E_5 = \mathfrak{C}_1 + \mathfrak{C}_2 + \mathfrak{C}_3 + \mathfrak{C}_4 \tag{5.46}$$

such that the intersections of these graded cycles in the graded surface $\mathcal{S}^{sl_{3|2}}$ having an $SL(3|2)$ geometry is described by

$$\mathcal{I}_{AB}^{sl_{3|2}} = \mathfrak{C}_A.\mathfrak{C}_B \tag{5.47}$$

and

$$\mathfrak{C}_A = E_A - E_{A+1} \tag{5.48}$$

Moreover, by using

$$E_A.E_B = -g_{AB} \tag{5.49}$$

we find that

$$\mathcal{I}_{AB}^{sl_{3|2}} = \begin{pmatrix} -2 & 1 & 0 & 0 \\ 1 & -2 & 1 & 0 \\ 0 & 1 & 0 & -1 \\ 0 & 0 & -1 & 2 \end{pmatrix} \tag{5.50}$$

meaning that the self intersections of the 2-cycles of the graded $\mathcal{S}^{sl_{3|2}}$ take the values

$$\mathfrak{C}_1^2 = \mathfrak{C}_2^2 = -2 \quad , \quad \mathfrak{C}_3^2 = 0 \quad , \quad \mathfrak{C}_4^2 = 2 \tag{5.51}$$

We think of these as closed Rieman surfaces Σ_g without boundary such that their topology is given by the Euler characteristics

$$\chi_g = 2g - 2 \tag{5.52}$$

Here, the positive integer g is the genus of Σ_g, and the topological χ_g has an indefinite sign in agreement with the values of (5.51). The value $g = 0$ yields to the 2-sphere $\chi_0 = 2$, $g = 1$ yields a 2-torus, while for $g = 2$ we obtain the double 2-torus with $\chi_2 = -2$ which characterizes these graded surfaces having higher genus Rieman surfaces Σ_g. These 2-cycles associated to the graded surface $\mathcal{S}^{sl_{3|2}}$ are depicted in **Figure 5.8**.

Figure 5.8: Rieman surfaces with genus g and Euler characteristics $2 - 2g$. The $g = 0$ corresponds to the 2-sphere. The $g = 1$ gives the 2-torus. The $g = 2$ describes the genus 2 Rieman surface.

5.3 Superspin chain realization in superstring theory

Thanks to the algebraic features of the symmetries of the superspin chain investigated above, we can embed this integrable system in superstring theory. We will consider here the distinguished $sl(3|2)$ superspin chain, and yield the type II strings realization and then uplift to M-theory. But before that, we begin by listing the relevant symmetry elements, in particular the weight vectors and the roots that will play a major role in the brane interpretations.

5.3.1 Ground state of the superspin chain

The system we will focus on here concerns the distinguished $sl(3|2)$ superspin chain of L nodes characterized by the total symmetry $U(L) \times SL(3|2)$, and the atomic states

$$\left|\Psi^l_A\right\rangle = \left|\epsilon_A\right\rangle_{sl_{3|2}} \otimes \left|\mathbf{e}^l\right\rangle_{u_L} \tag{5.53}$$

Notice that this factorisation of the wave function is permitted thanks to the commutation of the $SL(3|2)$ and $U(L)$ gauge symmetries. We write for the elements $g \in sl(3|2)$ and $\tilde{g} \in u(L)$

$$[\tilde{g}, g] = 0 \tag{5.54}$$

The superspin states (5.53) are expressed in terms of the following elements

algebra	simple roots	weight basis vectors
$sl(3\|2)$	$\alpha_1, ..., \alpha_4$	$\epsilon_1, ..., \epsilon_5$
$su(L)$	$\tilde{\alpha}_1, ..., \tilde{\alpha}_L$	$\mathbf{e}_1, ..., \mathbf{e}_L$

(5.55)

where the quantum states $|\epsilon_A\rangle$ correspond to the vector basis of the fundamental representation $\mathcal{R}(\omega_1)$ of $\mathbf{3|2}$. They obey the $sl(3|2)$ super-traceless condition

$$\sum_{A=1}^{5} (-)^{|A|} \epsilon_A = 0 \qquad , \qquad |\epsilon_A| \equiv |A| \tag{5.56}$$

and are linked to the simple roots α_A. Concerning the roots, notice that the transition from $|\epsilon_A\rangle$ to its neighbour $|\epsilon_{A+1}\rangle$ is generated by the step operator $E_{-\alpha_A}$ of $sl(3|2)$

$$|\epsilon_{A+1}\rangle = E_{-\alpha_A}|\epsilon_A\rangle \tag{5.57}$$

which can also be represented in terms of roots as $|\epsilon_A - \alpha_A\rangle$. Moreover, by using $E_{-\alpha_A} = |\epsilon_{A+1}\rangle\langle\epsilon_A|$ and the formal identification $E_{-\alpha_A} \sim \underline{\alpha}_A$, we can think about α_A as

$$\underline{\alpha}_A \sim |\epsilon_{A+1}\rangle\langle\epsilon_A| \tag{5.58}$$

For a generic transition $|\epsilon_A\rangle \to |\epsilon_B\rangle$, the needed root is given by $\alpha_{AB} = \epsilon_A - \epsilon_B$.

Concerning the states $|\mathbf{e}_l\rangle$ associated to the flavor symmetry, the Highest Weight vector of $U(L) = U(1) \times SU(L)$ is given by $\mathbf{e}^1$, and the traceless condition for $SU(L)$ by

$$\sum_{l=1}^{N_f} \mathbf{e}^l = 0 \tag{5.59}$$

Similarly to the internal symmetry, we can write the roots of the flavor symmetry sector such that

$$\begin{array}{rcl} |\mathbf{e}_{l+1}\rangle & = & \tilde{E}_{-\tilde{\alpha}_l}|\mathbf{e}_l\rangle \\ \underline{\tilde{\alpha}}_l & \sim & |\mathbf{e}_{l+1}\rangle\langle\mathbf{e}_l| \end{array}$$

Finally, the transition from a quantum state $|\epsilon_A\rangle \otimes |\mathbf{e}_l\rangle$ of the superspin chain to the state $|\epsilon_B\rangle \otimes |\mathbf{e}_{l'}\rangle$ is generated by the tensor product $E_{-\alpha_{AB}} \otimes \tilde{E}_{-\tilde{\alpha}_{ll'}}$. For neighbors, the transition from $|\epsilon_A\rangle \otimes |\mathbf{e}_l\rangle$ to $|\epsilon_{A+1}\rangle \otimes |\mathbf{e}_{l+1}\rangle$ is given by

$$E_{-\alpha_A} \otimes \tilde{E}_{-\tilde{\alpha}_l} \sim \underline{\alpha}_A \otimes \underline{\tilde{\alpha}}_l \tag{5.60}$$

5.3.2 Embedding in Type IIA branes

We give now the brane construction of the superspin chain quantum state in the framework of type II superstrings. Notice that this construction follows the approach of [122] which treated the Type IIB realization in the same context by taking advantage of the correspondence with 4D Chern Simons and line defects.

First of all, recall that the type IIA superstring theory is defined on a 10 dimensional space-time that we denote as $\mathcal{M}_{1,9}$, it contains three pairs of p-branes given by :

- F1 strings associated NS5
- Electric D0 and magnetic D6.
- Electric D2 and its dual D4.

The weight vectors and roots of (5.55) are translated in terms of these branes following Table (5.2) which describes the dictionary of the quantum state symmetries in the context of type IIA strings.

Since the $sl(3|2)$ weight vectors are of graded nature, we have the following brane intersections where $\mathcal{K}_{AB}$ is the distinguished $sl(3|2)$ Cartan matrix.

$$\begin{array}{rcl} \alpha_A.\epsilon_A & = & (-)^{|A|} \\ \alpha_A.\epsilon_{A+1} & = & -(-)^{|A+1|} \\ \alpha_A.\alpha_B & = & \mathcal{K}_{AB} \end{array} \tag{5.61}$$

Similar relations hold for the flavor sector but with bosonic Cartan matrix values. We deduce that the realization of the $|\Psi_A^l\rangle$ states of the distinguished $sl(3|2)$ superspin chain in terms of type IIA branes includes two stacks of branes : The first one given by $\{NS5_{\mathbf{A}}\}$ labeled by the subscript $A = 1, ..., 5$, and the second one by the $\{D6^l\}$ with upperscript $l = 1, ..., L$. These are transversed by four types of transitions as described below:

super chain	type IIA brane		
$\|\epsilon_A\rangle$	NS5_{ϵ_A}	$\equiv$	NS5_A
$\underline{\alpha}_A$	D2_{α_A}	$\equiv$	D2_{AA+1}
$\|e^l\rangle$	D6_{e^l}	$\equiv$	D6^l
$\underline{\tilde{\alpha}}^l$	$\text{D2}_{\tilde{\alpha}^l}$	$\equiv$	D2^{ll+1}
$\|\epsilon_A, e^l\rangle$	$\text{D4}_{\epsilon_A,e^l}$	$\equiv$	D4^l_A

Table 5.2: Lie superalgebra/Type IIA brane correspondence: Basic weight vectors are associated with NS5 and D4 branes. Simple roots are associated with D2 branes.

- The transition between two neighboring $\text{NS5}_{\mathbf{A}}$ and $\text{NS5}_{\mathbf{A+1}}$ is insured by the $\text{D2}_{\mathbf{AA+1}}$ brane between them. Hence, for a generic transition between $\text{NS5}_{\mathbf{A}}$ and $\text{NS5}_{\mathbf{B}}$, the mediator is $\text{D2}_{\mathbf{AB}}$
- The transition between the D6^l and its neighbor D6^{l+1} is mediated by the flavored $\text{D2}^{l,l+1}$ brane, meaning that D6^l and $\text{D6}^{l'}$ are mediated by a flavored $\text{D2}^{ll'}$.
- For the neighboring $\text{D4}^l_{\mathbf{A}}$ and $\text{D4}^l_{\mathbf{A+1}}$, they are mediated by a $\text{D2}_{\mathbf{AA+1}}$. At the same time, we have between a $\text{D4}^l_{\mathbf{A}}$ and a $\text{D4}^{l+1}_{\mathbf{A}}$ a D2^{ll+1}. Eventually, the transition between $\text{D4}^l_{\mathbf{A}}$ and $\text{D4}^{l+1}_{\mathbf{A+1}}$ is obtained by two steps given by $\text{D2}_{\mathbf{AA+1}}\text{D2}^{ll+1}$.
- The last type of transitions emerges between the gauge $\text{NS5}_{\mathbf{A}}$ and the flavored D6^l, it is realized by the $\text{D4}^l_{\mathbf{A}}$ brane.

The full type IIA branes included in this realization intersect in the 10D space-time as represented in Table 5.62.

10D	$\mathbb{R}_0$	$\mathbb{R}_1$	$\mathbb{C}_{23}$	$\mathbb{R}_4$	$\mathbb{R}_5$	$\tilde{\mathbb{R}}^4$
$NS5_{\mathbf{A}}$	x	x	x	$\{\xi^4_A\}$	$\{\xi^5_A\}$	$\tilde{\mathbb{R}}^2_{\|\mathbf{A}\|}$
$D2_{\mathbf{AA+1}}$	x	x	$\{z_{\mathbf{A}}\}$	$[\xi^4_A, \xi^4_{A+1}]$	$\{\xi^5_A\}$	0^4
$D4^l_{\mathbf{A}}$	x	x	$\{w^l_{\mathbf{A}}\}$	$\{\xi^4_A\}$	$[\xi^5_A, \varrho^5_l]$	$\tilde{\mathbb{R}}^2_{\|\mathbf{A}\|}$
$D6^l$	x	x	$\{u^l\}$	x	$\{\varrho^5_l\}$	$\tilde{\mathbb{R}}^4$

(5.62)

Concerning this representation, notice the following features :

- The cross (x) means that the dimension of type IIA is filled while the other boxes generate the transverse spaces of the branes; they give the precise positions of the branes which can be interpreted as scalar fields in super QFT at low energies.
- The four dimension euclidian $\tilde{\mathbb{R}}^4$ with coordinates (X^6, X^7, X^8, X^9) factorises like $\tilde{\mathbb{R}}^2_{\bar{\mathbf{0}}} \times \tilde{\mathbb{R}}^2_{\bar{\mathbf{1}}}$ where $\bar{\mathbf{0}}$ and $\bar{\mathbf{1}}$ refer to the $\mathbb{Z}_2$-degree of $|A|$.
- The singleton $\{\xi^4_A\}$ (resp. $\{\varrho^5_l\}$) means that the $NS5_{\mathbf{A}}$ brane (resp. D6^l) is located on the fourth-axis at the point $X^4 = \xi^4_A$ (resp. the fifth-axis $\{X^5 = \varrho^5_l\}$).
- The positions are ordered like $\xi^4_A < \xi^4_{A+1}$ and $\xi^5_A < \varrho^5_l$ as well as $\varrho^5_l < \varrho^5_{l+1}$.
- The interval $[\xi^4_A, \xi^4_{A+1}]$ belongs to the fourth-axis, it is filled by $D2_{\mathbf{AA+1}}$ stretching between NS5_A and NS5_{A+1}. The lengths $|\xi^4_A - \xi^4_{A'}|$ give the masses of the propagating quantum states between the NS5 branes.

- The interval $[\xi_A^5, \varrho_l^5]$ belongs to the fifth-axis, and is filled by $D4_A^l$ stretching between NS5_A and D6^l.

- The positions of the ϱ_l^5's must be pushed far away (say to infinity) from the ξ_A^4s since the D6^ls are flavor branes with symmetry $U(N_f)$ containing the diagonal $U(1)^{N_f}$. Therefore, the intervals $[\xi_A^5, \varrho_l^5]$ of the $D4_{\mathbf{A}}^l$ branes should be thought of as $[\xi_A^5, +\infty[$ as required by the flavor symmetry and the realisation given in [122].

We can moreover distinguish the bosonic and fermionic sectors underlying the $SL(3|2)$ gauge symmetry in the brane realization 5.62. In particular, the five states dispatch like

$$|\epsilon_A\rangle = |\varepsilon_a\rangle_{\frac{2}{5}} \oplus |\delta_i\rangle_{\frac{3}{5}} \qquad , \qquad |\varepsilon_a| = 0, \qquad |\delta_i| = 1 \tag{5.63}$$

where the even graded states $|\varepsilon_a\rangle$ carry charge $\frac{2}{5}$ with respect to $sl(1)$, and the odd graded $|\delta_i\rangle$ carry the charge $\frac{3}{5}$. This is due to the form of the even part of the $sl(3|2)$ Lie superalgebra

$$sl(3|2)_{\bar{0}} = sl(3) \oplus sl(1) \oplus sl(2) \tag{5.64}$$

such that $|\varepsilon_a\rangle$ is a triplet of $sl(3)$, and $|\delta_i\rangle$ is a doublet of $sl(2)$. This $\mathbb{Z}_2$-grading is manifested on the level of the p-branes $\text{NS5}_{\mathbf{A}}$, $\text{D2}_{\mathbf{AA+1}}$, D6^l and $D4_{\mathbf{A}}^l$ by distinguishing the label $\mathbf{A}$ to $|a| = \bar{0}$ and $|i| = \bar{1}$ leading to two sectors :

- The $sl(3)$ sector :
  It includes three bosonic weight vectors ε_a in addition to the bosonic simple roots α_1, α_2. Their corresponding type IIA branes are given by : (i) three bosonic like NS5_a expanding in $\mathbb{R}_0 \times \mathbb{R}_1$, $\mathbb{C} = \mathbb{R}_2 + i\mathbb{R}_3$ and $\mathbb{R}_6 \times \mathbb{R}_7$, (ii) two $\text{D2}_{a,a+1}$ branes with $a = 1, 2$ stretching along $\mathbb{R}_0 \times \mathbb{R}_1$ and in the one-dimensional space $[\xi_a^4, \xi_{a+1}^4]$ between NS5_a and NS5_{a+1}, and (iii) $3L$ bosonic D4_a^l expanding in $\mathbb{R}_0 \times \mathbb{R}_1 \times [\xi_a^5, \infty[\times \mathbb{R}_6 \times \mathbb{R}_7$. This configuration is collected in Table (5.65)

10D	$\mathbb{R}_0$	$\mathbb{R}_1$	$\mathbb{C}_{23}$	$\mathbb{R}_4$	$\mathbb{R}_5$	$\mathbb{R}_6$	$\mathbb{R}_7$	$\mathbb{R}_8$	$\mathbb{R}_9$
$NS5_a$	x	x	x	$\{\xi_a^4\}$	$\{\xi_a^5\}$	x	x	0	0
$D2_{a,a+\mathbf{1}}$	x	x	$\{z_a\}$	$[\xi_a^4, \xi_{a+1}^4]$	$\{\xi_a^5\}$	0	0	0	0
$D4_a^l$	x	x	$\{w_a^l\}$	$\{\xi_a^4\}$	$[\xi_a^5, \infty[$	x	x	0	0

(5.65)

- The $sl(2)$ sector :
  This sector corresponds to the two odd-graded weight vectors δ_1 and δ_2 and the bosonic-like simple root α_4. It involves the branes listed below in Table (5.66), where the D2 and D4 branes have similar configurations as before but we can see that the fermionic like $NS5_{3+i}$ with $i = 1, 2$ differ than the $NS5_a$ in the sense that they expand in $\mathbb{R}_8 \times \mathbb{R}_9$ instead of $\mathbb{R}_6 \times \mathbb{R}_7$.

10D	$\mathbb{R}_0$	$\mathbb{R}_1$	$\mathbb{C}_{23}$	$\mathbb{R}_4$	$\mathbb{R}_5$	$\mathbb{R}_6$	$\mathbb{R}_7$	$\mathbb{R}_8$	$\mathbb{R}_9$
$NS5_{3+i}$	x	x	x	$\{\xi_{3+i}^4\}$	$\{\xi_{3+i}^5\}$	0	0	x	x
$D2_{45}$	x	x	$\{z_4\}$	$[\xi_4^4, \xi_6^4]$	$\{\xi_4^5\}$	0	0	0	0
$D4_{3+i}^l$	x	x	$\{w_{3+i}^l\}$	$\{\xi_{3+i}^4\}$	$[\xi_{3+i}^5, \infty[$	0	0	x	x

(5.66)

- The $sl(1)$ sector :
  This one links the previous $sl(3)$ and $sl(2)$ sectors by means of the fermionic-like D2_{34} brane, it stretches between the bosonic NS5_3 and the fermionic NS5_4 as described below.

10D	$\mathbb{R}_0$	$\mathbb{R}_1$	$\mathbb{C}_{23}$	$\mathbb{R}_4$	$\mathbb{R}_5$	$\mathbb{R}_6$	$\mathbb{R}_7$	$\mathbb{R}_8$	$\mathbb{R}_9$
D2_{34}	x	x	$\{z_3\}$	$[\xi_3^4, \xi_4^4]$	$\{\xi_3^5\}$	0	0	0	0

(5.67)

5.3.3 Embedding in M- theory

The distinguished $sl(3|2)$ superspin chain system studied here can be realized in the 11-dimensional M-theory by direct uplifting of the of type IIA string realization described before. In particular, the 11-dimensional space-time is obtained from the ten dimensional $\mathcal{M}_{1,9}$ by means of the circle $\mathbb{S}^1_M \sim R_M e^{i\vartheta}$ such that

$$\mathcal{M}_{1,10} = \mathcal{M}_{1,9} \times \mathbb{S}^1_M \tag{5.68}$$

As a result of this compactification, the NS5 and D4 branes of type IIA both become M5-branes of M-theory, while the D2 merges into an M2 brane. We have the equivalence

	$\mathcal{M}_{1,10}$	$\mathcal{M}_{1,9}$
i)	$M5$	$NS5$
ii)	$M5$	$M5/\mathbb{S}^1_M \sim D4$

,

	$\mathcal{M}_{1,10}$	$\mathcal{M}_{1,9}$
i)	$M2$	$D2$
ii)	$M2$	$M2/\mathbb{S}^1_M \sim F1$

(5.69)

The worlvolumes in 11D are such

11D	:	10D	$\mathbb{S}^1_M$
$\mathrm{M5}_A$	:	$\mathrm{NS5}_A$	
$\mathrm{M5}^l_A$	:	$\mathrm{D4}^l_A$	x

,

11D	:	10D	$\mathbb{S}^1_M$
$\mathrm{M2}_{AA+1}$	:	$\mathrm{D2}_{AA+1}$	
M2	:	F1	x

(5.70)

with the cross (x) indicating that the M5 merging from the D4 fills the direction of the compactification circle. The same holds for the M2 brane merging from the one-dimensional F1.

Concerning the geometrical singularity description, for example the A_{L-1} ALE singularity distinguishing the L coincident D6-branes with the flavour symmetry $U(L)$, it can be understood in the framework of M-theory in terms of the orbifold $\mathbb{C}^2/\mathbb{Z}_{N_f}$ with discrete group $\mathbb{Z}_{N_f}$ acting on complex parameters z and z' in $\mathbb{C}_{23}$ as

$$z \to e^{\frac{2i\pi}{N}} z \qquad , \qquad z' \to e^{-\frac{2i\pi}{N}} z' \tag{5.71}$$

Or, it can be represented in $\mathbb{C}^3[u, v, w]$ by the equation

$$uv = w^N \tag{5.72}$$

or more particularly by

$$uv = \prod_{l=1}^{N} (w - \zeta_l) \tag{5.73}$$

involving L complex parameters ζ_l. In the language of 2-cycle homology, the A_{N-1} topology is thought of in terms of the fibration $\mathcal{S}_N = \Sigma_N \times \mathbb{C}$ with Σ_N being a complex curve (2-cycle) given by the intersection of generating 2-cycles C_l with complexified Kahler moduli $t_l = \zeta_l - \zeta_{l+1}$. The algorithm of the M-theory realizations for the superspin chain symmetries is given in this case by Table (5.3.3)

super chain	type IIA	M-branes		
$\vert\epsilon_A\rangle$	$\mathrm{NS5}_{\epsilon_A}$	$\mathrm{M5}_{\epsilon_A}$	$\equiv$	$\mathrm{M5}_A$
$\underline{\alpha}_A$	$\mathrm{D2}_{\alpha_A}$	$\mathrm{M2}_{\alpha_A}$	$\equiv$	$\mathrm{M2}_{AA+1}$
$\vert e^l\rangle$	$\mathrm{D6}_{e^l}$	C^2/Z_{N_f}		
$\vert\epsilon_A, e^l\rangle$	$\mathrm{D4}_{\epsilon_A,e^l}$	$\mathrm{M5}_{\epsilon_A,e^l}$	$\equiv$	$\mathrm{M5}^l_A$

Table 5.3: Symmetry/M-brane correspondence.

The M-branes intersections are written in terms of the Cartan matrix $\mathcal{A}^{sl_L}_{ll'}$ of $sl\,(L)$ as

$$\begin{array}{lcl} \tilde{\alpha}_l.\mathbf{e}_l & = & +1 \\ \tilde{\alpha}_l.\mathbf{e}_{l+1} & = & -1 \\ \tilde{\alpha}_l.\tilde{\alpha}_{l'} & = & \mathcal{A}^{sl_L}_{ll'} \end{array} \tag{5.74}$$

Thanks to these promotions, we can directly translate the type IIA configuration of table (5.62) into the wanted M-theory realization of the $sl(3|2)$ superspin chain state

11D	$\mathbb{R}_0$	$\mathbb{R}_1$	$\mathcal{S}_N$	$\mathbb{R}_4$	$\tilde{\mathbb{R}}^4$
$M5_{\mathbf{A}}$	x	x	Σ_A	$\{\xi^4_A\}$	$\tilde{\mathbb{R}}^2_{\lvert\mathbf{A}\rvert}$
$M2_{\mathbf{AA+1}}$	x	x	(z_A, z'_A)	$[\xi^4_A, \xi^4_{A+1}]$	0^4
$M5^l_{\mathbf{A}}$	x	x	Σ^l_A	$\{\xi^4_A\}$	$\tilde{\mathbb{R}}^2_{\lvert\mathbf{A}\rvert}$

(5.75)

where we have :

- Five $\mathrm{M5}_{\mathbf{A}}$ branes for the $sl_{3|2}$ supersymmetry, expanding in the complex surface $\mathcal{S}_N$ along the complex line Σ_A given by the fibration $\mathbb{C} \times \{z_A\}$ with $z_A = X^2_A + iX^3_A$.
- Four $\mathrm{M2}_{\mathbf{AA+1}}$ mediating between the $\mathrm{M5}_{\mathbf{A}}$ and $\mathrm{M5}_{\mathbf{A+1}}$ where the complex z'_A reads as $e^{X^5_A + i\vartheta_A}$ with $X^5_A = \xi^5_A$.
- $5L$ super $\mathrm{M5}^l_{\mathbf{A}}$ stretching along the complex curve Σ^l_A identified with a half line ending on left at z'_A and on right at $\zeta_l = e^{X^5_l + i\vartheta_l}$ with $X^5_l = \varrho^5_l$ and $|\zeta_l| \to \infty$.

This superstring configuration is illustrated in Figure **5.9** where the intersections of the M-branes are represented by five basic $\mathrm{M5}_{\mathbf{A}}$ stacks are represented in Figure 5.9

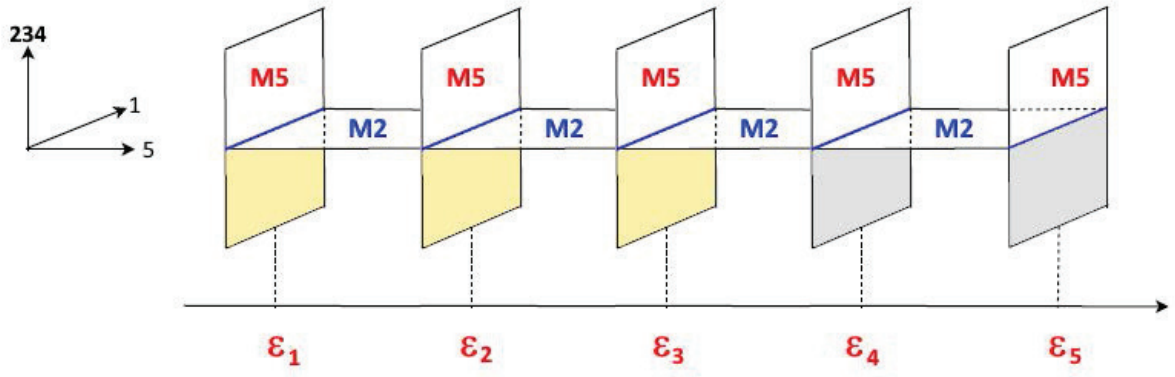

Figure 5.9: Horizontal M2 branes stretching between pairs of vertical M5s located at X_A and X_{A+1}. The M2 and the M5 intersect along an "M-string" (the 1-direction in blue). The positions X_A can be put in correspondence with the unit weights ϵ_A and the $X_{A+1} - X_A$ with the simple roots.

Similarly to the type IIA brane realization, we can use here the algebraic properties of the $sl(3|2)$ superalgebra, in particular the $\mathbb{Z}_2$ charges, to split the branes involved in (5.75) into three sectors. These are in one to one with the algebras appearing in the bosonic part of $sl(3|2)$ as in (5.64). We have :

- The $sl(3)$ sector given by

11D	$\mathbb{R}_0$	$\mathbb{R}_1$	$\mathcal{S}_N$	$\mathbb{R}_4$	$\mathbb{R}_6$	$\mathbb{R}_7$	$\mathbb{R}_8$	$\mathbb{R}_9$
$\mathrm{M5}_a$	x	x	Σ_a	$\{\xi^4_a\}$	x	x	0	0
$\mathrm{M2}_{aa+1}$	x	x	(z_a, z'_a)	$[\xi^4_a, \xi^4_{a+1}]$	x	x	0	0
$\mathrm{M5}^l_a$	x	x	Σ^l_a	$\{\xi^4_a\}$	0	0	0	0

(5.76)

- The $sl\,(2)$ sector given by

11D	$\mathbb{R}_0$	$\mathbb{R}_1$	$\mathcal{S}_N$	$\mathbb{R}_4$	$\mathbb{R}_6$	$\mathbb{R}_7$	$\mathbb{R}_8$	$\mathbb{R}_9$
$\mathrm{M5}_{3+i}$	x	x	Σ_{3+i}	$\{\xi^4_{3+i}\}$	0	0	x	x
$\mathrm{M2}_{\mathbf{45}}$	x	x	(z_{34}, z'_{34})	$[\xi^4_3, \xi^4_4]$	0	0	x	x
$\mathrm{M5}^l_{3+i}$	x	x	Σ^l_{3+i}	$\left\{\xi^4_{3+i}\right\}$	0	0	0	0

(5.77)

- The $sl(1)$ sector which only contains the $\mathrm{M2}_{\mathbf{34}}$ interpolating between a bosonic $\mathrm{M5}_{\mathbf{3}}$ and a fermionic $\mathrm{M5}_{\mathbf{4}}$ with worldvolume

11D	$\mathbb{R}_0$	$\mathbb{R}_1$	$\mathcal{S}_N$	$\mathbb{R}_4$	$\mathbb{R}_6$	$\mathbb{R}_7$	$\mathbb{R}_8$	$\mathbb{R}_9$
$\mathrm{M2}_{\mathbf{34}}$	x	x	$z_{\mathbf{34}}$	$[\xi^4_3, \xi^4_4]$	0	0	0	0

(5.78)

CHAPTER 6

CONCLUSION

The investigation carried in this thesis represents an extension of the results of the correspondence linking two-dimensional integrable models to four-dimensional Chern-Simons theory. In particular, we relied on the finding that an XXX spin chain with internal symmetry g can be realized as a lattice of line defects in the dual 4D CS with gauge symmetry G, and the L-operators solving its RLL equations of integrability are equivalent to the phase space of magnetic 't Hooft line defects. This interpretation yields a simple and direct formula for the oscillator realization of minuscule L-operators based on Levi decompositions of the chain's internal symmetry algebra, which are in turns deduced by nodes cutting from the associated Dynkin diagram. This general formula allowed us here to explicitly compute Lax operators for spin chains with bosonic $ABCDE$ symmetries from dual gauge theories, where some of these solutions are missing from the spin chain literature. The rest are in perfect agreement with the results obtained using Yangian representations -based techniques, and serve as more evidence to the strength of the duality in question.

These calculations were carried in the third chapter where we studied the Levi decompositions of these $ABCDE$ Lie algebras and applied the general formula (2.37), in order to calculate the desired Lax matrices for minuscule nodes of the associated Dynkin Diagrams. These solutions are expressed in matrix form in terms of oscillator degrees of freedom of the auxiliary phase space, and the spectral parameter z. By manipulating these different families of matrices, we elaborated what we called "quiver" diagrams as a unifying representation of the intrinsic data carried by this type of Lax operators. These diagrams also allowed us to understand the behaviour of the quantum states carried by a Wilson line under the singular action of a magnetic 't Hooft line.

The list of bosonic minuscule oscillator Lax matrices computed in the framework of 4D Chern-Simons theories as well as their associated Quiver descriptions are collected in Table (6.1) for the ABCDE spin chain systems. We also refer for each solution to the Levi decompositions behind its construction.

Symmetry	Levi decompositions	L-matrix	Quiver
A_{N-1}	$sl_N \to sl_k \oplus sl_1 \oplus sl_{N-k} \oplus \mathbf{k}\,(\mathbf{N-k})_{\pm}$	(3.39)	(3.7)
B_N	$so_{2N+1} \to so_2 \oplus so_{2N-1} \oplus (\mathbf{2N-1})_{\pm}$	(3.65)	(3.14)
C_N	$sp_{2N} \to so_2 \oplus sl_N \oplus \left(\frac{\mathbf{N(N+1)}}{\mathbf{2}}\right)_{\pm}$	(3.78)	(3.17)
$D_N(vect)$	$so_{2N} \to so_2 \oplus so_{2N-2} \oplus (\mathbf{2N-2})_{\pm}$	(3.100)	(3.25)
$D_N(spin)$	$so_{2N} \to sl_1 \oplus sl_N \oplus \frac{\mathbf{N(N-1)}}{\mathbf{2}}{}_{\pm}$	(3.111)	(3.26)
E_6	$e_6 \to so_2 \oplus so_{10} \oplus \mathbf{16}_{\pm}$	(3.141)	(3.32)
E_7	$e_7 \to so(2) \oplus e_6 \oplus \mathbf{27}_{\pm}$	(3.167)	(3.36)

(6.1)

The Lax matrices given here above are all realized in the fundamental representation of the corresponding Lie algebra. Their associated quiver diagrams allow to observe a unifying property of the E_7 Chern-Simons gauge theory, or equivalently the e_7 spin chain. By analyzing minuscule coweights for the ADE symmetries, one can notice a chain of decompositions starting from the e_7 Lie algebra which leads to e_6, and then to so_{10}, which yields so_8 or $sl5$ by different splitting patterns; these all lead finally to the linear sl_N with $N \leq 4$. This sequence is straightforwardly manifested on the level of quiver diagrams, where the Q_{E_7} can be thought of as the unifying quiver for ADE minuscule L-operators. The fundamental states in **56** of Q_{E_7} split by giving a subset in the node **27**. This node can be understood as Q_{E_6} where the 27 substates of the 56 states, split themself into subsates in the nodes **10** and **16**. This means that in the node **27**, we can identify sub-quivers $\mathrm{Q}^{vect}_{SO_{10}}$ and $\mathrm{Q}^{spin}_{SO_{10}}$, which both lead after two decompositions into $\mathrm{Q}_{SL_4} \simeq \mathrm{Q}_{SO_6}$, where the vector and spinor coweights are equivalent. These breaking patterns are explained in Figure 6.1. Regarding states of orthogonal B and symplectic C types, they are equivalent in this chain of decompositions to the vectorial and spinorial D states respectively. Recall that we have $\mathrm{Q}_{B_N} \sim \mathrm{Q}^{vect}_{D_N}$, and $\mathrm{Q}_{C_N} \sim \mathrm{Q}^{spin}_{D_N}$.

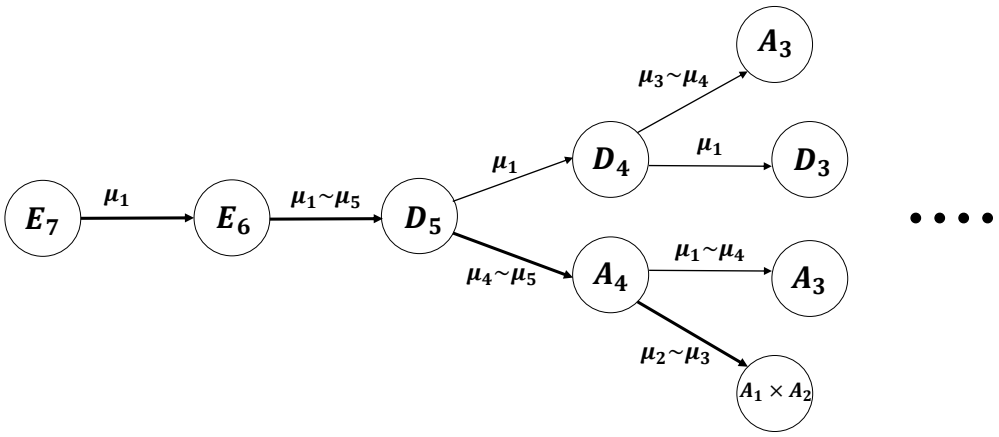

Figure 6.1: Breaking chains of the E_7 symmetry by following Levi decompositions with respect to minuscule coweights. The bold arrows describe the exceptional sequence leading to the Standard model group. The minuscule coweights μ correspond to the Lie algebra from which the arrow starts

Moreover, we have stated that the quiver description represented here for minuscule Lax operators, can offer a glimpse on the inner structure of solutions without having to make explicit calculations. By directly using the branching rules of representations beyond the fundamental with respect to minuscule coweights of the ADE algebras, we give in Figures 6.2,6.3 and 6.4 quiver diagrams describing the general behavior of internal states in Lax matrices for different representations of the simply laced bosonic symmetries.

The positive results obtained by exploiting this Integrability/ 4D CS correspondence have prompted us to extend this duality into the super symmetries case in order to study integrable superspin chain systems and their graded solutions in Chapter 4. In analogy to the bosonic construction, we realized the super Lax operators solving the graded RLL equations by analyzing Levi-like decompositions of Lie superalgebras. Following this approach, we built a list of super Lax matrices for superspin chains with internal symmetries given by the basic $ABCD$ Lie superalgebras. These solutions are to our knowledge, still missing in the superspin chain literature, except for the solutions of the linear $sl(m|n)$ models that were recovered from the 4D Chern-Simons with $SL(m|n)$ symmetry and compared with those constructed using degenerate solutions of the graded Yang-Baxter equation. For this linear symmetry, all simple nodes are

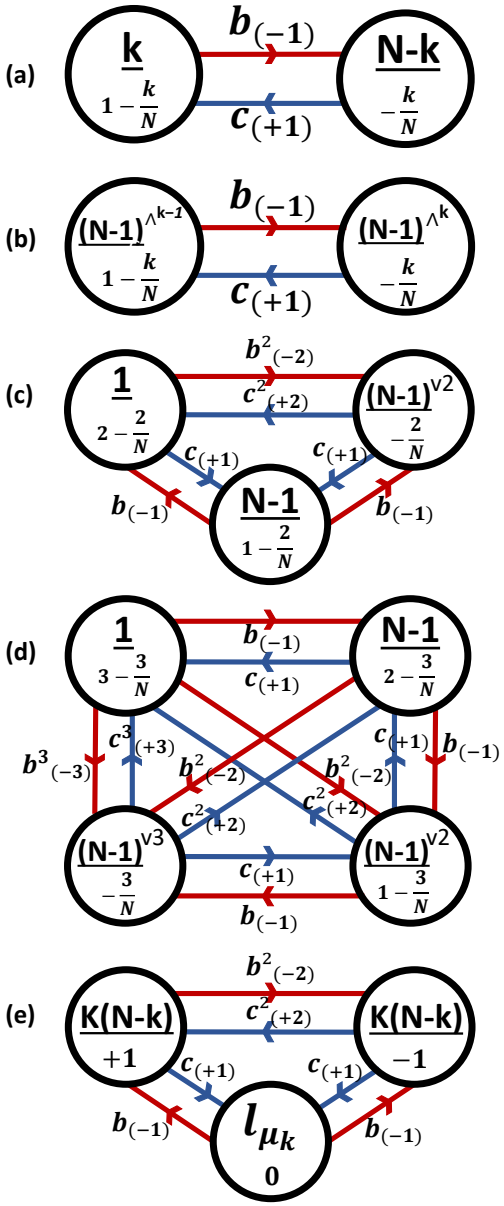

Figure 6.2: Leading elements of topological quiver diagrams for the L-operators of A- type. These quivers are classified by the magnetic charge μ_k of the 't Hooft line and the representation $\boldsymbol{R}$. (**a**) Wilson line with charge $\boldsymbol{R} = \boldsymbol{N}$. (**b**) Wilson line with $\boldsymbol{R} = \boldsymbol{N}^{\wedge k}$. (**c**) Wilson line with $\boldsymbol{R} = \boldsymbol{N}^{\vee 2}$. (**d**) Wilson line with $\boldsymbol{R} = \boldsymbol{N}^{\vee 3}$. (**e**) Wilson line with charge $\boldsymbol{R} = \boldsymbol{adj}\, sl_N$.

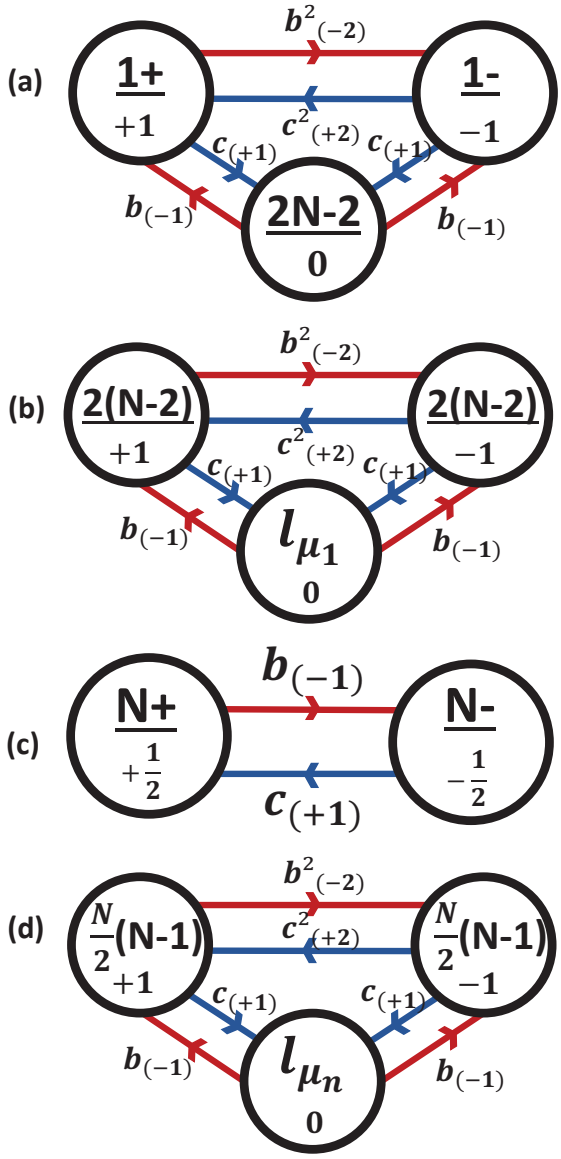

Figure 6.3: Leading elements of topological quiver diagrams for the L-operators of D- type. The first two quivers correspond to the Levi decomposition with respect to the (vectorial) minuscule coweight μ_1: (**a**) Wilson line with charge $\boldsymbol{R = 2N}$**.** (**b**) Wilson line with $\boldsymbol{R = adjso_{2N}}$. The other two quivers correspond to the Levi decomposition with respect to the (spinorial) minuscule coweight μ_N: (c) Wilson line with $\boldsymbol{R = 2^{N-1}}$. (d) Wilson line with $\boldsymbol{R = adjso_{2N}}$.

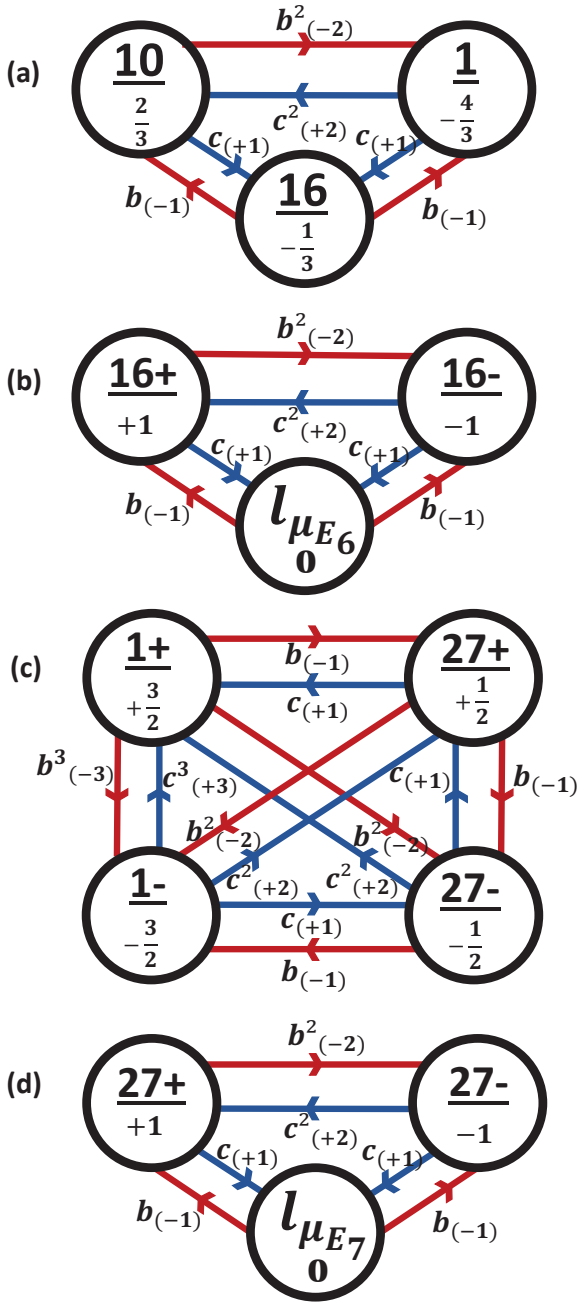

Figure 6.4: Leading elements of topological quiver diagrams for the L-operators of E- type. The first two quivers for the E_6 gauge theory. (**a**) for the fundamental **27** of E_6; and (**b**) for the adjoint representation. The last two quivers regard the E_7 Chern-Simons theory. (**c**) for the fundamental **56** of E_7 and (**d**) for the adjoint representation.

associated to minuscule-like coweights, and lead to Levi-like decompositions. We therefore gave a more general expression for super Lax matrices for any node of any super Dynkin diagram of $sl(m|n)$. Notice that the bosonic L-operators of the $sl(m)$ spin chain [123] can be recovered as a special case of the graded distinguished solutions by simply taking $n = 0$.

For the $B\,(m|n)$, $C(n)$ and $D(m|n)$ superspin chains, we focus on the distinguished super Dynkin diagrams, and in particular on nodes leading to Levi-like decompositions. For the $B(m|n)$ superalgebra, we find one super Lax operator which is similar the bosonic minuscule Lax operator of the B-type spin chain. This can be justified by the fact that the coweight leading to the Levi-like decomposition of $osp(2m+1|2n)$ coincides with the vector-like minuscule node in the B_m part of the distinguished Dynkin diagram of $B\,(m|n)$. For $C(n)$, we calculated two graded Lax operators; the first corresponds to the fermionic node, and the second is equivalent to the minuscule Lax matrix of the bosonic C_n algebra. Regarding the $D(m|n)$ Lie superalgebra, we had three possible minuscule-like nodes equivalent to the minuscule node of the bosonic D_N algebra. We calculated their associated super Lax operators that also appear of vector, spinor and cospinor nature in analogy to the D_N Lax operators.

The expressions of these graded solutions are collected in the Table (6.2) below, where we mention the superalgebras' decompositions associated to each solution such that $g = \boldsymbol{l}_\mu \oplus N_+ \oplus N_-$. Notice also that all these graded matrices are given in fundamental representations of the corresponding super Lie algebra.

Superalgebra	Subalgebra $\boldsymbol{l}_\mu$	Nilpotent N_+	L-operators	Equations
$sl_{m\|n}$	$sl_{k\|l} \oplus sl_{m-k\|n-l} \oplus gl_1$	$(k+l)^c(m-k+n-l)$	$\mathcal{L}^{\mu}_{sl(m\|n)}$	(4.67)
$osp_{2m+1\|2n}$	$osp_{2m-1\|2n} \oplus gl_1$	$2m+2n-1$	$\mathcal{L}^{\mu_{n+1}}_{B_{m\|n}}$	(4.95)-(4.99)
$osp_{2\|2n-2}$	$sp_{2n-2} \oplus gl_1$ $sl_{1\|n-1} \oplus gl_1$	$2\,(n-1)$ $\frac{n(n+1)}{2} - 1$	$\mathcal{L}^{\mu_1}_{C(n)}$ $\mathcal{L}^{\mu_n}_{C(n)}$	(4.120) (4.135)-(4.138)
$osp_{2m\|2n}$	$osp_{2m-2\|2n} \oplus gl_1$ $sl_{m\|n} \oplus gl_1$	$2\,(m+n-1)$ $\frac{(m+n)(m+n+1)}{2} - m$	$\mathcal{L}^{\mu_{m+n}}_{D_{m\|n}}$ $\mathcal{L}^{\mu_{n+1}}_{D_{m\|n}}$	(4.169)-(4.171) (4.155)

(6.2)

Finally, in Chapter 5, we studied the embedding of integrable superspin chains in M-theory and type II strings, by focusing on the linear $sl(m|n)$ model, and by using the rich dualities within string theory to justify the brane realization of such integrable system. Steps and outcomes of this investigation can be summarized in the following points:
(i) The determination of degrees of freedom and symmetries of the integrable superspin chain system in general, and the linear $sl(m|n)$ with superspins in the fundamental $\mathbf{m}|\mathbf{n}$ in particular.
(ii) The translation of elements of these symmetries in terms of brane systems by using relationships between the triad: root and weight systems of Lie algebras, homology cycles of complex manifolds with singularities and branes in type II strings and M-theory.
(iii) Linking the exotic features of the superspin states of the super chain to the exotic properties of colored Dynkin super diagrams of Lie superalgebras.
(iv) Extending the Algebra/ Homology correspondence in the so-called ADE geometries of Du Val to super groups (Super Algebra/ Homology) with super singularity.
(v) Construction of the brane system realizing the $sl(3|2)$ superspin chain in the type IIA string theory, by involving varieties of NS5-, D2- and flavored D4-branes as well as F1 strings.
(vi) Lifting the Type IIA brane realization to the 11-dimensional M-theory, where the $sl(3|2)$ emerges from M5 and M2 branes. (vii) Linking the grading of the internal space of the superspin chain that manifests on brane realization, to the super geometry emerging from graded roots.

To end this conclusion, we stress the main perspectives of the present work, in particular by relying on the very interesting discovery of the Integrability/ 4D CS Correspondence, as well as its extensions. Future research directions may involve:

• Working out a generalized Lax operator formula allowing to generate oscillator Lax operators even for non minuscule coweights, i.e. for all nodes of a Dynkin diagram. This would include the interpretation of algebras' 5-gradings, like those listed in [231]-[233], in terms of singular gauge configuration.

• Linking the quiver description elaborated here to a supersymmetric Quiver gauge theory, dual to the four-dimensional Chern-Simons and the two-dimensional integrable models. A strong candidate is the N = 4 quiver gauge theory whose quantum Coulomb branches are identified with the phase space of 't Hooft lines in [123].

• Exploiting the general super Lax operator formula for superspin chains with exceptional Lie super symmetries $F(4)$, $G(3)$ and $D(1,2;\alpha)$. Such calculation should be based on 3-gradings generated by nodes cutting from the Dynkin diagrams of these Lie superalgebras.

• Investigating the derivation of RLL solutions in the string theory, by relying on the brane realization of spin chain systems and their dual line defects constructions.

• Deepening the brane realization of superspin chains by studying the embedding of orthosymplectic chains, in particular with $osp(2m|2n)$ symmetry.

• Connecting the present correspondence to other well known theories and dualities in theoretical physics, such as the AdS/ CFT. This would allow to enlarge the network of dualities in the framework of string theory.

BIBLIOGRAPHY

[1] Costello, K., Witten, E., Yamazaki, M. (2017). Gauge theory and integrability, I. arXiv preprint arXiv:1709.09993.

[2] Costello, K., Witten, E., Yamazaki, M. (2018). Gauge theory and integrability, II. arXiv preprint arXiv:1802.01579.

[3] Costello, K., Yamazaki, M. (2019). Gauge theory and integrability, III. arXiv preprint arXiv:1908.02289.

[4] Saidi, E. H. (2020). Quantum line operators from Lax pairs. Journal of Mathematical Physics, 61(6).

[5] Vicedo, B. (2021). 4D Chern–Simons theory and affine Gaudin models. Letters in Mathematical Physics, 111(1), 24.

[6] Fukushima, O., Sakamoto, J. I., Yoshida, K. (2020). Yang-Baxter deformations of the AdS5× S5 supercoset sigma model from 4D Chern-Simons theory. Journal of High Energy Physics, 2020(9), 1-23.

[7] Delduc, F., Lacroix, S., Magro, M., Vicedo, B. (2020). A unifying 2d action for integrable σ-models from 4d Chern–Simons theory. Letters in Mathematical Physics, 110(7), 1645-1687.

[8] Bykov, D. (2023). Quantum flag manifold σ-models and Hermitian Ricci flow. Communications in Mathematical Physics, 401(1), 1-32.

[9] Bittleston, R., Skinner, D. (2019). Gauge theory and boundary integrability. Journal of High Energy Physics, 2019(5), 1-53.

[10] Bittleston, R., Skinner, D. (2020). Gauge theory and boundary integrability. Part II. Elliptic and trigonometric cases. Journal of High Energy Physics, 2020(6), 1-35.

[11] Costello, K. (2013). Supersymmetric gauge theory and the Yangian. arXiv preprint arXiv:1303.2632.

[12] Costello, K., Yagi, J. (2018). Unification of integrability in supersymmetric gauge theories. arXiv preprint arXiv:1810.01970.

[13] Costello, K., Stefański Jr, B. (2020). Chern-Simons origin of superstring integrability. Physical Review Letters, 125(12), 121602.

[14] Nekrasov, N. (2019). Superspin chains and supersymmetric gauge theories. Journal of High Energy Physics, 2019(3), 1-17.

[15] Nekrasov, N. (2017). Open-closed (little) string duality and Chern-Simons-Bethe/gauge correspondence. Talk at String Math, 24-28.

[16] Dorey, N., Lee, S., Hollowood, T. J. (2011). Quantization of integrable systems and a 2d/4d duality. Journal of High Energy Physics, 2011(10), 1-42.

[17] Ashwinkumar, M., Tan, M. C., Zhao, Q. (2018). Branes and categorifying integrable lattice models. arXiv preprint arXiv:1806.02821.

[18] Yamazaki, M. (2014). New integrable models from the gauge/YBE correspondence. Journal of Statistical Physics, 154(3), 895-911.

[19] Orlando, D., Reffert, S. (2010). Relating gauge theories via gauge/Bethe correspondence. Journal of High Energy Physics, 2010(10), 1-30.

[20] Orlando, D. (2013). A stringy perspective on the quantum integrable model/gauge correspondence. arXiv preprint arXiv:1310.0031.

[21] Okuda, T. (2015). Line operators in supersymmetric gauge theories and the 2d-4d relation. In New dualities of supersymmetric gauge theories (pp. 195-222). Cham: Springer International Publishing.

[22] Nekrasov, N. A., Shatashvilli, S. L. (2009). QUANTIZATION OF INTEGRABLE SYSTEMS. arXiv preprint arXiv:0908.4052.

[23] Nekrasov, N. A., Shatashvili, S. L. (2009). Supersymmetric vacua and Bethe ansatz. arXiv preprint arXiv:0901.4744.

[24] Yamazaki, M. (2014). New integrable models from the gauge/YBE correspondence. Journal of Statistical Physics, 154(3), 895-911.

[25] Orlando, D., Reffert, S. (2010). Relating gauge theories via gauge/Bethe correspondence. Journal of High Energy Physics, 2010(10), 1-30.

[26] Orlando, D. (2013). A stringy perspective on the quantum integrable model/gauge correspondence. arXiv preprint arXiv:1310.0031.

[27] Ashwinkumar, M., Tan, M. C. (2019). Unifying lattice models, links and quantum geometric Langlands via branes in string theory. arXiv preprint arXiv:1910.01134.

[28] Costello, K. (2014, December). Integrable lattice models from four-dimensional field theories. In Proc. Symp. Pure Math (Vol. 88, p. 3).

[29] Witten, E. (2016). Integrable lattice models from gauge theory. arXiv preprint arXiv:1611.00592.

[30] Das, A. (1989). Integrable models (Vol. 30). World scientific.

[31] Bogoliubov, N. M., Malyshev, C. L. (2015). Integrable models and combinatorics. Russian Mathematical Surveys, 70(5), 789.

[32] Bogoliubov, N. M., Izergin, A. G., Korepin, V. E. (1986). Critical exponents for integrable models. Nuclear Physics B, 275(4), 687-705.

[33] Borsi, M., Pozsgay, B., Pristyák, L. (2021). Current operators in integrable models: a review. Journal of Statistical Mechanics: Theory and Experiment, 2021(9), 094001.

[34] Faddeev, L. (1982). Integrable models in 1+ 1 dimensional quantum field theory (No. CEA-CONF–6565). CEA Centre d'Etudes Nucleaires de Saclay.

[35] Faddeev, L. D., Korchemsky, G. P. (1995). High energy QCD as a completely integrable model. Physics Letters B, 342(1-4), 311-322.

[36] Lou, S. Y. (1997). Conformal invariance and integrable models. Journal of Physics A: Mathematical and General, 30(13), 4803.

[37] Lukyanov, S. (1995). Free field representation for massive integrable models. Communications in Mathematical Physics, 167, 183-226.

[38] Di Francesco, P., Zuber, J. B. (1990). SU (N) lattice integrable models associated with graphs. Nuclear Physics B, 338(3), 602-646.

[39] Sirker, J. (2012). The Luttinger liquid and integrable models. International Journal of Modern Physics B, 26(22), 1244009.

[40] Warner, N. P. (1995). Supersymmetry in boundary integrable models. Nuclear Physics B, 450(3), 663-694.

[41] Batchelor, M. T., Foerster, A. (2016). Yang–Baxter integrable models in experiments: from condensed matter to ultracold atoms. Journal of Physics A: Mathematical and Theoretical, 49(17), 173001.

[42] Faddeev, L. D., Takhtajan, L. A. (1987). Hamiltonian methods in the theory of solitons (Vol. 23). Berlin: Springer.

[43] Jimbo, M. (1990). Yang-Baxter equation in integrable systems (Vol. 10). World Scientific.

[44] Wadati, M., Akutsu, Y. (1988). From solitons to knots and links. Progress of Theoretical Physics Supplement, 94, 1-41.

[45] Perk, J. H., Au-Yang, H. (2006). Yang-baxter equations. arXiv preprint math-ph/0606053.

[46] Zamolodchikov, A. B., Zamolodchikov, A. B. (1979). Factorized S-matrices in two dimensions as the exact solutions of certain relativistic quantum field theory models. Annals of physics, 120(2), 253-291.

[47] Bazhanov, V. V., Lukyanov, S. L., Zamolodchikov, A. B. (1999). Integrable structure of conformal field theory III. The Yang–Baxter relation. Communications in mathematical physics, 200, 297-324.

[48] Bethe, H. (1931). Zur theorie der metalle: I. Eigenwerte und eigenfunktionen der linearen atomkette. Zeitschrift für Physik, 71(3-4), 205-226.

[49] Onsager, L. (1944). Crystal statistics. I. A two-dimensional model with an order-disorder transition. Physical Review, 65(3-4), 117.

[50] McGuire, J. B. (1964). Study of exactly soluble one-dimensional N-body problems. Journal of Mathematical Physics, 5(5), 622-636.

[51] Yang, C. N. (1967). Some exact results for the many-body problem in one dimension with repulsive delta-function interaction. Physical Review Letters, 19(23), 1312.

[52] Baxter, R. J. (1971). Eight-vertex model in lattice statistics. Physical Review Letters, 26(14), 832.

[53] Zamolodchikov, A. B., Zamolodchikov, A. B. (1979). Factorized S-matrices in two dimensions as the exact solutions of certain relativistic quantum field theory models. Annals of physics, 120(2), 253-291.

[54] Bazhanov, V. V., Łukowski, T., Meneghelli, C., Staudacher, M. (2010). A shortcut to the Q-operator. Journal of Statistical Mechanics: Theory and Experiment, 2010(11), P11002.

[55] Bazhanov, V. V., Frassek, R., Łukowski, T., Meneghelli, C., Staudacher, M. (2011). Baxter Q-operators and representations of Yangians. Nuclear Physics B, 850(1), 148-174.

[56] Frassek, R. (2020). Oscillator realisations associated to the D-type Yangian: Towards the operatorial Q-system of orthogonal spin chains. Nuclear Physics B, 956, 115063.

[57] Ferrando, G., Frassek, R., Kazakov, V. (2021). QQ-system and Weyl-type transfer matrices in integrable SO (2r) spin chains. Journal of High Energy Physics, 2021(2), 1-47.

[58] Frassek, R., Pestun, V., Tsymbaliuk, A. (2022). Lax matrices from antidominantly shifted Yangians and quantum affine algebras: A-type. Advances in Mathematics, 401, 108283.

[59] Frassek, R., Tsymbaliuk, A. (2022). Rational Lax matrices from antidominantly shifted extended Yangians: BCD types. Communications in Mathematical Physics, 392(2), 545-619.

[60] Frassek, R. (2014). Q-operators, Yangian invariance and the quantum inverse scattering method. arXiv preprint arXiv:1412.3339.

[61] Frassek, R., Łukowski, T., Meneghelli, C., Staudacher, M. (2011). Oscillator construction of su (n| m) Q-operators. Nuclear Physics B, 850(1), 175-198.

[62] Volin, D. (2012). String hypothesis for spin chains: a particle/hole democracy. Letters in Mathematical Physics, 102(1), 1-29.

[63] Saidi, E. H., Sedra, M. B. (1994). Hyper-Kähler metrics building and integrable models. Modern Physics Letters A, 9(34), 3163-3173.

[64] Baxter, R. J. (2016). Exactly solved models in statistical mechanics. Elsevier.

[65] Nekrasov, N., Witten, E. (2010). The omega deformation, branes, integrability and Liouville theory. Journal of High Energy Physics, 2010(9), 1-83.

[66] Bao, S., Wang, J., Wang, W., Cai, Z., Li, S., Ma, Z., ... Wen, J. (2018). Discovery of coexisting Dirac and triply degenerate magnons in a three-dimensional antiferromagnet. Nature communications, 9(1), 2591.

[67] Yang, C. N. (1967). Some exact results for the many-body problem in one dimension with repulsive delta-function interaction. Physical Review Letters, 19(23), 1312.

[68] Baxter, R. J. (1972). Partition function of the eight-vertex lattice model. Annals of Physics, 70(1), 193-228.

[69] Jimbo, M., Miwa, T. (1994). Algebraic analysis of solvable lattice models (Vol. 85). American Mathematical Soc..

[70] Bazhanov, V. V., Lukyanov, S. L., Zamolodchikov, A. B. (1997). Integrable structure of conformal field theory II. Q-operator and DDV equation. Communications in Mathematical Physics, 190(2), 247-278.

[71] Turaev, V. (1990). The Yang-Baxter equation and invariants of links. New Developments in the Theory of Knots, 11, 175.

[72] Borsato, R., Sax, O. O., Sfondrini, A., Stefanski, B., Torrielli, A. (2013). The all-loop integrable spin-chain for strings on AdS3× S 3× T 4: the massive sector. Journal of High Energy Physics, 2013(8), 1-43.

[73] Delduc, F., Lacroix, S., Magro, M., Vicedo, B. (2019). Integrable coupled σ models. Physical review letters, 122(4), 041601.

[74] Saidi, E. H., Sedra, M. B. (1994). On N= 4 integrable models. International Journal of Modern Physics A, 9(06), 891-913.

[75] Beshetikhin, N. Y. (1985). Hamiltonian structures for integrable field theory models. II. Models with O (n) and Sp (2k) symmetry on a one-dimensional lattice. Theor. Math. Phys.;(United States), 63(2).

[76] Saidi, E. H. (1995). Matrix representation of higher integer conformal spin symmetries. Journal of Mathematical Physics, 36(8), 4461-4475.

[77] Zamolodchikov, A. B., Zamolodchikov, A. B. (1979). Factorized S-matrices in two dimensions as the exact solutions of certain relativistic quantum field theory models. Annals of physics, 120(2), 253-291.

[78] De Vega, H. J., Karowski, M. (1987). Exact Bethe ansatz solution of O (2N) symmetric theories. Nuclear Physics B, 280, 225-254.

[79] Faddeev, L. D. (1996). How algebraic Bethe ansatz works for integrable model. arXiv preprint hep-th/9605187.

[80] Sklyanin, E. K. (1982). Some algebraic structures connected with the Yang–Baxter equation. Funktsional'nyi Analiz i ego Prilozheniya, 16(4), 27-34.

[81] Bytsko, A. G., Teschner, J. (2006). Quantization of models with non-compact quantum group symmetry: Modular XXZ magnet and lattice sinh-Gordon model. Journal of Physics A: Mathematical and General, 39(41), 12927.

[82] Frassek, R., Łukowski, T., Meneghelli, C., Staudacher, M. (2013). Baxter operators and Hamiltonians for "nearly all" integrable closed gl (n) spin chains. Nuclear Physics B, 874(2), 620-646.

[83] Kazakov, V., Leurent, S., Tsuboi, Z. (2012). Baxter's Q-operators and operatorial Bäcklund flow for quantum (super)-spin chains. Communications in Mathematical Physics, 311, 787-814.

[84] Pronko, G. P. (2000). On Baxter's Q-operator for the XXX spin chain. Communications in Mathematical Physics, 212, 687-701.

[85] Dancer, K. A., Gould, M. D., Links, J. (2007). Lax Operator for the Quantised Orthosymplectic Superalgebra U q [osp (m| n)]. Algebras and Representation Theory, 10, 593-617.

[86] Frahm, H., Martins, M. J. (2015). Finite-size effects in the spectrum of the OSp (3| 2) superspin chain. Nuclear Physics B, 894, 665-684.

[87] Beisert, N. (2004). The dilatation operator of N= 4 super Yang–Mills theory and integrability. Physics Reports, 405(1-3), 1-202.

[88] Dolan, L., Nappi, C. R., Witten, E. (2003). A relation between approaches to integrability in superconformal Yang-Mills theory. Journal of High Energy Physics, 2003(10), 017.

[89] Donagi, R., Witten, E. (1996). Supersymmetric Yang-Mills theory and integrable systems. Nuclear Physics B, 460(2), 299-334.

[90] D'Hoker, E., Phong, D. H. (2002). Lectures on supersymmetric Yang-Mills theory and integrable systems. Theoretical Physics at the End of the Twentieth Century: Lecture Notes of the CRM Summer School, Banff, Alberta, 1-125.

[91] Guica, M., Maslyuk, F. L., Zarembo, K. (2017). Integrability in dipole-deformed super Yang–Mills. Journal of Physics A: Mathematical and Theoretical, 50(39), 394001.

[92] Gromov, N., Vieira, P. (2013). Quantum integrability for three-point functions of maximally supersymmetric Yang-Mills theory. Physical Review Letters, 111(21), 211601.

[93] Kasperczuk, S. (1994). Integrability of the Yang-Mills hamiltonian system. Celestial Mechanics and Dynamical Astronomy, 58, 387-391.

[94] Ablowitz, M. J., Chakravarty, S., Halburd, R. G. (2003). Integrable systems and reductions of the self-dual Yang–Mills equations. Journal of Mathematical Physics, 44(8), 3147-3173.

[95] Dubois-Violette, M., Madore, J. (1987). Conservation laws and integrability conditions for gravitational and Yang-Mills field equations. Communications in mathematical physics, 108, 213-223.

[96] Belitsky, A. V., Braun, V. M., Gorsky, A. S., Korchemsky, G. P. (2004). Integrability in QCD and beyond. International Journal of Modern Physics A, 19(28), 4715-4788.

[97] Roiban, R., Volovich, A. (2004). Yang-Mills correlation functions from integrable spin chains. Journal of High Energy Physics, 2004(09), 032.

[98] Llibre, J., Valls, C. (2016). Darboux integrability of generalized Yang–Mills Hamiltonian system. Journal of Nonlinear Mathematical Physics, 23(2), 234-242.

[99] Staudacher, M. (2012). Review of AdS/CFT integrability, chapter III. 1: Bethe ansätze and the R-matrix formalism. Letters in Mathematical Physics, 99, 191-208.

[100] Beisert, N., Ahn, C., Alday, L. F., Bajnok, Z., Drummond, J. M., Freyhult, L. Zoubos, K. (2012). Review of AdS/CFT integrability: an overview. Letters in Mathematical Physics, 99, 3-32.

[101] Kazakov, V. A., Marshakov, A., Minahan, J. A., Zarembo, K. (2004). Classical/quantum integrability in AdS/CFT. Journal of High Energy Physics, 2004(05), 024.

[102] Serban, D. (2011). Integrability and the AdS/CFT correspondence. Journal of Physics A: Mathematical and Theoretical, 44(12), 124001.

[103] Kazakov, V. A., Zarembo, K. (2004). Classical/quantum integrability in non-compact sector of AdS/CFT. Journal of High Energy Physics, 2004(10), 060.

[104] Klose, T. (2012). Review of AdS/CFT integrability, chapter iv. 3: Chern–Simons and strings on AdS4× CP3. Letters in Mathematical Physics, 99(1-3), 401-423.

[105] Vieira, P., Volin, D. (2012). Review of AdS/CFT integrability, chapter III. 3: the dressing factor. Letters in Mathematical Physics, 99, 231-253.

[106] Zoubos, K. (2012). Review of AdS/CFT integrability, chapter IV. 2: deformations, orbifolds and open boundaries. Letters in Mathematical Physics, 99(1-3), 375-400.

[107] de Mello Koch, R., Ramgoolam, S. (2012). A double coset ansatz for integrability in AdS/CFT. Journal of High Energy Physics, 2012(6), 1-30.

[108] Gromov, N., Kazakov, V., Kozak, A., Vieira, P. (2009). Integrability for the full spectrum of planar AdS/CFT II. arXiv preprint arXiv:0902.4458.

[109] Minahan, J. A. (2012). Review of AdS/CFT Integrability, Chapter I. 1: Spin Chains in Super Yang-Mills. Letters in Mathematical Physics, 99(1-3), 33-58.

[110] Tseytlin, A. A. (2012). Review of AdS/CFT integrability, chapter II. 1: classical AdS 5× S 5 string solutions. Letters in Mathematical Physics, 99, 103-125.

[111] Staudacher, M. (2012). Review of AdS/CFT integrability, chapter III. 1: Bethe ansätze and the R-matrix formalism. Letters in Mathematical Physics, 99, 191-208.

[112] Kristjansen, C. (2012). Review of AdS/CFT integrability, chapter IV. 1: aspects of nonplanarity. Letters in Mathematical Physics, 99(1-3), 349-374.

[113] Drummond, J. M. (2012). Review of AdS/CFT integrability, chapter V. 2: dual superconformal symmetry. Letters in Mathematical Physics, 99(1-3), 481-505.

[114] Kapustin, A. (2006). Wilson-'t Hooft operators in four-dimensional gauge theories and S-duality. Physical Review D, 74(2), 025005.

[115] Saidi, E. H. (2019). Gapped gravitinos, isospin particles, and partial breaking. Progress of Theoretical and Experimental Physics, 2019(1), 013B01.

[116] Kapustin, A., Witten, E. (2006). Electric-magnetic duality and the geometric Langlands program. arXiv preprint hep-th/0604151.

[117] Yagi, J. (2017). Surface defects and elliptic quantum groups. Journal of High Energy Physics, 2017(6), 1-32.

[118] Okuda, T. (2015). Line operators in supersymmetric gauge theories and the 2d-4d relation. In New dualities of supersymmetric gauge theories (pp. 195-222). Cham: Springer International Publishing.

[119] Brennan, T. D., Dey, A., Moore, G. W. (2019). 't Hooft defects and wall crossing in SQM. Journal of High Energy Physics, 2019(10), 1-101.

[120] Hayashi, H., Okuda, T., Yoshida, Y. (2021). ABCD of't Hooft operators. Journal of High Energy Physics, 2021(4), 1-69.

[121] Maruyoshi, K., Yagi, J. (2016). Surface defects as transfer matrices. Progress of Theoretical and Experimental Physics, 2016(11), 113B01.

[122] Ishtiaque, N., Moosavian, S. F., Zhou, Y. (2020). Topological holography: The example of the D2-D4 brane system. SciPost Physics, 9(2), 017.

[123] Costello, K., Gaiotto, D., Yagi, J. (2021). Q-operators are't Hooft lines. arXiv preprint arXiv:2103.01835.

[124] Maruyoshi, K., Ota, T., Yagi, J. (2021). Wilson-'t Hooft lines as transfer matrices. Journal of High Energy Physics, 2021(1), 1-31.

[125] Hietarinta, J. (1984). Classical versus quantum integrability. Journal of mathematical physics, 25(6), 1833-1840.

[126] Holt, C. R. (1982). Construction of new integrable Hamiltonians in two degrees of freedom. Journal of Mathematical Physics, 23(6), 1037-1046.

[127] Retore, A. L. (2022). Introduction to classical and quantum integrability. Journal of Physics A: Mathematical and Theoretical, 55(17), 173001.

[128] Przybylska, M. (2009). Darboux points and integrability of homogeneous Hamiltonian systems with three and more degrees of freedom. Regular and Chaotic Dynamics, 14(2), 263-311.

[129] Bracken, P. (2020). Classical and Quantum Integrability: A Formulation That Admits Quantum Chaos. In A Collection of Papers on Chaos Theory and Its Applications. IntechOpen.

[130] Weigert, S. (1992). The problem of quantum integrability. Physica D: Nonlinear Phenomena, 56(1), 107-119.

[131] Cambiaggio, M. C., Rivas, A. M. F., Saraceno, M. (1997). Integrability of the pairing Hamiltonian. Nuclear Physics A, 624(2), 157-167.

[132] Prigogine, I., Petrosky, T. Y., Hasegawa, H. H., Tasaki, S. (1991). Integrability and chaos in classical and quantum mechanics. Chaos, Solitons Fractals, 1(1), 3-24.

[133] Olshanetsky, M. A., Perelomov, A. M. (1983). Quantum integrable systems related to Lie algebras. Physics Reports, 94(6), 313-404.

[134] Lamers, J. (2015). A pedagogical introduction to quantum integrability, with a view towards theoretical high-energy physics. arXiv preprint arXiv:1501.06805.

[135] Evnin, O., Piensuk, W. (2018). Quantum resonant systems, integrable and chaotic. Journal of Physics A: Mathematical and Theoretical, 52(2), 025102.

[136] Faddeev, L. D. (1996). How algebraic Bethe ansatz works for integrable model. arXiv preprint hep-th/9605187.

[137] Levkovich-Maslyuk, F. (2016). The bethe ansatz. Journal of Physics A: Mathematical and Theoretical, 49(32), 323004.

[138] Frahm, H., Grelik, J. H., Seel, A., Wirth, T. (2010). Functional Bethe ansatz methods for the open XXX chain. Journal of Physics A: Mathematical and Theoretical, 44(1), 015001.

[139] Wang, Y., Yang, W. L., Cao, J., Shi, K. (2015). Off-diagonal Bethe ansatz for exactly solvable models. Springer Berlin Heidelberg.

[140] Belliard, S., Crampé, N. (2013). Heisenberg XXX model with general boundaries: eigenvectors from algebraic Bethe ansatz. SIGMA. Symmetry, Integrability and Geometry: Methods and Applications, 9, 072.

[141] Martins, M. J. (1999). Unified algebraic Bethe ansatz for two-dimensional lattice models. Physical Review E, 59(6), 7220.

[142] Mezincescu, L., Nepomechie, R. I. (1992). Analytical Bethe Ansatz for quantum-algebra-invariant spin chains. Nuclear Physics B, 372(3), 597-621.

[143] Frenkel, E., Koroteev, P., Sage, D. S., Zeitlin, A. M. (2020). q-opers, QQ-systems, and Bethe ansatz. arXiv preprint arXiv:2002.07344.

[144] Ekhammar, S. (2023). An Exploration of Q-Systems: From Spin Chains to Low-Dimensional AdS/CFT (Doctoral dissertation, Acta Universitatis Upsaliensis).

[145] Sklyanin, E. K., Takhtadzhyan, L. A., Faddeev, L. D. (1979). Quantum inverse problem method. I. Teoreticheskaya i Matematicheskaya Fizika, 40(2), 194-220.

[146] Sklyanin, E. K. (1992). Quantum inverse scattering method. Selected topics. arXiv preprint hep-th/9211111.

[147] Korepin, V. E., Bogoliubov, N. M., Izergin, A. G. (1997). Quantum inverse scattering method and correlation functions (Vol. 3). Cambridge university press.

[148] Maillet, J. M., Terras, V. (2000). On the quantum inverse scattering problem. Nuclear Physics B, 575(3), 627-644.

[149] Faddeev, L. (1995). Instructive history of the quantum inverse scattering method. In KdV'95: Proceedings of the International Symposium held in Amsterdam, The Netherlands, April 23–26, 1995, to commemorate the centennial of the publication of the equation by and named after Korteweg and de Vries (pp. 69-84). Springer Netherlands.

[150] Martins, M. J., Ramos, P. B. (1998). The quantum inverse scattering method for Hubbard-like models. Nuclear Physics B, 522(3), 413-470.

[151] Volkov, A. Y., Faddeev, L. D. (1992). Quantum inverse scattering method on a spacetime lattice. Theoretical and Mathematical Physics, 92, 837-842.

[152] Bogoliubov, N. M., Izergin, A. G., Korepin, V. E. (2005, July). Quantum inverse scattering method and correlation functions. In Exactly Solvable Problems in Condensed Matter and Relativistic Field Theory: Proceedings of the Winter School and International Colloquium Held at Panchgani, January 30–February 12, 1985 and Organized by Tata Institute of Fundamental Research, Bombay (pp. 220-316). Berlin, Heidelberg: Springer Berlin Heidelberg.

[153] Sukumar, C. V. (1985). Supersymmetric quantum mechanics and the inverse scattering method. Journal of Physics A: Mathematical and General, 18(15), 2937.

[154] Sklyanin, E. K. (1982). Quantum version of the method of inverse scattering problem. Journal of Soviet Mathematics, 19, 1546-1596.

[155] Doikou, A., Evangelisti, S., Feverati, G., Karaiskos, N. (2010). Introduction to quantum integrability. International Journal of Modern Physics A, 25(17), 3307-3351.

[156] Wadati, M. (1985). Quantum inverse scattering method. In Dynamical Problems in Soliton Systems: Proceedings of the Seventh Kyoto Summer Institute, Kyoto, Japan, August 27–31, 1984 (pp. 68-80). Berlin, Heidelberg: Springer Berlin Heidelberg.

[157] Sogo, K., Wadati, M. (1982). Quantum inverse scattering method and Yang-Baxter relation for integrable spin systems. Progress of Theoretical Physics, 68(1), 85-97.

[158] Bazhanov, V. V., Lukyanov, S. L., Zamolodchikov, A. B. (1996). Integrable structure of conformal field theory, quantum KdV theory and thermodynamic Bethe ansatz. Communications in Mathematical Physics, 177(2), 381-398.

[159] Bazhanov, V. V., Lukyanov, S. L., Zamolodchikov, A. B. (1997). Integrable structure of conformal field theory II. Q-operator and DDV equation. Communications in Mathematical Physics, 190(2), 247-278.

[160] Bazhanov, V. V., Lukyanov, S. L., Zamolodchikov, A. B. (1999). Integrable structure of conformal field theory III. The Yang–Baxter relation. Communications in mathematical physics, 200, 297-324.

[161] Jimbo, M. (1989). Introduction to the Yang-Baxter equation. International Journal of Modern Physics A, 4(15), 3759-3777.

[162] Weinstein, A., Xu, P. (1992). Classical solutions of the quantum Yang-Baxter equation. Communications in mathematical physics, 148, 309-343.

[163] Hietarinta, J. (1993). Solving the two-dimensional constant quantum Yang–Baxter equation. Journal of mathematical physics, 34(5), 1725-1756.

[164] DING, J., HODGES, T. J. (2000). The Yang-Baxter equation for operators on function fields.

[165] Belavin, A. A., Drinfeld, V. G. (1982). Solutions of the classical Yang–Baxter equation for simple Lie algebras. Funktsional'nyi Analiz i ego Prilozheniya, 16(3), 1-29

[166] Chicherin, D., Derkachov, S. (2015). Matrix factorization for solutions of the Yang-Baxter equation. arXiv preprint arXiv:1502.07923.

[167] Derkachov, S. E., Chicherin, D. (2016). Matrix factorization for solutions of the Yang–Baxter equation. Journal of Mathematical Sciences, 213, 723-742.

[168] Derkachov, S. È., Spiridonov, V. P. (2013). Yang–Baxter equation, parameter permutations, and the elliptic beta integral. Russian Mathematical Surveys, 68(6), 1027.

[169] Jimbo, M. (1994). Introduction to the Yang-Baxter equation. Braid Group, Knot Theory, and Statistical Mechanics, 153-176.

[170] Frenkel, I. B., Reshetikhin, N. Y. (1992, January). Quantum affine algebras, commutative systems of difference equations and elliptic solutions to the Yang-Baxter equations. In Proceedings of the XXth International Conference on Differential Geometric Methods in Theoretical Physics, New York, 1991 (pp. 46-107). Singapore: World Scientific.

[171] Chicherin, D., Derkachov, S. E., Spiridonov, V. P. (2016). From principal series to finite-dimensional solutions of the Yang-Baxter equation. SIGMA. Symmetry, Integrability and Geometry: Methods and Applications, 12, 028.

[172] Nepomechie, R. I. (1998). A spin chain primer. arXiv preprint hep-th/9810032.

[173] Grabowski, M. P., Mathieu, P. (1994). Quantum integrals of motion for the Heisenberg spin chain. Modern Physics Letters A, 9(24), 2197-2206.

[174] Korepin, V. E., Pâtu, O. I. (2007). XXX spin chain: from Bethe solution to open problems. arXiv preprint cond-mat/0701491.

[175] Boos, H. E., Korepin, V. E. (2002). Evaluation of integrals representing correlations in the XXX Heisenberg spin chain. In MathPhys Odyssey 2001: Integrable Models and Beyond In Honor of Barry M. McCoy (pp. 65-108). Boston, MA: Birkhäuser Boston.

[176] Kitanine, N. (2001). Correlation functions of the higher spin XXX chains. Journal of Physics A: Mathematical and General, 34(39), 8151.

[177] Grabowski, M. P., Mathieu, P. (1996). The structure of conserved charges in open spin chains. Journal of Physics A: Mathematical and General, 29(23), 7635.

[178] Klümper, A., Scheeren, C. (2019). The thermodynamics of the spin-1 2 XXX chain: free energy and low-temperature singularities of correlation lengths. Classical and Quantum Nonlinear Integrable Systems, 234-255.

[179] Grabowski, M. P., Mathieu, P. (1995). Structure of the conservation laws in quantum integrable spin chains with short range interactions. Annals of Physics, 243(2), 299-371.

[180] Zhang, J., Rajabpour, M. A. (2022). Entanglement of magnon excitations in spin chains. Journal of High Energy Physics, 2022(2), 1-45.

[181] Affleck, I. (1989). Quantum spin chains and the Haldane gap. Journal of Physics: Condensed Matter, 1(19), 3047.

[182] Sun, C. F., Xue, K., Wang, G. C., Zhou, C. C., , Du, G. J. (2011). The topological basis realization and the corresponding XXX spin chain. Europhysics Letters, 94(5), 50001.

[183] Wang, X., Zanardi, P. (2002). Quantum entanglement and Bell inequalities in Heisenberg spin chains. Physics Letters A, 301(1-2), 1-6.

[184] Fisher, D. S. (1994). Random antiferromagnetic quantum spin chains. Physical review b, 50(6), 3799.

[185] Du, G., Xue, K., Zhou, C. (2021). The Yangian relations of Heisenberg spin chain model. Scientific Reports, 11(1), 14615.

[186] Kwek, L. C., Takahashi, Y., Choo, K. W. (2009, December). Spin chain under next nearest neighbor interaction. In Journal of Physics: Conference Series (Vol. 143, No. 1, p. 012014). IOP Publishing.

[187] Coordinate Bethe Ansatz and Quantum Group Symmetry of the Spin-1 XXZ Heisenberg Spin Chain S.I. Tolmaya.

[188] Ilievski, E. (2014). Exact solutions of open integrable quantum spin chains. arXiv preprint arXiv:1410.1446.

[189] Derkachov, S. E., Manashov, A. N. (2011). Noncompact sl (N) spin chains: BGG-resolution, Q-operators and alternating sum representation for finite-dimensional transfer matrices. Letters in Mathematical Physics, 97(2), 185-202.

[190] Schlottmann, P. (1988). Integrable spin-1 Heisenberg chain with impurity. Physical Review B, 37(1), 379.

[191] Lazarescu, A., Pasquier, V. (2014). Bethe Ansatz and Q-operator for the open ASEP. Journal of Physics A: Mathematical and Theoretical, 47(29), 295202.

[192] Andrei, N., Johannesson, H. (1984). Heisenberg chain with impurities (an integrable model). Physics Letters A, 100(2), 108-112.

[193] Frahm, H., Grelik, J. H., Seel, A., Wirth, T. (2010). Functional Bethe ansatz methods for the open XXX chain. Journal of Physics A: Mathematical and Theoretical, 44(1), 015001.

[194] Claeys, P. W., Herzog-Arbeitman, J., Lamacraft, A. (2022). Correlations and commuting transfer matrices in integrable unitary circuits. SciPost Physics, 12(1), 007.

[195] Alcaraz, F. C., Lazo, M. J. (2003). The Bethe ansatz as a matrix product ansatz. Journal of Physics A: Mathematical and General, 37(1), L1.

[196] Lulek, T., Topolewicz, S. (2010). A complete set of commuting operators for the Bethe ansatz. Journal of Physics A: Mathematical and Theoretical, 43(49), 495201.

[197] Gross, B. H. (2000). On minuscule representations and the principal SL2. Represent. Theory, 4(200), 225-244.

[198] Slansky, R. (1981). Group theory for unified model building. Physics reports, 79(1), 1-128.

[199] Van Daele, A. (1970). General formula to derive branching rules. Journal of Mathematical Physics, 11(11), 3275-3282.

[200] McKay, W., Patera, J., Sankoff, D. (1977). The computation of branching rules for representations of semisimple Lie algebras. In Computers in nonassociative rings and algebras (pp. 235-277). Academic Press.

[201] Gould, M. D., Bracken, A. J., , Hughes, J. W. B. (1989). Branching rules for typical and atypical representations of gl (n| 1). Journal of Physics A: Mathematical and General, 22(15), 2879.

[202] Li, L. (2018). Branching Rules of Classical Lie Groups in Two Ways (Doctoral dissertation, Stanford University).

[203] Lanir, A., Nedelin, A., Sela, O. (2020). Black hole entropy function for toric theories via Bethe Ansatz. Journal of High Energy Physics, 2020(4), 1-52.

[204] Argurio, R., Bertolini, M., Ferretti, G., Petersson, C., Lerda, A. (2007). Stringy instantons at orbifold singularities. Journal of High Energy Physics, 2007(06), 067.

[205] Saidi, E. H., Drissi, L. B. (2022). 5D N= 1 super QFT: symplectic quivers. Nuclear Physics B, 974, 115632.

[206] Mattioli, P., Ramgoolam, S. (2015). Quivers, words and fundamentals. Journal of High Energy Physics, 2015(3), 1-74.

[207] Saidi, E. H. (2012). Mutation symmetries in BPS quiver theories: building the BPS spectra. Journal of High Energy Physics, 2012(8), 1-86.

[208] Bonelli, G., Sciarappa, A., Tanzini, A., Vasko, P. (2016). Quantum cohomology and quantum hydrodynamics from supersymmetric quiver gauge theories. Journal of Geometry and Physics, 109, 3-43.

[209] Garcia-Etxebarria, I., Saad, F., , Uranga, A. M. (2006). Quiver gauge theories at resolved and deformed singularities using dimers. Journal of High Energy Physics, 2006(06), 055.

[210] Uranga, A. M. (2001). From quiver diagrams to particle physics. In European Congress of Mathematics: Barcelona, July 10–14, 2000 Volume II (pp. 499-506). Basel: Birkhäuser Basel.

[211] Saidi, E. H. (1993). Chiral rings in the N= 4 SU (2) conformal theory. Physics Letters B, 300(1-2), 84-91.

[212] Hobuß, K. (2019). Spin chains and vertex models based on superalgebras.

[213] Frahm, H., Martins, M. J. (2015). Finite-size effects in the spectrum of the OSp (3| 2) superspin chain. Nuclear Physics B, 894, 665-684.

[214] Dancer, K. A., Gould, M. D., Links, J. (2007). Lax Operator for the Quantised Orthosymplectic Superalgebra U q [osp (m| n)]. Algebras and Representation Theory, 10, 593-617.

[215] Frassek, R., Marboe, C., Meidinger, D. (2017). Evaluation of the operatorial Q-system for non-compact super spin chains. Journal of High Energy Physics, 2017(9), 1-34.

[216] Foerster, A., Karowski, M. (1993). Algebraic properties of the Bethe ansatz for an $spl(2,1)$ -supersymmetric $t-J$ model. Nuclear Physics B, 396(2-3), 611-638.

[217] Frassek, R., Marboe, C., Meidinger, D. (2017). Evaluation of the operatorial Q-system for non-compact super spin chains. Journal of High Energy Physics, 2017(9), 1-34.

[218] Tsuboi, Z. (2014). Asymptotic representations and q-oscillator solutions of the graded Yang–Baxter equation related to Baxter Q-operators. Nuclear Physics B, 886, 1-30.

[219] Mayer, L. (2023). Many-Body Invariants for Super Spin Chains with Antiunitary Symmetries (Doctoral dissertation, Universität zu Köln).

[220] Shevchenko, Y., Makarov, A., Nefedev, K. (2017). Effect of long-and short-range interactions on the thermodynamics of dipolar spin ice. Physics Letters A, 381(5), 428-434.

[221] Ye, J., Baldauf, T., Mattauch, S., Paul, N., Paul, A. (2019). Topologically stable helices in exchange coupled rare-earth/rare-earth multilayer with superspin-glass like ordering. Communications Physics, 2(1), 114.

[222] Belim, S. V. (2023). Study of ordering in 2D ferromagnetic nanoparticles arrays: Computer simulation. AIMS Materials Science, 10(6), 948-964.

[223] Hagendorf, C. (2013). Spin chains with dynamical lattice supersymmetry. Journal of Statistical Physics, 150(4), 609-657.

[224] Zirnbauer, M. R. (1994). Towards a theory of the integer quantum Hall transition: From the nonlinear sigma model to superspin chains. Annalen der Physik, 506(7-8), 513-577.

[225] Belitsky, A. V., Braun, V. M., Gorsky, A. S., , Korchemsky, G. P. (2004). Integrability in QCD and beyond. International Journal of Modern Physics A, 19(28), 4715-4788.

[226] Beisert, N., Staudacher, M. (2003). The N= 4 SYM integrable super spin chain. Nuclear Physics B, 670(3), 439-463.

[227] Frappat, L., Sciarrino, A., Sorba, P. (1996). Dictionary on Lie superalgebras. arXiv preprint hep-th/9607161.

[228] Sthanumoorthy, N. (2016). Introduction to finite and infinite dimensional lie (super) algebras. Academic Press.

[229] Frappat, L., Sciarrino, A., Sorba, P. (1989). Structure of basic Lie superalgebras and of their affine extensions. Communications in Mathematical Physics, 121, 457-500.

[230] Dynkin, E. B. (1960). Semisimple subalgebras of semisimple Lie algebras. Amer. Math. Soc. Transl. Ser. 2, 6, 111-244.

[231] Stoilova, N. I., Van der Jeugt, J. (2005). A classification of generalized quantum statistics associated with classical Lie algebras. Journal of mathematical physics, 46(3).

[232] Stoilova, N. I., Van der Jeugt, J. (2007). Classification of generalized quantum statistics associated with the exceptional Lie (super) algebras. Journal of mathematical physics, 48(4).

[233] Stoilova, N. I., Van der Jeugt, J. (2008, August). Algebraic generalization of quantum statistics. In Journal of Physics: Conference Series (Vol. 128, No. 1, p. 012061). IOP Publishing.

[234] Van der Jeugt, J. (1987). Regular subalgebras of Lie superalgebras and extended Dynkin diagrams. Journal of mathematical physics, 28(2), 292-301.

[235] Stoilova, N. I., Van der Jeugt, J. (2005). Lie superalgebraic framework for generalization of quantum statistics. arXiv preprint math-ph/0511058.

[236] Stoilova, N. I., Van der Jeugt, J. (2005). A classification of generalized quantum statistics associated with basic classical Lie superalgebras. Journal of mathematical physics, 46(11).

[237] Boujakhrout, Y., Saidi, E. H., Laamara, R. A., Drissi, L. B. (2022). Lax operator and superspin chains from 4D CS gauge theory. Journal of Physics A: Mathematical and Theoretical, 55(41), 415402.